QUANTITY AND QUALITY OF GROUND-WATER INFLOW TO THE SAN JOAQUIN RIVER, CALIFORNIA

By Steven P. Phillips, Sherrill Beard, *and* R.J. Gilliom

U.S. GEOLOGICAL SURVEY

Water-Resources Investigations Report 91-4019

Prepared in cooperation with the

CALIFORNIA DEPARTMENT OF WATER RESOURCES and the

CALIFORNIA STATE WATER RESOURCES CONTROL BOARD

6439-64

Sacramento, California
1991

U.S. DEPARTMENT OF THE INTERIOR
MANUEL LUJAN, JR., *Secretary*

U.S. GEOLOGICAL SURVEY
Dallas L. Peck, *Director*

For sale by the Books and
Open-File Reports Section
U.S. Geological Survey
Federal Center, Box 25425
Denver, CO 80225

For additional information write to:
District Chief
U.S. Geological Survey
Federal Building, Room W-2234
2800 Cottage Way
Sacramento, CA 95825

CONTENTS

FIGURES

TABLES

CONVERSION FACTORS AND VERTICAL DATUM

Conversion Factors

Multiply	By	To obtain
cubic foot per second (ft^3/s)	0.0283	cubic meter per second
cubic foot per second per foot [(ft^3/s)/ft]	0.0930	cubic meter per second per meter
cubic foot per second per mile [(ft^3/s)/mi]	0.0176	cubic meter per second per kilometer
foot (ft)	0.3048	meter
foot per mile (ft/mi)	0.1894	meter per kilometer
foot per second (ft/s)	0.3048	meter per second
foot per year (ft/yr)	0.3048	meter per year
inch (in.)	25.4	millimeter
mile (mi)	1.609	kilometer

Water temperature is given in degrees Celsius (°C), which can be converted to degrees Fahrenheit (°F) by the following equation:

$$\text{Temp. } °F = 1.8(\text{temp. } °C) + 32.$$

Vertical Datum

Sea Level: In this report "sea level" refers to the National Geodetic Vertical Datum of 1929--a geodetic datum derived from a general adjustment of the first-order level nets of the United States and Canada, formerly called Sea Level Datum of 1929.

QUANTITY AND QUALITY OF GROUND-WATER INFLOW TO THE SAN JOAQUIN RIVER, CALIFORNIA

By Steven P. Phillips, Sherrill Beard, *and* R.J. Gilliom

Abstract

Concern over high concentrations of dissolved solids and trace elements in the San Joaquin River has focused attention on ground water as a potentially significant source of contamination. Two approaches were used to assess the quantity of ground-water inflow to a 19-mile reach of the San Joaquin River. The first approach was to develop cross-sectional ground-water-flow models using data collected from observation wells installed at three sites along the reach. The average quantity of ground-water inflow simulated by the flow models was 2.0 cubic feet per second per mile.

The second approach was a surface-water-flow balance. During synoptic studies in 1986 and 1989, streamflow and specific conductance were measured at the upstream and downstream ends of the 19-mile reach and at all known points of inflow and outflow along the reach. Residual inflow and salt load were attributed to ground water. The estimated ground-water inflow for the 1986 and 1989 synoptic studies was 6.7 and 3.2 cubic feet per second per mile, respectively.

The quality of ground-water inflow was assessed through the synthesis of model results and measured ground-water chemistry and through salt-balance calculations from the results of synoptic studies. The average chemical composition of ground-water inflow estimated by combining results from the flow models and chemical analyses is 1,590 milligrams per liter for dissolved solids, 1,321 micrograms per liter for boron, 0.9 microgram per liter for selenium, 6.6 micrograms per liter for molybdenum, and an average specific conductance of 2,230 microsiemens per centimeter at 25 degrees Celsius. The average specific conductance of ground-water inflow was estimated from the salt balance to be 1,730 and 1,216 microsiemens per centimeter at 25 degrees Celsius in 1986 and 1989, respectively.

The dissolved-solids loads (specific conductance times flow) implied by the results of both approaches are within 20 percent of each other, using the data from the 1989 synoptic study. The results of the 1986 and 1989 water-balance synoptic studies indicate that the quantity and quality of ground-water inflow to the San Joaquin River can vary significantly with changes in hydrologic conditions.

INTRODUCTION

The San Joaquin River has high concentrations of dissolved solids, selenium, boron, and sometimes molybdenum (Kratzer and others, 1987). Concern that these or other contaminants may adversely affect water quality and use has focused attention on the sources of contamination. Ground water is a potential source of dissolved solids and trace elements to the San Joaquin River that has not been well characterized.

The U.S. Geological Survey, in cooperation with the California Department of Water Resources and the California State Water Resources Control Board, began a study in 1988 to assess the quantity and quality of ground-water inflow to the San Joaquin River. The specific objectives of the study were to test preliminary estimates of ground-water inflow and dissolved-solids contributions, enhance present knowledge to include contributions of selected trace elements, and improve understanding of the processes that govern the quantity and quality of ground-water inflow to the San Joaquin River.

This report describes the results of the study and presents

(1) Descriptive analysis of the hydrogeologic characteristics of the ground-water-flow system adjacent to the river;
(2) Quantitative analysis of ground-water flow into the river using two-dimensional ground-water-flow models developed for three cross sections of the flow system;

(3) Quantitative analysis of ground-water flow into the river by a water-balance approach using measured surface-water flows;
(4) Descriptive analysis of the chemistry and isotopic composition of ground water adjacent to the river with implications of the age, origin, and quality of ground water in different parts of the flow system; and
(5) Comparative evaluation of independent assessments of the quantity and quality of ground-water inflow to the San Joaquin River.

The study focused on a 19-mile reach of the lower San Joaquin River between Newman and Patterson (fig. 1). Data for hydrogeologic and geochemical characterization and for model analysis were collected at the upstream end, middle, and downstream end of the 19-mile reach. The water-balance approach based on measured streamflow was applied to the entire reach.

DESCRIPTION OF STUDY AREA

The San Joaquin Valley is bounded by the Coast Ranges to the west and the Sierra Nevada to the east. The axis of the valley is delineated by the San Joaquin River, which flows northward to the Sacramento-San Joaquin Delta. Important sources of water to the river are Sierra Nevada runoff, surface agricultural-return flows, tile-drain discharges, and ground water. The relative importance of each of these sources of flow varies seasonally with the semiarid climate of the valley and with irrigation cycles as agriculture is the dominant land use (Clifton and Gilliom, 1989).

The segment of the San Joaquin River studied in this report is a 19-mile reach in the northern San Joaquin Valley (fig. 1). Streamflow is perennial in the study reach and increases downstream as water from small tributaries, irrigation-return flows, and ground-water inflow enters the river. Streamflow was measured continuously during the study near Newman, Crows Landing, and Patterson, where the major eastbound roads from these towns cross the river. The Newman and Patterson study sites are at the upstream and downstream ends of the 19-mile reach, respectively, and the Crows Landing study site is near the midpoint of the reach.

PREVIOUS STUDIES

Previous studies indicated that ground-water inflow to the San Joaquin River is probably a small proportion of total riverflow but a substantial proportion of the river salt load. A regional-scale water-budget model was developed to simulate the water budget for a 60-mile reach of the river (Kratzer and others, 1987; Rashmawi and others, 1989). The water-budget

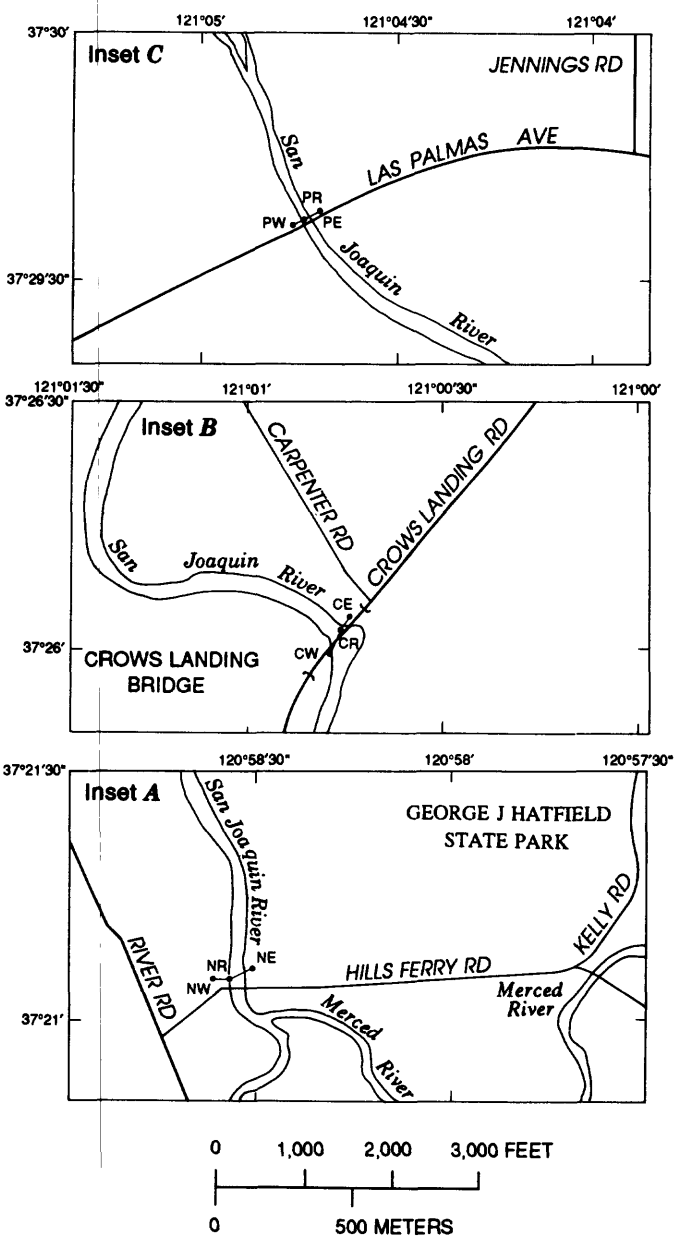

Figure 1. Location of study area and study sites.

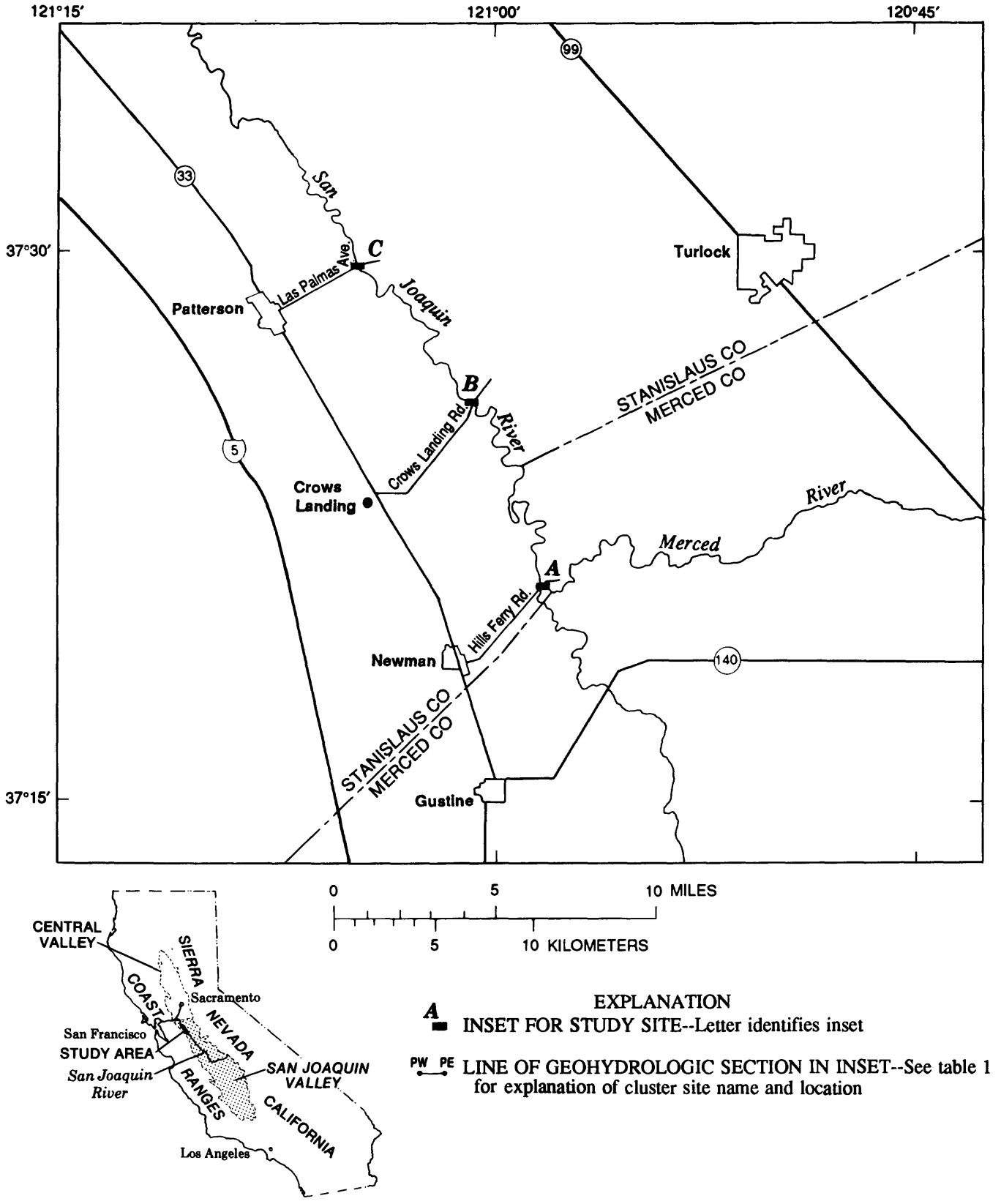

Figure 1. Continued.

model includes a ground-water-flow model that was used to estimate ground-water inflow to the river. Ground-water inflow was estimated to contribute 3 to 4 percent of the total flow in the river. Because of the high salinity of ground water, this relatively small quantity of water was estimated to contribute about 16 percent of the dissolved solids. On the basis of streamflow data for October 1986, Clifton and Gilliom (1989) estimated that about 2 percent of San Joaquin River flow was from ground-water inflow to the 19-mile reach of river between the Merced River inflow and the town of Patterson (the middle third of the 60-mile reach of the river).

WELL CONSTRUCTION AND GEOLOGIC LOGGING

Ground-water observation wells were installed near the Newman, Crows Landing, and Patterson sites to measure water levels and to collect ground-water samples for chemical analyses near the San Joaquin River. Three clusters of observation wells were installed at each of the study sites--one cluster site within the river and one on each side of the river within 200 ft of the bank. Each cluster site consists of two or three wells completed at different depths. A total of 22 wells were installed at depths ranging from 5 to 107.5 ft below land surface.

For the purposes of this report, all wells were assigned an identifier consisting of two letters and a number (table 1). The first letter corresponds to the first letter in the name of the cluster site, which is named by the nearest town, and the second letter corresponds to the location with respect to the river: east of (E), west of (W), or within (R) the river. The number associated with the well identifier is the depth, in feet, from land surface to the midpoint of the screened interval or from the river bottom to the bottom of the wells within the river. For example, PW-11.5 is a well at the Patterson site on the west side of the river, and the midpoint of the well screen is 11.5 feet below land surface. Figure 2 shows the locations and depths of the observation wells at each cluster site.

Two procedures were used to install and complete the wells for this project. Wells on the riverbank (land wells) were drilled using a standard 6-inch flight-auger bit. These wells were cased with 2-inch diameter polyvinyl chloride (PVC) well casing and have a 5-foot screened interval 3 ft above the closed bottom of the casing. A natural sandpack was allowed to form to the top of the screened interval for wells completed within coarse-grained materials, and 16×30 mesh sand was used for wells completed within fine-grained materials. The rest of the annulus was filled with bentonite grout to the land surface. All land wells are protected with a steel casing cover and locking cap. Construction of a typical land well is shown in figure 3.

Wells installed in the river (river wells) were jetted by hand using a high-pressure water jet. These wells are cased with 2-inch diameter PVC well casing, except for the deep river well at the Patterson site, which is 1.5 in. in diameter. All river wells are open-ended with 1 ft of washed sand at the bottom of the casing. River wells at the Crows Landing and Patterson sites are secured to existing stream gaging equipment, and river wells at the Newman site are free-standing about 5 ft from the west bank.

Lithologic logs were compiled from onsite descriptions of drill cuttings and core samples and from observations recorded during drilling and jetting procedures. When possible, core samples were collected continuously during the drilling of the deepest well at each land site. When coarse-grained deposits made coring difficult, drill cuttings and noted observations, such as variations in drill speed, were used to complete the lithologic log. Lithologic logs of the wells jetted into the riverbed were based on observations noted during the jetting procedure and from several samples recovered from the jetwash.

Table 1. Cluster site names, location, and depth, and well identifiers and corresponding State well number

[Depth: Depth is in feet below land surface to the midpoint of the screened interval or from the river bottom to the bottom of the well within the river. --, no data]

Cluster site name	Location	Depth	Well identifier	State well No.
Newman (N)	West	14.5	NW-14.5	007S009E04J05
	West	47.5	NW-47.5	007S009E04J06
	West	107.5	NW-107.5	007S009E04J07
	River	7.0	NR-7.0	007S009E04J03
	River	20.0	NR-20.0	007S009E04J04
	East	14.5	NE-14.5	007S009E03M01
	East	35.5	NE-35.5	007S009E03M02
	East	107.5	NE-107.5	007S009E03M03
Crows Landing (C)	West	12.8	CW-12.8	007S009E07H03
	West	18.2	CW-18.2	006S009E07H02
	West	97.7	CW-97.7	006S009E07H01
	River	5.0	CR-5.0	006S009E07A03
	River	20.0	CR-20.0	006S009E07A04
	East	19.5	CE-19.5	006S009E07A01
	East	107.5	CE-107.5	006S009E07A02
Patterson (P)	West	11.5	PW-11.5	005S008E15M07
	West	22.5	PW-22.5	005S008E15M06
	West	89.0	PW-89.0	005S008E15M05
	River	5.0	PR-5.0	005S008E15M04
	River	30.7	PR-30.7	005S008E15M03
	East	9.5	PE-9.5	005S008E15M01
	East	98.3	PE-98.3	005S008E15M02

Drill cuttings and core samples were described by texture, color, and other significant features. Texture descriptions were based on the National Research Council grain-size classification (National Research Council, 1947). The color of dry samples was recorded using numerical color designations from the Munsell Soil Color Charts (Munsell Color, 1975). Other characteristics of drill cuttings and core samples were determined using Compton's field manual (Compton, 1985) and American Geological Institute data sheets (Dietrich and others, 1982).

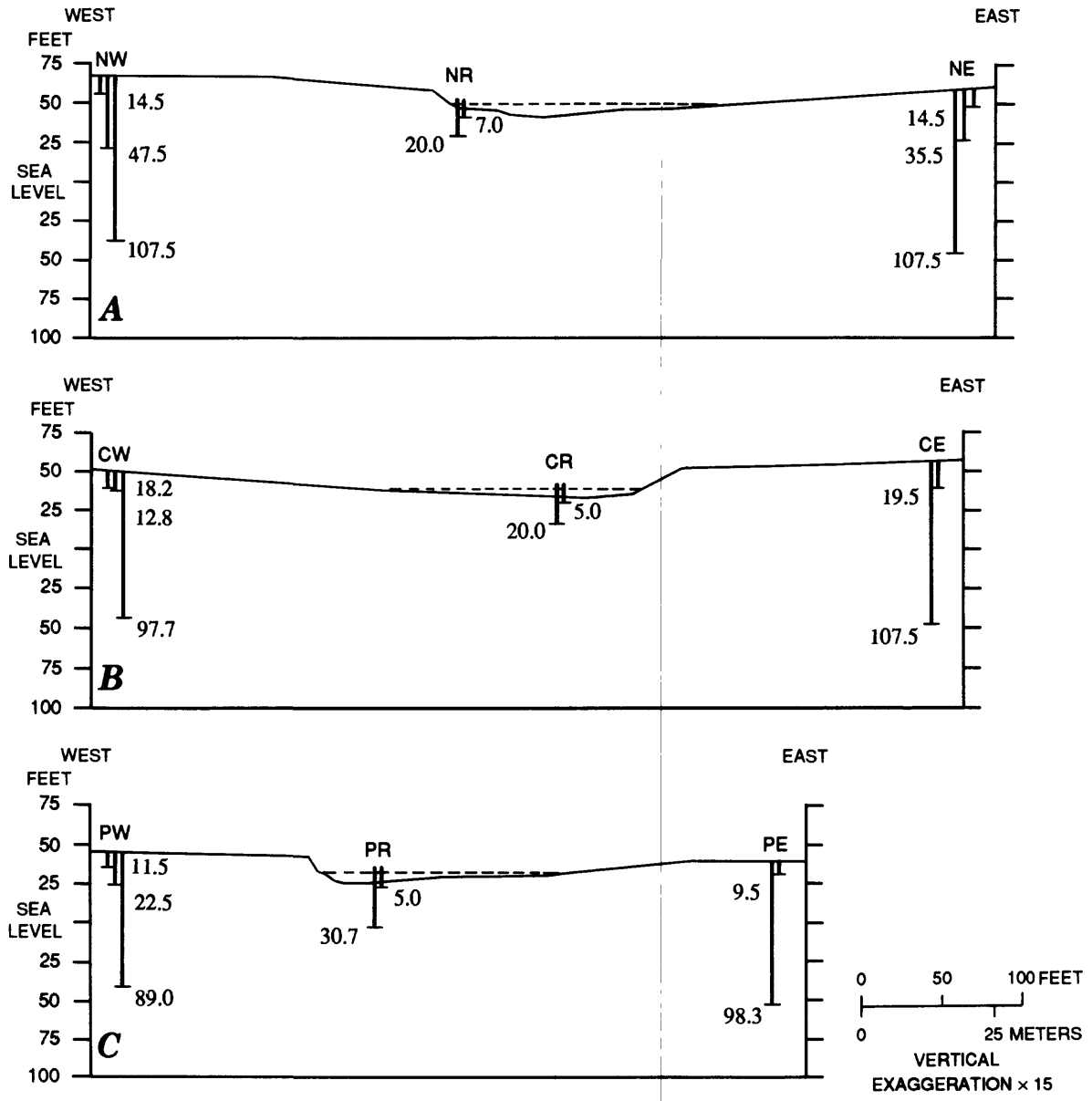

EXPLANATION

——— LAND SURFACE--Approximately located between cluster sites

- - - - - SAN JOAQUIN RIVER--Approximately located

CR 5.0 / 20.0 CLUSTER SITE--Site at which two or more observation wells are installed at different depths. See table 1 for explanation of cluster site name and location

MIDPOINT OF 5-FOOT SCREENED INTERVAL OF INDIVIDUAL LAND WELL OR TOTAL DEPTH OF RIVER WELL--Number is depth, in feet, below land surface or river bottom

Figure 2. Locations and depths of the observation wells at each cluster site. *A*, Newman site. *B*, Crows Landing site. *C*, Patterson site.

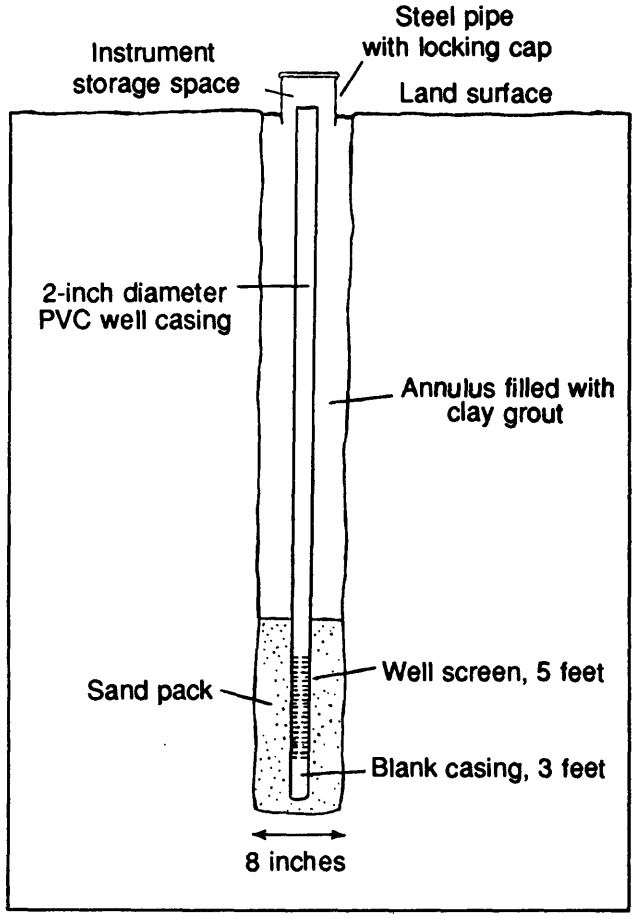

Figure 3. Construction of a typical land well.

SAMPLING AND ANALYTICAL METHODS

Ground-water samples for chemical analyses were collected with a peristaltic pump, submersible piston pump, or a Teflon bailer. Prior to sampling, about 1.5 to 3 consecutive well-casing volumes of water were pumped from each well. All sampling apparatus and containers were rinsed at least three times with the well water. Samples to be analyzed for major ions and dissolved trace elements were pumped through 0.45-µm (micrometer) membrane filters with a peristaltic pump and stored in polyethylene bottles, except for the mercury sample, which was collected in a glass bottle with a Teflon-lined cap. Samples for nitrogen and phosphorus analysis were chilled. Unfiltered samples were collected for tritium analysis and for analyses of stable isotopes of oxygen and hydrogen.

All samples except those for tritium were analyzed at U.S. Geological Survey laboratories. Major-ion and trace-element samples were analyzed using standard procedures described by Fishman and Friedman (1989). Selenium concentrations were analyzed using hydride generation and atomic absorption spectrometry (Fishman and Bradford, 1982). Oxygen-18 isotope composition was determined using a modification of the carbon dioxide equilibration method of Epstein and Mayeda (1953), and stable hydrogen-isotopic composition (delta deuterium) was determined by analyzing hydrogen quantitatively extracted from water (Kendall and Coplen, 1985). The tritium samples were analyzed at the Environmental Isotope Laboratory of the University of Waterloo in Ontario, Canada, using electrolytic enrichment and liquid scintillation counting techniques.

Specific conductance, pH, and alkalinity were measured in the field during the collection of samples for laboratory analysis. Specific conductance and pH were measured using meters that were calibrated at each site using standard solutions. Alkalinity was measured by titrating 50 mL (milliliter) samples with dilute sulfuric acid.

Specific conductance also was measured periodically in the San Joaquin River and the ground water. The specific conductance of the river was monitored hourly at the Newman and Patterson sites, and dip-samples were measured periodically at all sites. A minimum of eight ground-water samples were collected bimonthly, and specific conductance was measured onsite or in the laboratory within 1 day of collection using a digital conductivity meter. The specific conductance data collected for selected wells over time were used to evaluate the temporal variability of ground-water salinity.

HYDROGEOLOGY

GEOLOGIC SETTING

The three primary hydrogeologic units in the study area are: the Corcoran Clay Member of the Tulare Formation, Sierran sand, and flood-basin deposits. The Corcoran is present throughout most of the western San Joaquin Valley. This low-permeability unit is a lacustrine deposit composed of silt and silty clay (Bull and Miller, 1975). The Corcoran is about 80 ft thick in the study area, and the top of the unit is located at a depth of about 180 ft below the land surface (Page, 1986). Overlying the Corcoran is the Sierran sand, which is typically more than 150 ft thick. The Sierran sand is a high permeability unit composed primarily of medium- to coarse-grained sand derived from the Sierra Nevada to the east. Generally, 10 to 30 ft of flood-basin deposits overlie the Sierran sand. The flood-basin deposits are composed of interbedded sand, silt, and clay of Sierran and Coast Ranges source, and permeability is highly variable.

The distribution and source of aquifer materials at the cluster sites were interpreted from lithologic logs compiled from drill cuttings, cores, and field observations recorded during installation of the observation wells (fig. 4). Complete logs are presented in table 8 (at back of report). The geologic origin of aquifer materials sampled during well installation was determined from visual appearance and texture. This approach works reasonably well because of the generally oxic and fine-grained nature of Coast Ranges sediments compared with reduced and coarse-grained Sierra Nevada sediments. The flood-basin deposits are of mixed origin with intermittent deposits that are dominantly from Coast Ranges or Sierra Nevada sources.

Individual layers within the flood-basin deposits could not be correlated across the river with any degree of certainty. At each cluster site, however, clay or sandy clay layers of variable thickness were present within the shallow flood-basin deposits. The consistent occurrence of fine-grained layers, which have much lower permeability than adjacent sand deposits, probably is a key control on the ground-water-flow system near the river.

HYDROLOGIC SETTING

The Corcoran Clay Member divides the ground-water-flow system into an upper unconfined zone and a lower confined zone. Flow between the unconfined and confined zones is believed to be negligible in the study area. Contour maps of water-table altitude and the potentiometric surface below the Corcoran, which were prepared by the California Department of Water Resources (Ben B. Igawa, written commun., 1989), indicate little or no vertical hydraulic gradient across the Corcoran, and the results of previous studies indicate that the hydraulic conductivity of the Corcoran is at least 10,000 times lower than that of the Sierran sand (Johnson and others, 1968; Phillips and Belitz, 1990).

Agricultural practices greatly influence the ground-water-flow system in the study area. Irrigation is the primary source of recharge, supplementing much smaller amounts of natural recharge from precipitation and infiltration from streams. Although most irrigation recharge is farther away from the river than the location of the observation wells, local irrigation near the river occurs at some locations. Table 2 gives the general character of irrigation practices near the cluster sites on land and also indicates whether or not the site was inundated during the 1986 flood. Pumping of ground water from agricultural wells is a primary discharge mechanism, supplementing the natural mechanisms of evapotranspiration and discharge to the San Joaquin River. The effects of irrigation and withdrawal of water from wells can be seen in the regional water table and in water levels recorded in the observation wells.

Figure 5 shows the altitude of the water table in and around the study area in spring of 1987. Horizontal hydraulic gradients west of the San Joaquin River (5 to 32 ft/mi) generally are greater than those east of the river (3 to 11 ft/mi). The water table west of the San Joaquin River is a subdued replica of the topography, sloping gently toward the river from the Coast Ranges. East of the river, agricultural pumpage has resulted in the formation of a ground-water divide about 12 mi northeast of the Newman-Patterson reach. East of the divide, which is parallel to the river, the water table slopes eastward toward a cone of depression. West of the divide, the water table slopes gently toward the river.

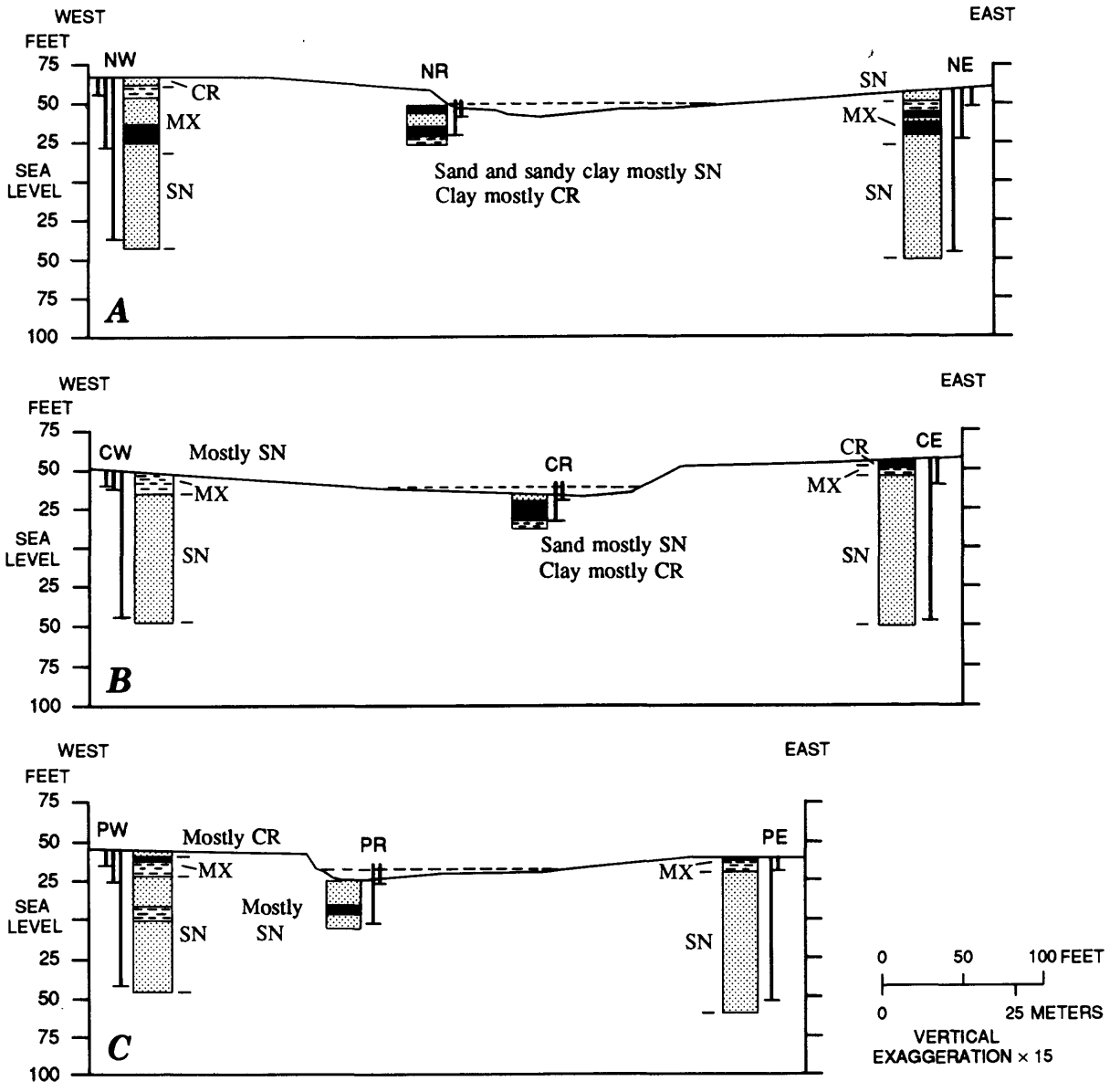

EXPLANATION

LITHOLOGY

- Clay
- Sandy clay--Mixture of sand and clay or silt
- Sand

GEOLOGIC SOURCE

- MX Mixed (Coast Ranges and Sierra Nevada)
- CR Coast Ranges
- SN Sierra Nevada

—— LAND SURFACE--Approximately located between cluster sites

---- SAN JOAQUIN RIVER--Approximately located

PR CLUSTER SITE--Site at which two or more observation wells are installed at different depths. See table 1 for explanation of cluster site name and location

Figure 4. Generalized lithology and geologic source of aquifer materials at cluster sites. *A*, Newman site. *B*, Crows Landing site. *C*, Patterson site.

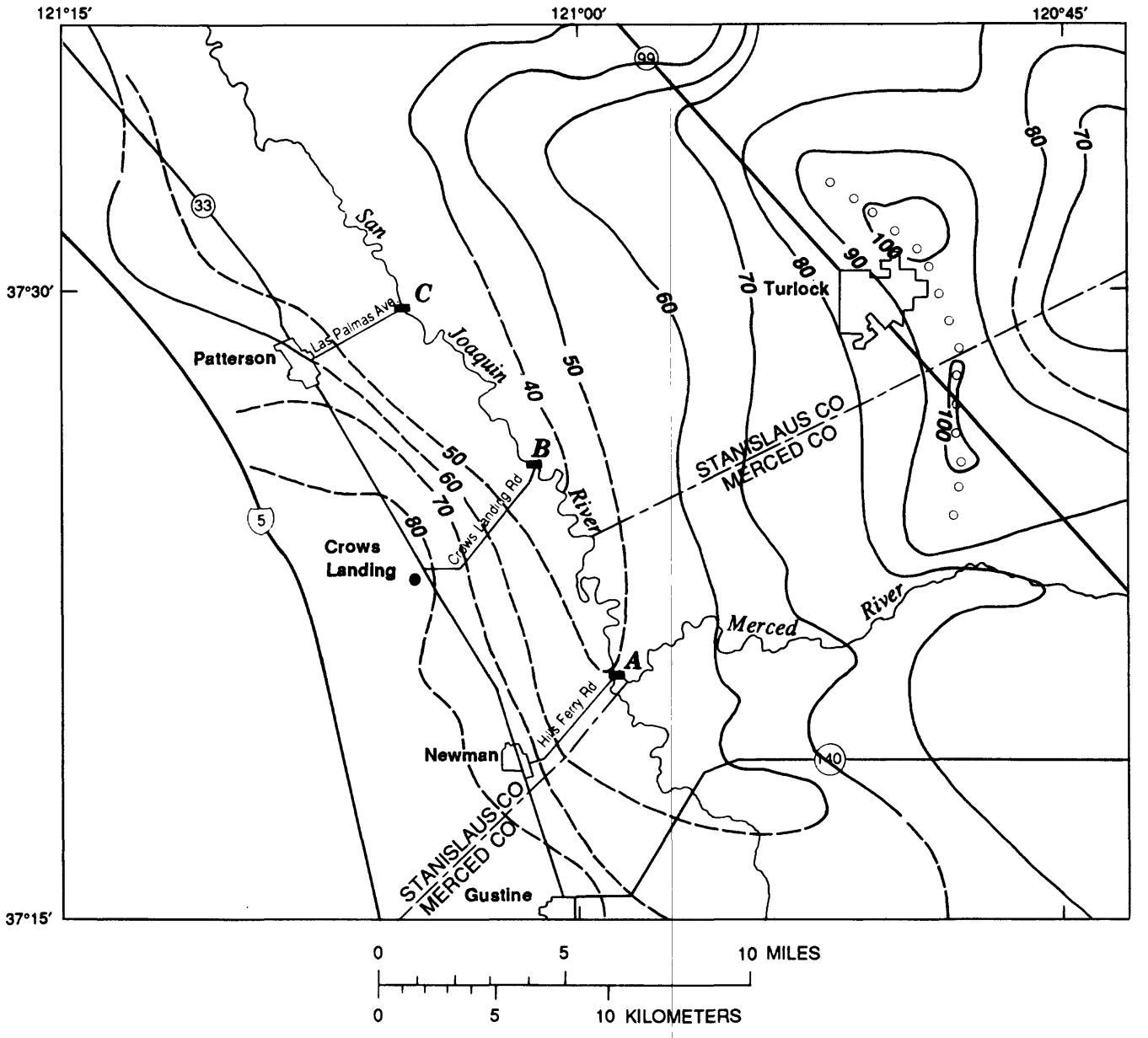

Figure 5. Water-table altitude in and around the study area, spring 1987. Modified from a map by the California Department of Water Resources (Ben B. Igawa, written commun., 1989).

Table 2. Land use, irrigation, and other surface applications of water near cluster sites on land

Cluster site name and location (see table 1)	Inundated during 1986 flood	Land use and water-application history
NW	Yes	Cultivated field--Irrigated with local ground water
NE	Yes	Natural pasture--No irrigation and a grass lawn within 100 feet that is watered with local shallow ground water
CW	Yes	Natural riverbank--Cultivated field about 500 yards northwest of cluster site
CE	No	Pasture--Irrigated during the summer months with river water and a small pond about 20 feet west of cluster site that receives overflow drainage that was originally pumped from the river
PW	Yes	Pasture--Occasionally wetted down with river water and historically was cultivated and irrigated with river water
PE	Yes	Natural riverbank--Pasture about 300 feet east of the cluster site which is currently used as a catch for secondary treated wastewater and historically was cultivated and irrigated with either secondary treated wastewater or water from local reservoirs containing Sierra Nevada runoff

Water levels in the observation wells installed at the study sites were measured weekly from October 1988 through August 1989 (fig. 6). All wells show a seasonal variation in water levels to some degree, with declining water levels in the late summer and early autumn and rising water levels in the late winter and spring. The effects of agricultural practices on water levels can be seen clearly in the hydrograph of the west side of the Newman site. In June 1989, ground-water pumping caused a downward spike in the deep and intermediate wells, and subsequent irrigation caused a corresponding upward spike in the shallow water-table well. This same pattern was repeated in the following month. Seasonal variations in water levels result in seasonal variations in ground-water inflow to the river if the hydraulic gradients are affected.

A key to evaluating ground-water inflow to the river is an understanding of the distribution and variability of hydraulic gradients between the ground water and the river. Horizontal hydraulic gradients near the river, vertical gradients between the deep land wells and the shallow water-table wells, vertical gradients between the deep river wells and the river, and horizontal gradients between the deep land wells on opposite sides of the river are shown in figures 7-10.

Horizontal hydraulic gradients between shallow water-table wells and the San Joaquin River are toward the river and generally do not have a strong seasonal trend over the period measured (fig. 7). An exception to this generalization is the west side of the Newman site, which is adjacent to an irrigation ditch, where the horizontal gradient increases rapidly during the late spring and summer irrigation periods. The horizontal gradient is relatively weak on the east side of the Newman site and is subject to frequent reversals. Horizontal gradients on both sides of the Crows Landing site are average in magnitude and are only subject to reversal during sharp rises in river stage. At the Patterson site, horizontal gradients on both sides of the river are relatively strong and did not reverse during the period measured.

Vertical hydraulic gradients between the deep and shallow land wells are highly variable from site to site but generally are constant over time (fig. 8). The vertical gradient on the west side of the Newman site is highly variable because of the close proximity to an

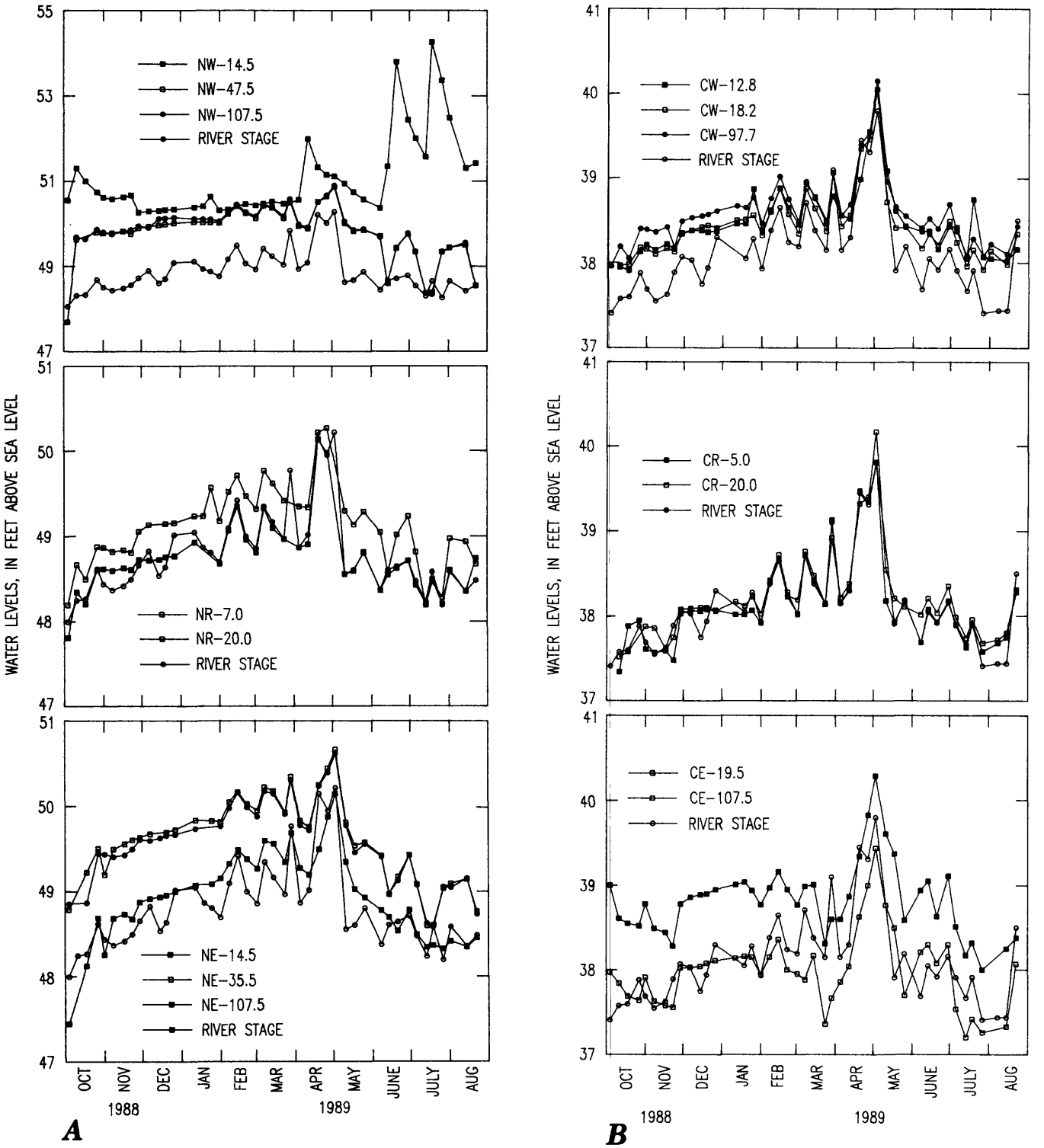

Figure 6. Water levels in observation wells at each cluster site. *A*, Newman site. *B*, Crows Landing site. *C*, Patterson site. See table 1 for explanation of well identifier. Vertical scale for cluster site NW is twice that of other sites.

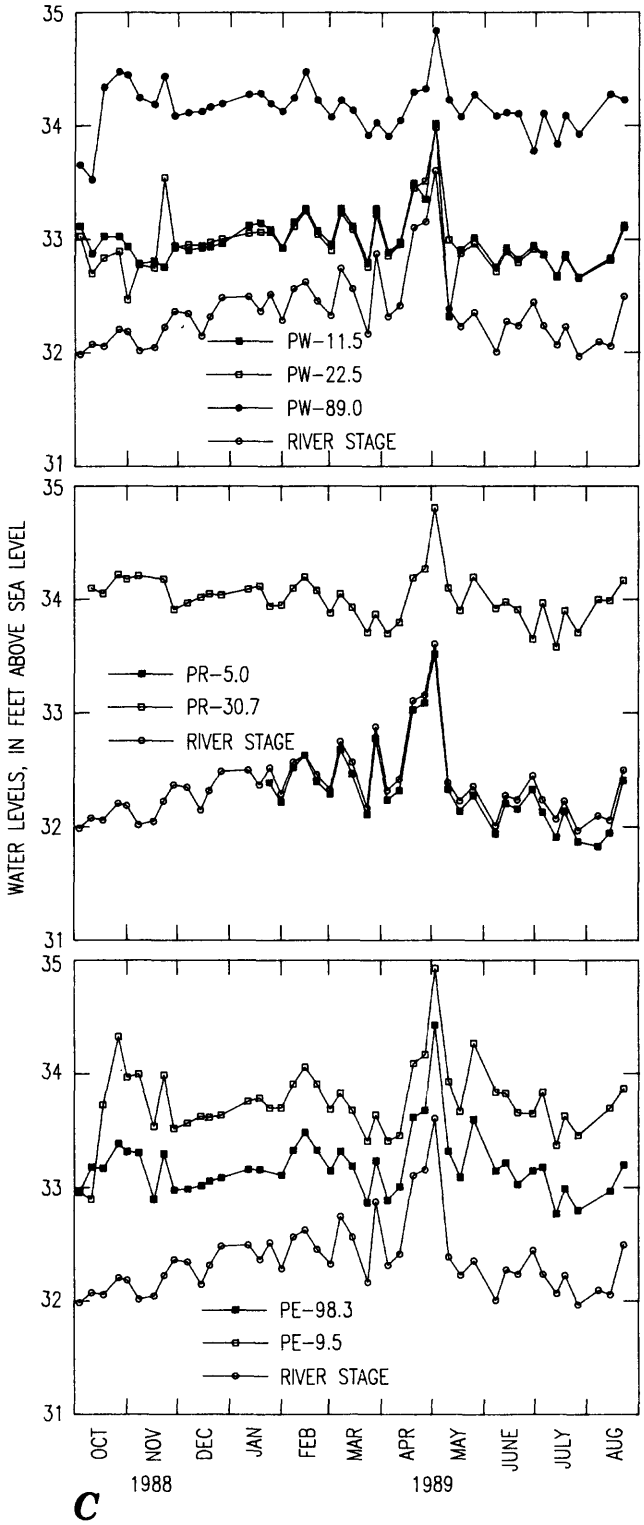

Figure 6. Continued

irrigation ditch and is almost exclusively downward. The vertical gradients at the remaining sites are virtually constant, including the east side at the Newman site, where the gradient is exclusively upward. On the west side of the Crows Landing site, the vertical gradient generally is upward but relatively weak and subject to frequent reversals. The gradient on the east side of the Crows Landing site is exclusively downward and relatively strong. At the Patterson site, the vertical gradients on both sides are almost exclusively upward and are stronger than those at the other sites.

Vertical hydraulic gradients between the deep river wells and the river show little seasonal trend, with the possible exception of the Patterson site (fig. 9). The data for all sites generally indicate an upward gradient but show considerable variability from site to site. At the Newman site, the vertical gradient is upward except for two brief reversals in mid-summer. The vertical gradient beneath the river at the Crows Landing site, though generally upward, is subject to frequent reversals throughout the period measured. At the Patterson site, the vertical gradient is exclusively upward and stronger than at other sites.

Horizontal hydraulic gradients between the deep land wells on opposite sides of the river are toward the east and do not show a distinct seasonal trend (fig. 10). There are a few brief periods when the gradient is reversed. Data for the Newman site show several reversals that are most likely a result of ground-water pumpage for irrigation of the field adjacent to the wells on the west side of the river. Apart from these brief reversals, the gradients at the Newman site are relatively constant. At the Crows Landing site, the gradient is almost exclusively eastward and is the strongest of the three sites. Several upward spikes in the gradients probably are related to local east-side pumping. The horizontal hydraulic gradient between the deep land wells at the Patterson site is intermediate and reversed once during spring irrigation.

The hydraulic gradients and the water-level hydrographs indicate that ground-water pumping has a significant effect on the ground-water-flow system near the San Joaquin River. An understanding of the distribution of pumping is an important aspect of the conceptualization of the flow system. Detailed pumpage data were not available for the study area, but

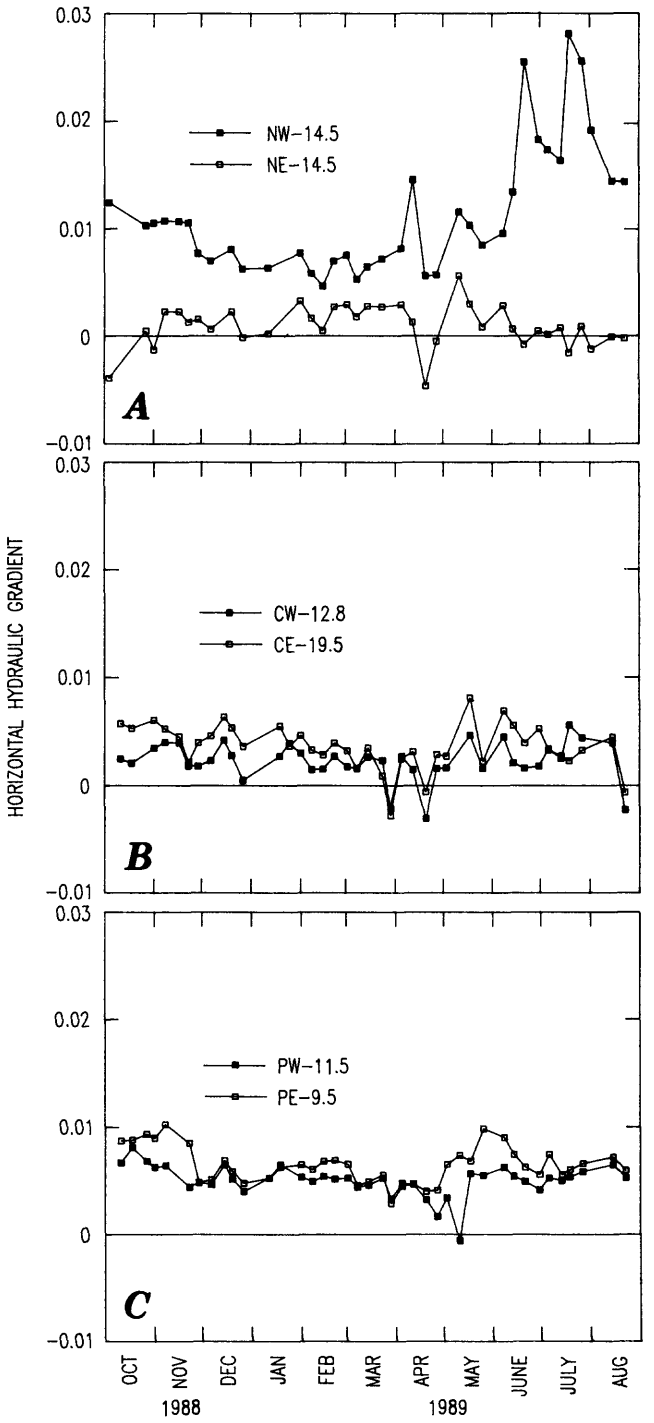

Figure 7. Horizontal hydraulic gradients between shallow water-table wells and the San Joaquin River. *A*, Newman site. *B*, Crows Landing site. *C*, Patterson site. Positive gradients indicate flow toward the river. See table 1 for explanation of well identifier.

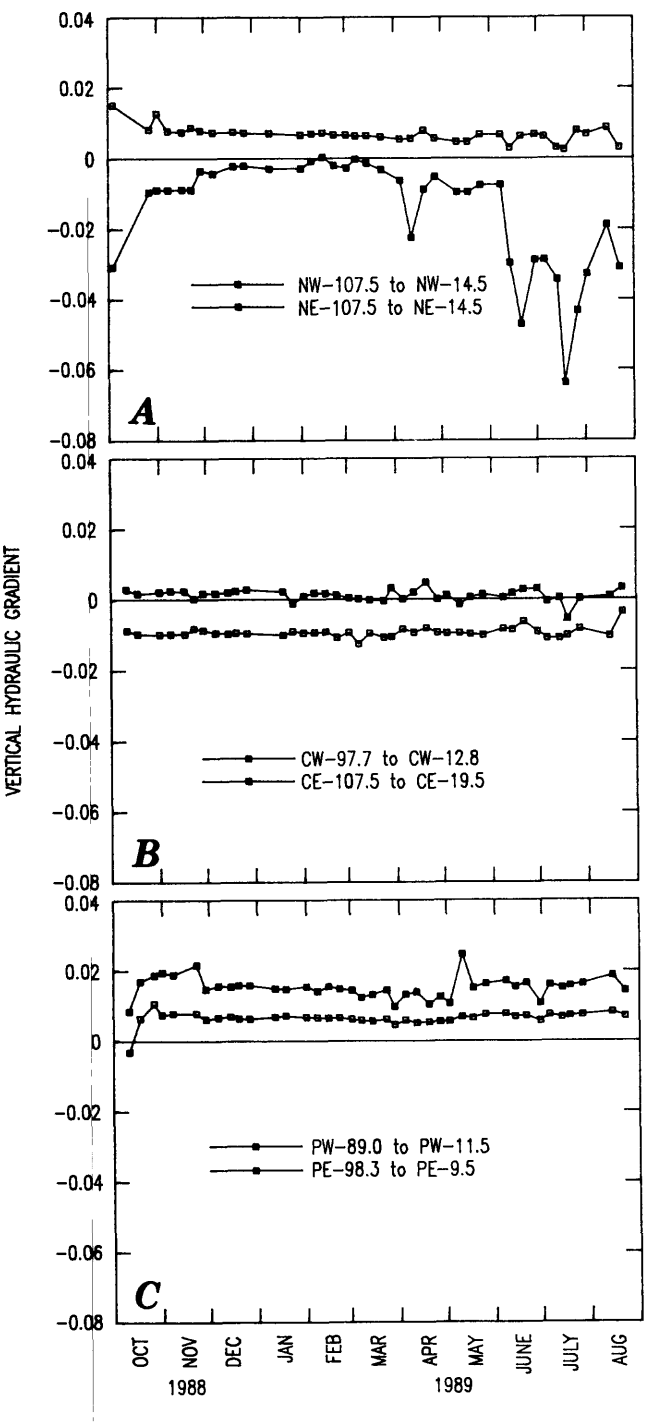

Figure 8. Vertical hydraulic gradients between the deep and shallow land wells. *A*, Newman site. *B*, Crows Landing site. *C*, Patterson site. Positive gradients indicate upward flow. See table 1 for explanation of well identifier.

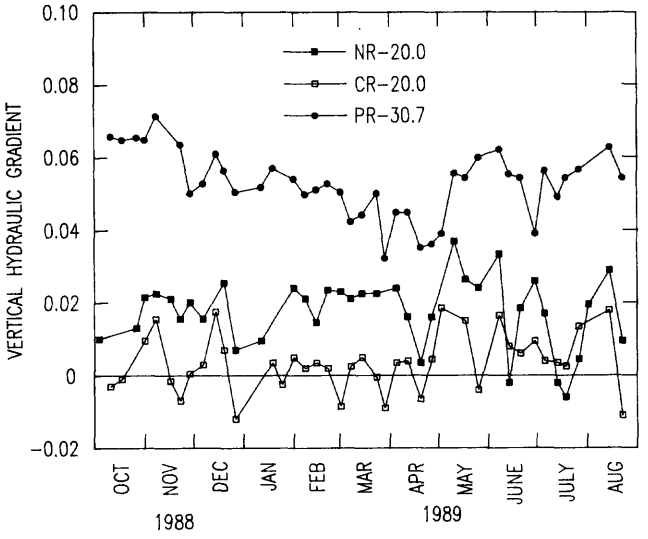

Figure 9. Vertical hydraulic gradients between the deep river wells and the river. Positive gradients indicate upward flow. See table 1 for explanation of well identifier.

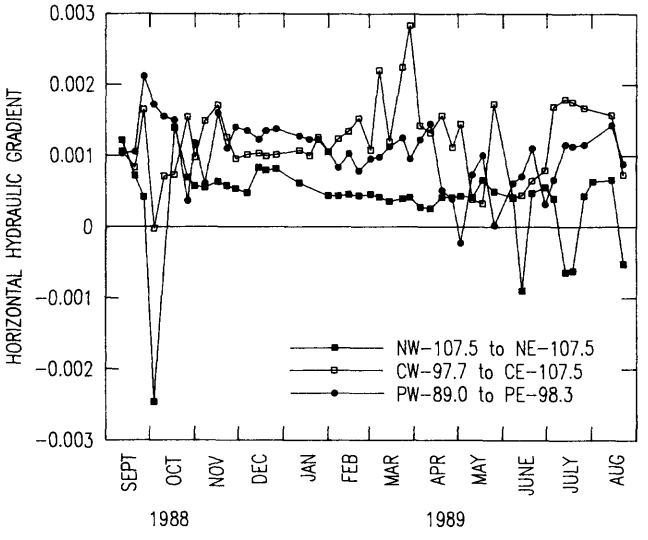

Figure 10. Horizontal hydraulic gradients between the deep land wells on opposite side of the river. Positive gradients indicate eastward flow. See table 1 for explanation of well identifier.

several indirect lines of evidence suggest that ground-water withdrawal from the unconfined zone overlying the Corcoran Clay Member takes place primarily east of the river.

Local evidence of eastern pumping includes the eastward horizontal hydraulic gradients between deep land wells and relatively low water levels in deep wells on the east side in comparison to those in other wells and to the river stage. At the Crows Landing site, the water level in the deep land well on the east side was, on average, lower than the river stage. Ground-water pumping on the east side of the Crows Landing site results in (1) a diversion of water from the natural discharge zone (the San Joaquin River) and (2) a component of flow underneath the San Joaquin River from west to east across the valley trough. Similarly, the water level in the deep land well on the east side of the Patterson site is considerably lower than the water levels in the deep well on the west side and in the deep river well. At the Newman site, the water level in the deep land well on the east side is lower than that on the west side but higher than the water level in the deep river well. Based on local water-level data only, significant east-side pumping and flow underneath the San Joaquin River from west to east is evident at the Crows Landing and Patterson sites and to a lesser extent at the Newman site.

Regional evidence suggesting that ground-water pumping from the unconfined zone takes place primarily on the east side of the river includes regional water-table data and the results from previous studies. As described earlier, there is a large cone of depression east of the ground-water divide northeast of the study reach. There is no corresponding feature on the west side of the valley. This holds true throughout the central and northern San Joaquin Valley with the exception of a linear trough adjacent to the Coast Ranges in the central part of the western valley, which is thought to be related to pumping in the confined zone (Belitz and Heimes, 1990).

Belitz and Heimes (1990) also concluded that there is flow across the valley trough toward eastern pumping centers in the central part of the valley. This general pattern of water flowing from west to east underneath the San Joaquin River has two major implications: (1) water that would naturally discharge to the San Joaquin River is being diverted and (2) water that originated on the west side of the valley, which under natural conditions would not cross the San Joaquin River to any great extent, is being transported to the east side of the valley.

ESTIMATION OF GROUND-WATER INFLOW USING GROUND-WATER-FLOW MODELS

Two-dimensional steady-state ground-water-flow models were created to estimate ground-water inflow to the San Joaquin River at each of the study sites. The three models were constructed using the U.S. Geological Survey modular three-dimensional finite-difference ground-water-flow model (McDonald and Harbaugh, 1988). These flow models represent vertical cross sections oriented perpendicular to the river near the Newman, Crows Landing, and Patterson sites. The approach is similar to that taken in a previous study to estimate ground-water return flow to the lower Colorado River (Loeltz and Leake, 1983).

The three-dimensional flow equation used in the model was altered by setting the dimension parallel to the San Joaquin River to unity (1 ft). The resulting two-dimensional ground-water-flow equation for steady-state flow in an anisotropic medium can be written as follows:

$$\frac{\partial}{\partial x}(K_H\frac{\partial h}{\partial x})+\frac{\partial}{\partial z}(K_V\frac{\partial h}{\partial z}) = 0, \qquad (1)$$

where

h = hydraulic head (L);
K_H = horizontal hydraulic conductivity (L/t);
K_V = vertical hydraulic conductivity (L/t); and
x,z = cartesian coordinates.

MODEL GEOMETRY AND BOUNDARY CONDITIONS

The size and discretization of the model grid are identical for each of the three sites. The model cross section is about 0.67 mi wide and 180 ft deep (fig. 11). The San Joaquin River is at the midpoint of the grid and is approximated by a block of cells 160 ft wide by 6 ft deep. These dimensions are based on approximate measurements of river width and measured depth profiles. The model grid is divided horizontally into a total of 32 columns, 16 on each side of the river midpoint. Horizontal cell dimensions are a minimum of 20 ft wide, periodically increasing in width with distance from the river. The grid is divided vertically into 20 layers of variable thickness. Layers 1-5, 6-8, 9-17, and 18-20 are 3, 5, 10, and 20 ft thick, respectively.

The types of boundary conditions are identical for all three models (fig. 11). The vertical sides of the cross section perpendicular to the river are no-flow boundaries. These boundaries are based on the assumption that flow is parallel to the cross section. The water-table map presented in figure 5 shows that this is a reasonable assumption, although small-scale flow patterns may exist near the river. The lower boundary also is a no-flow boundary and is delineated by the contact between the Sierran sand and the Corcoran Clay Member.

Specified-head cells with high hydraulic conductivity are used to simulate the San Joaquin River, which is the central part of the upper boundary. The effect of accumulated riverbed sediments on hydraulic conductivity is assumed to be negligible, and the aquifer interacts directly with the river. This is believed to be a reasonable assumption because during river well installation, it was observed that the river bottom was sandy and that the jetwash was sandy for at least the first 5 ft below the riverbed. The remainder of the upper boundary consists of a water-table surface on each side of the river. The water table is allowed to vary as a function of head.

The east and west model faces are specified-flux boundaries, which are used for simulating the effects of ground-water recharge and discharge (pumpage) outside the model boundaries. Specifying recharge and discharge only at the east and west boundaries neglects the occurrence of these processes within 0.34 mi of the river, even though local irrigation takes place at some sites (table 2). This assumption is believed to be justified because 0.34 mi represents a maximum of 6 percent of the distance between the valley walls and the valley trough in the study area; therefore, a maximum of 6 percent of the area in which recharge and discharge may occur is neglected.

Recharge to the model cross section was applied to the east and west boundaries and distributed in amounts proportional to the transmissivity of each model layer, ensuring horizontal flow under homogeneous isotropic conditions. Recharge allocated to the west side was applied to all model layers; however, recharge allocated to the east side was applied only to the top one-half of the eastern boundary. The lower one-half of the eastern boundary was used to specify discharge from the model cross section in the form of ground-water withdrawal for agricultural use. As

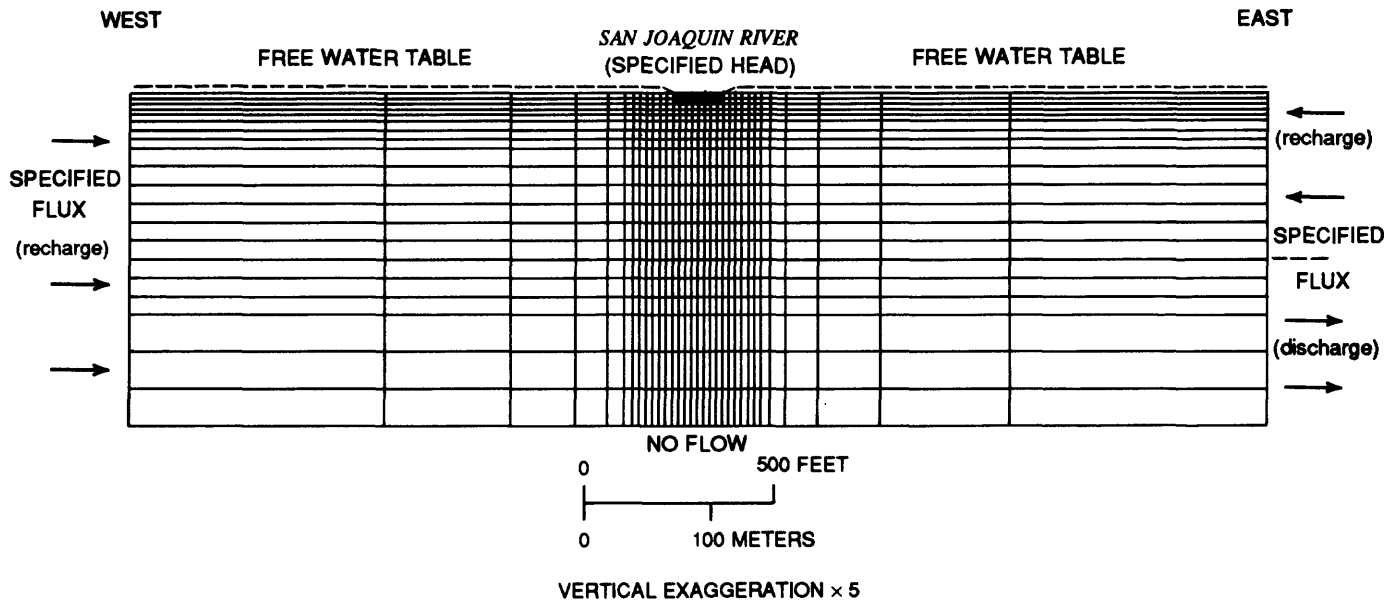

Figure 11. Dimensions and discretization of the model grid, and specification of the boundary conditions.

discussed earlier, ground-water pumping from the unconfined zone is believed to be primarily on the east side of the river. Pumpage, like recharge, was distributed in amounts proportional to the transmissivity of each model layer. The lower one-half of the boundary was designated for pumpage because screening production wells in the lower parts of the unconfined aquifer is a common practice in the study area.

The decision to position the lateral model boundaries 0.34 mi from the river, as opposed to extending them to the natural flow boundaries, was based on several factors. First, the natural flow boundaries are not clearly defined, particularly east of the river. The ground-water divide certainly acts as a recharge divide, as recharge is applied from above, but probably does not act as a discharge divide because heavy pumping east of the divide probably induces eastward flow across the divide at greater depths in the unconfined zone. Second, the distribution of pumping in the area between the ground-water divide and the river is unknown, except that analysis of hourly water-level data showed definite pumping cycles that probably were related to the pumping of local wells. If the boundaries were extended farther from the river, this unknown pumpage would have to be included explicitly in the model. Finally, positioning the lateral model boundaries close to the river provides a sensitive boundary condition that can be used qualitatively during model calibration.

ESTIMATION OF MODEL PARAMETERS

Values of model parameters were either estimated or calibrated. Horizontal hydraulic conductivity was estimated from results of analysis of slug-test data. Vertical hydraulic conductivity was determined through model calibration, given various conceptual models for the distribution of aquifer materials controlling vertical flow. Recharge and discharge at the east and west boundaries also were calibrated on the basis of specific assumptions about the distribution of each.

Slug tests were conducted in 10 of the 22 observation wells to estimate horizontal hydraulic conductivity. River wells were not tested because of the uncertainty in determining an effective horizontal screened interval for an open-ended pipe. Water-table wells also are not suitable for slug-test analysis. The 10 wells tested are screened in the Sierran sand. Both forward (slug) and reverse (bail) tests were done using an impermeable object as a displacement device. The data from these tests were interpreted

using the method of Cooper and others (1967) as expanded by Papadopulos and others (1973). Data from six of the wells were readily interpreted using this methodology, and the results are presented in table 3. The median value for horizontal hydraulic conductivity of 2.0×10^{-3} ft/s was used for all the models. The data from the four remaining wells show oscillatory behavior caused by inertial effects (fig. 12). Kipp (1985) presented a method for interpreting this type of data, but these data were not analyzed for this study.

Vertical hydraulic conductivity was determined by calibration on the basis of three conceptual models for the distribution of aquifer materials that control vertical flow. The following conceptual models were considered: (1) isotropic homogeneous, (2) anisotropic, and (3) single layer. In the isotropic homogeneous model, horizontal and vertical hydraulic conductivities were assumed to be identical. In the anisotropic model, a constant horizontal-to-vertical anisotropy was assigned to the entire cross section. The single layer, or layered model, is identical to the isotropic homogeneous model, with the exception of a single 5-ft thick layer of relatively low hydraulic conductivity. This low-conductivity model layer is continuous, within 30 ft of the land surface, and conceptually represents fine-grained flood-basin deposits. These conceptual models are not intended to be accurate representations of the observed lithology at each cross section. Instead, they represent a range of conditions that seems possible based on the limited amount of lithologic data collected.

Table 3. Estimated horizontal hydraulic conductivities of the Sierran sand from analysis of slug- and bail-test data

[ft/s, foot per second; --, no data]

Well identifier (see table 1)	Horizontal hydraulic conductivity (ft/s)	
	Slug test	Bail test
NW-47.5	2.0×10^{-3}	1.5×10^{-3}
NE-35.5	2.0×10^{-3}	1.7×10^{-3}
NE-107.5	6.9×10^{-5}	--
CW-18.2	3.5×10^{-3}	2.8×10^{-3}
CE-107.5	9.3×10^{-4}	1.2×10^{-3}
PW-22.5	4.6×10^{-3}	2.8×10^{-3}

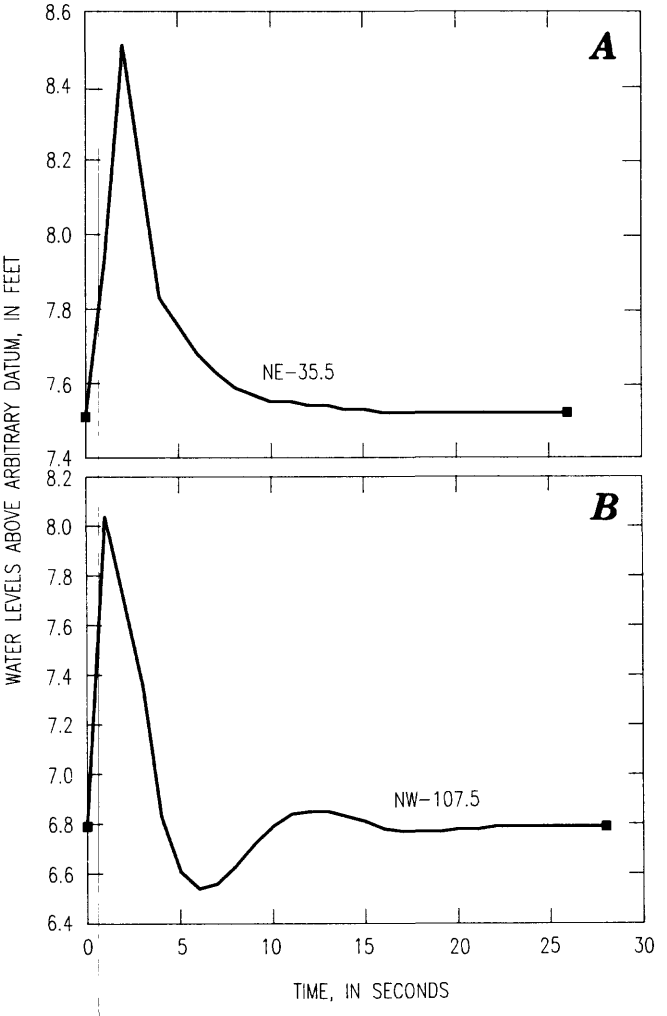

Figure 12. Measured water levels over time. *A*, Normal slug test. *B*, Slug test influenced by inertial effects.

The quantities of total recharge entering the model cross sections were calibrated. The division of total recharge into quantities entering the eastern and western model boundaries was calculated on the basis of the assumption of a constant areal recharge rate along flowlines connecting the three sites with the flow boundaries to the east and west. Thus, the length of each of these flowlines is proportional to the recharge area on the east and west sides of each site. At all sites, the natural flow boundary to the west is closer than that to the east. The quantity of recharge entering the western boundary was estimated to be 43, 37, and 34 percent of the total for the Newman, Crows Landing, and Patterson models, respectively. As discussed earlier, discharge by ground-water pumping was calibrated on the basis of the assumption that pumping in the unconfined zone takes place primarily east of the San Joaquin River.

CALIBRATION AND SENSITIVITY

Cross-sectional models of the Newman, Crows Landing, and Patterson sites were tested using the three conceptual models for the distribution of materials controlling vertical flow. Model calibration was conducted in two steps. The first step was a trial-and-error process that yielded calibrated versions of each conceptual model that was capable of producing a reasonable hydraulic head distribution. The second step was systematic alteration of values of calibrated model parameters to determine the uniqueness of the solutions and the sensitivity of the calibrated models to changes in these parameters. Additional testing determined the sensitivity of the calibrated models to noncalibrated parameters.

CALIBRATION CRITERIA

Water levels measured in observation wells and river stages recorded at the study sites were used to calibrate each of the three models. The error between the measured water levels and simulated hydraulic heads served as a calibration criterion. Steady-state hydraulic heads were approximated by the median values of weekly water-level measurements from October 1988 through August 1989. For modeling purposes, the median river stage was subtracted from each of the median water levels in observation wells, thus changing the baseline from sea level to river stage. The resulting values are presented on the cross sections in figure 13.

Four of the values shown in figure 13 were not used quantitatively during model calibration. Two shallow land wells probably are affected by local sources of recharge not accounted for in the models: NW-14.5 on the west side of the Newman site and CE-19.5 on the east side of the Crows Landing site. The west side of the Newman site is adjacent to an irrigated field bordered by a ditch. This ditch was often full of water during and after periods of irrigation. At the Crows Landing site, a small pond is about 20 ft from the shallow observation well. This pond is used as an overflow disposal area and was full during most of the study period.

The remaining two values not used quantitatively during calibration are those in the deep river wells at the Newman and Crows Landing sites. Slug tests were done in these wells to confirm that the wells were completed in the flood-basin deposits rather than the Sierran sand as originally interpreted from lithologic logs (table 8). The values of hydraulic conductivity interpreted from the slug-test data from the river wells, which are open-ended pipes, were used for comparison purposes only. The results for the deep river well at the Patterson site, which was believed to be within the Sierran sand, were 100 times higher than those for the deep river well at the Crows Landing site. This was considered to be sufficient evidence that the well at Crows Landing is not in the Sierran sand. The deep river well at the Newman site is physically difficult to test, but the stratigraphic relations shown in figure 4 suggest that the well is not deep enough to have reached the Sierran sand.

MODEL CALIBRATION--STEP 1

In the first step of calibration, models representing the isotropic homogeneous, anisotropic, and layered conceptual models for all three cross sections were calibrated by trial and error. Vertical hydraulic conductivity, recharge, and pumpage were varied until the solution best matched measured conditions. The primary measure of model fit was the quantitative comparison of measured water levels and simulated hydraulic heads using the root mean square error (RMSE). Qualitative measures of model fit also were used because two different sets of parameters would sometimes yield similar RMSE but different hydraulic head distributions. The differences were often apparent on comparison of the simulated water-table altitudes at the east and west boundaries. For example, solutions were rejected if the water table at the eastern boundary was below the river stage because this constitutes a large-scale depression in the water table for which there is no supporting evidence. Other similar qualitative criteria were used in selecting the best model.

The calibrated anisotropic and layered models for all three cross sections produced solutions that matched measured water levels reasonably well. Table 4 shows the median measured water level above river stage for each observation well and the corresponding simulated values for the anisotropic and layered models. For the Newman and Crows Landing layered models, simulated values immediately above and below the low-conductivity layer are included for the deep river wells because the wells are believed to be in the flood-basin deposits. The isotropic homogeneous model is not included in the table because it failed to produce substantial hydraulic gradients and consequently failed to produce reasonable distributions of hydraulic head.

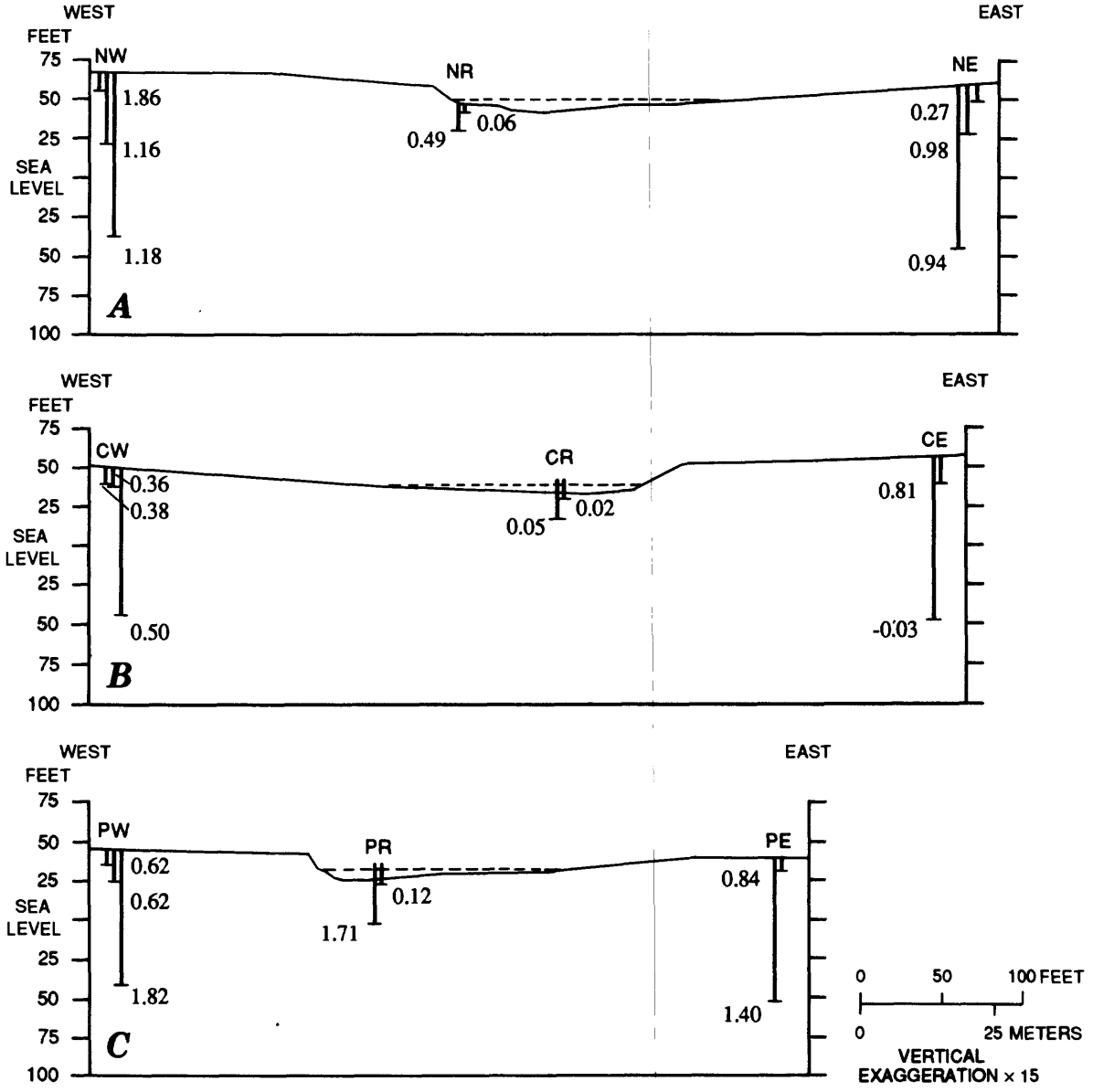

EXPLANATION

——— LAND SURFACE--Approximately located between cluster sites

- - - - - SAN JOAQUIN RIVER--Approximately located

PR
0.12
1.71

CLUSTER SITE--Site at which two or more observation wells are installed at different depths. See table 1 for explanation of cluster site name and location

MIDPOINT OF 5-FOOT SCREENED INTERVAL OF INDIVIDUAL LAND WELL OR TOTAL DEPTH OF RIVER WELL--Number is median weekly water level, in feet above or below (-) median weekly river stage

Figure 13. Median weekly water levels in observation wells relative to the median weekly river stage. *A*, Newman site. *B*, Crows Landing site. *C*, Patterson site.

Table 4. Measured water levels and simulated hydraulic heads above river stage for each observation well for the anisotropic and layered models of each cluster site

Cluster site name	Well identifier (see table 1)	Median measured water levels, in feet above river stage	Hydraulic head, in feet above river stage	
			Simulated by anisotropic model	Simulated by layered model
Newman (N)	NW-14.5[1]	1.86	0.74	0.46
	NW-47.5	1.16	1.00	1.12
	NW-107.5	1.18	1.29	1.12
	NR-7.0	.06	.30	0.01
	NR-20.0[1]	.49	.61	[2]0.02/1.02
	NE-14.5	.27	.44	0.27
	NE-35.5	.98	.73	0.94
	NE-107.5	.94	.94	0.94
Crows Landing (C)	CW-12.8	.38	.39	0.38
	CW-18.2	.36	.40	0.38
	CW-97.7	.50	.55	0.78
	CR-5.0	.02	.08	0.00
	CR-20.0[1]	.05	.20	[2]0.00/0.30
	CE-19.5[1]	.81	.10	0.06
	CE-107.5	-.03	.00	-0.13
Patterson (P)	PW-11.5	.62	.59	0.59
	PW-22.5	.62	.87	0.59
	PW-89.0	1.82	1.79	1.85
	PR-5.0	.12	.62	0.01
	PR-30.7	1.71	1.55	1.66
	PE-9.5	.84	.81	0.40
	PE-98.3	1.40	1.51	1.43

[1]Well was not used quantitatively during calibration.
[2]Simulated values above/below the low-conductivity layer.

The values in table 4 show that the layered models match measured values better than the anisotropic models at the Newman and Patterson sites but that neither model is clearly superior at the Crows Landing site. Note that the results of the layered and anisotropic models often complement each other. For example, the layered model reproduces measured water levels at the Patterson west side and river locations far better than does the anisotropic model. The anisotropic model produces superior results for the east side of the river at the Patterson site.

MODEL CALIBRATION--STEP 2

In the second step of calibration, the uniqueness of the calibrated solutions for each of the cross-section models was tested. Values of recharge and vertical hydraulic conductivity were varied systematically lower and higher than those of the calibrated solutions. These parameters were varied by amounts large enough to ensure that the calibrated model was bounded by inferior solutions but small enough to remain within a range of physically reasonable values.

Recharge was altered by a factor of 2 and vertical hydraulic conductivity by a factor of 3. For a given combination of recharge and vertical hydraulic conductivity, discharge at the eastern model boundary was adjusted until the measured water level in the deep eastern well was matched. The resulting distribution of hydraulic head was compared with measured water levels, and the RMSE was calculated. Figure 14 is a summary of the results. The center of each 3×3 grid represents the calibrated solution for a given site and conceptual model. The eight surrounding squares in each grid represent solutions resulting from systematic changes in recharge and (or) vertical hydraulic conductivity and the associated change in pumping. The RMSE for each solution is shown in the upper left-hand corner of each square.

All the original calibrated solutions in figure 14 are associated with relatively low values of RMSE. Some of the surrounding solutions have slightly lower RMSE than that of the associated calibrated solution. Through qualitative assessment of hydraulic head distributions, all these solutions were determined to be inferior. Most of these solutions were ruled out on the basis of the simulated values at the lateral boundaries, often because the water table at the eastern boundary was lower than the river stage. Thus, through the use of quantitative and qualitative measures, each of the calibrated model formulations was determined to be superior to the surrounding solutions.

MODEL SENSITIVITY

The sensitivity of the models to calibrated parameters was determined during calibration. The results in figure 14 show the sensitivity of simulated hydraulic heads and ground-water inflow to changes in the calibrated parameters. The differences between measured water levels and simulated hydraulic heads, which are represented by the RMSE, are clearly sensitive to the calibrated parameters. Ground-water inflow also is sensitive to the calibrated parameters but generally remains within a factor of 2 of the value simulated by the calibrated model even though parameter values were varied widely.

The sensitivity of the model to noncalibrated parameters was tested by varying those parameters for the calibrated models only. The noncalibrated parameters are horizontal hydraulic conductivity, distribution of discharge at the eastern boundary, and distribution of recharge. Horizontal hydraulic conductivity has a one-to-one correspondence with flux. If, for example, the conductivity is doubled, the identical solution is obtained by doubling the fluxes; consequently, the value of horizontal hydraulic conductivity has a strong effect on the resulting value of ground-water inflow. The horizontal hydraulic conductivity used in the models was the median result from the analysis of slug- and bail-test data. The results ranged from 9.3×10^{-4} to 4.6×10^{-3} ft/s, excluding the slug test at NE-107.5, which was inexplicably low. This range of values suggests that the horizontal hydraulic conductivity used in the models (2.0×10^{-3} ft/s) and the resulting estimates of ground-water inflow could vary by a factor of about 2.

The sensitivity of the model to the distribution of pumping was tested by moving the discharge zone representing agricultural pumping from the lower one-half of the eastern boundary to a location that increases the effect of pumping on hydraulic head in the deep eastern well. This alternative pumping zone includes only the layer in which the deep eastern well is screened, which is 10 ft thick and extends from the cell adjacent to the deep eastern well to the eastern boundary. Given the initial conditions of the calibrated models, each model was run again with the appropriate alternative pumping zone. The quantity of pumpage was then adjusted until simulated hydraulic heads in the deep eastern wells matched the median measured water levels. This resulted in virtually no change in hydraulic head at the calibration points for all the models. Ground-water inflow increased by 130 percent for the Crows Landing layered model and varied less than 20 percent for the remaining models.

The sensitivity to changes in the distribution of recharge was tested by varying the percentage of total recharge entering each side of the model cross sections by a factor of 2 upward and downward. Given the initial conditions of the calibrated models, the values of recharge and pumpage were adjusted for each recharge distribution until the best match between measured water levels and simulated hydraulic heads was achieved. The changes in the simulated hydraulic head distribution were minimal except for the Crows Landing layered model, which experienced the maximum change in ground-water inflow--an increase of 80 percent. Ground-water inflow for the other models changed by an average of 16 percent.

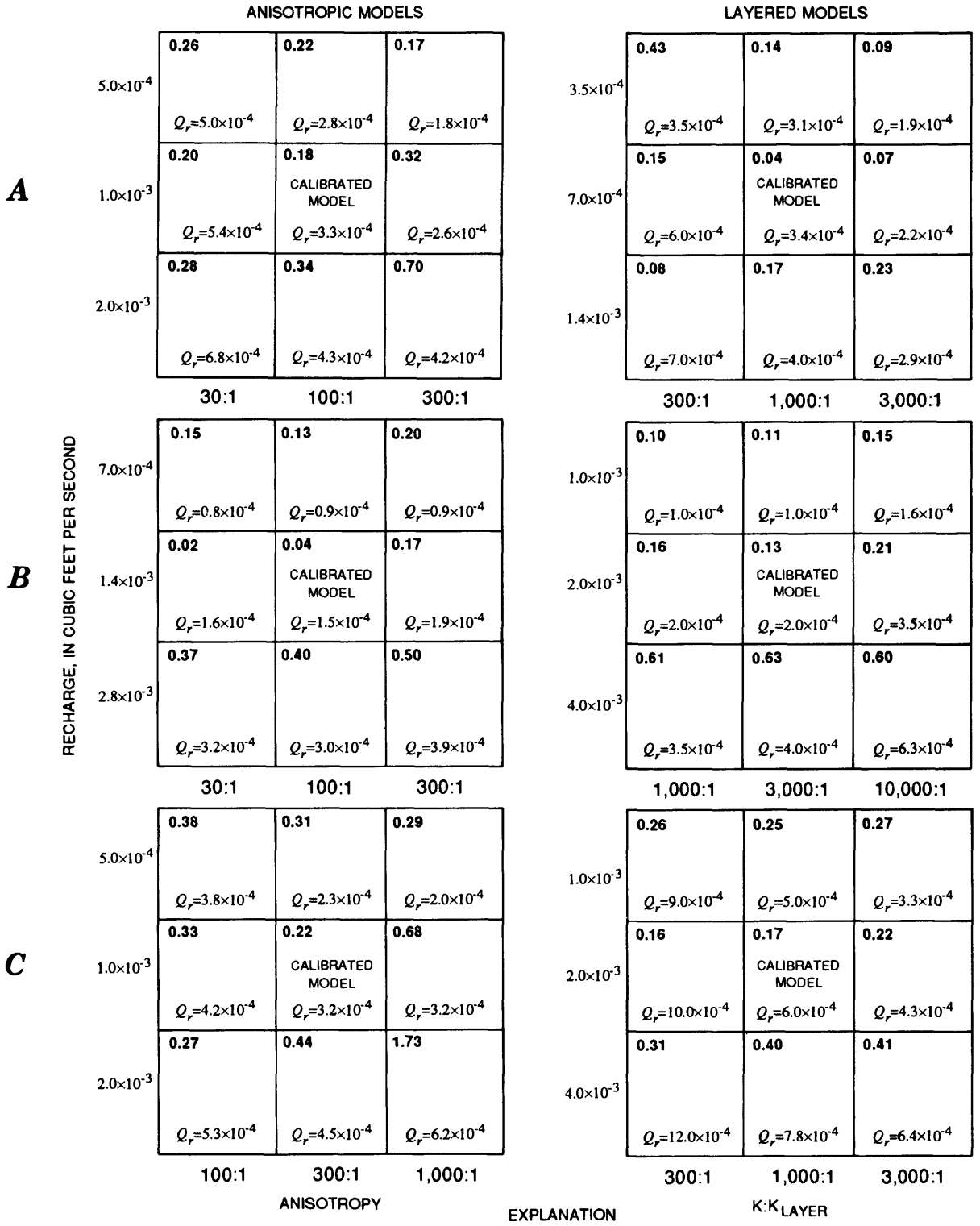

Figure 14. Summary of calibration results for anistropic and layered models. *A*, Newman site. *B*, Crows Landing site. *C*, Patterson site.

The Crows Landing layered model is clearly the most sensitive to changes in pumping and recharge. This sensitivity probably is a function of the relatively high pumping rates required to maintain the downward hydraulic gradient on the east side.

MODEL RESULTS

The results of the calibrated models are shown in figure 15 as simplified flow nets indicating general directions of ground-water flow. These flow directions are consistent with the general trends of the hydraulic gradients noted earlier. Simulated shallow horizontal flow is toward the river, and simulated vertical flow beneath the river is upward. Recall that the calculated horizontal gradients between the deep land wells suggested that there was a component of flow from west to east across the valley trough, particularly at the Crows Landing site. The model results suggest that eastward flow across the valley trough occurs at all three sites and is a substantial component of flow.

Calibrated formulations of the anisotropic and layered models for all three cross sections yielded reasonable results. However, the isotropic homogeneous model did not prove to be conceptually valid because it failed to produce substantial hydraulic gradients. The failure of the isotropic homogeneous model indicates that the existing vertical hydraulic gradients cannot be explained by the convergence of flowlines toward the river. Although some fraction of the existing gradients may be attributed to convergence, resistance to vertical flow is greater than the resistance to horizontal flow.

None of the conceptual models for the distribution of materials controlling vertical flow produce simulated hydraulic heads that match the measured water levels at all the measuring points. For a given cross section, the anisotropic and layered models reproduce the hydraulic head distribution in parts of the system and do poorly in others. Where one conceptual model does poorly the other often does well, suggesting that the real system may be some combination of the two simplified models. The best estimate of ground-water inflow to the river, therefore, may be some value between those simulated by the anisotropic and layered models. Table 5 shows ground-water inflow to the San Joaquin River for all calibrated models. If the hydrogeology at the three cross sections is representative of conditions along the entire reach, the average simulated ground-water inflow calculated from all the model results [1.7 $(ft^3/s)/mi$] also is representative of the reach.

The assumption that the hydrogeology at the three cross sections is representative of conditions along the entire reach may cause error in estimates of ground-water inflow to the reach. This is because the three cross sections are oriented parallel to the direction of regional ground-water flow, and a significant proportion of the river is oriented at an oblique angle to regional flow. The maximum overestimation of ground-water inflow would be about 50 percent based on the difference between the actual length of the reach and the length of a smooth curve following the general course of the river.

Sensitivity analyses of the six calibrated models showed that, with respect to the calibrated parameters, ground-water inflow for a given model generally is bounded within a factor of 2. The sensitivity with respect to the noncalibrated parameters was minimal, with the exception of the horizontal hydraulic conductivity, which may vary by a factor of 2 based on the range of results from the analysis of slug-test data from direct measurements at the study sites. Results from similar tests south of the study area in eight wells within Sierran sand, ranging in depth from 65 to 570 ft, show an average hydraulic conductivity of 1.2×10^{-3} ft/s (Phillips and Belitz, 1990). This value compares well with the median of results from slug and bail tests at the study sites (2.0×10^{-3} ft/s).

The regional-scale water-budget model for a 60-mile reach of the river (Kratzer and others, 1987; Rashmawi and others, 1989) produced average values of ground-water inflow for the San Joaquin River by river mile for 1979, 1981, 1982, 1984, and 1985. Based on the calibrated water-budget model, the average value of ground-water inflow for the 19-mile reach was about 2.0 $(ft^3/s)/mi$, which compares well with the average result from the six calibrated models developed in this study [1.7 $(ft^3/s)/mi$].

The average rate of recharge for the six calibrated models is 1.35×10^{-3} $(ft^3/s)/ft$, and the average rate of pumpage is 1.02×10^{-3} $(ft^3/s)/ft$. On the basis of the assumption that the three sites are representative of the 19-mile reach, the average estimated rates of recharge and pumpage along the reach are 7.1 and 5.4 $(ft^3/s)/mi$, respectively. A comparison of these values

Table 5. Simulated ground-water inflow to the San Joaquin River using the anisotropic and layered models

[$(ft^3/s)/mi$, cubic foot per second per mile]

Cluster site name	Simulated ground-water inflow [$(ft^3/s)/mi$]	
	Anistropic model	Layered model
Newman	1.7	1.8
Crows Landing	.8	1.1
Patterson	1.7	3.2
Average	1.4	2.0

indicates that, on average, about 76 percent of ground water entering the model cross sections is discharged through agricultural pumping and the remaining 24 percent is discharged into the river. These values indicate that the rate of agricultural pumping can have a strong effect on the rate of ground-water inflow.

The average simulated recharge and pumping rates for the study area can be compared, in a general sense, to estimated values from a previous study in the central part of the western San Joaquin Valley. A water-budget approach was used to estimate average 1980 areal recharge and pumpage rates of 0.74 and 0.47 ft/yr, respectively (J.M. Gronberg and Kenneth Belitz, U.S. Geological Survey, oral commun., 1990). Surface-water deliveries and climate were considered as average in 1980. Conversion of the average simulated volumetric recharge and pumping rates for the six calibrated models to average areal rates required estimation of the area over which recharge and pumping take place. This area is defined on the north and south by parallel flowlines east and west of the river between the endpoints of the reach and the flow boundaries and on the east and west by the natural flow boundaries. The distance between the Newman and Patterson sites is about 11.5 mi. Recharge is distributed over the distance between the Coast Ranges and the ground-water divide, which averages about 18 mi, and pumping is distributed over the distance between the river and the ground-water divide, which averages about 12 mi. The resulting conversion of the simulation results for the six calibrated models yields average areal recharge and pumping rates of 0.75 and 0.86 ft/yr, respectively. The recharge rates compare well, but the pumping rate estimated in this study is almost double that in the previous study. Several possible explanations for the higher pumping rate are: (1) drought conditions have resulted in higher demand for ground water for irrigation purposes; (2) there may be a heavier reliance on ground water on the east side of the valley compared with the west; and (3) the area over which pumping is distributed may have been underestimated, as pumping east of the ground-water divide probably induces eastward flow across the divide.

The calibrated models can be used to estimate the percentage of ground-water inflow coming from various locations in the unconfined zone, and ultimately, the quality of ground water entering the river. For these estimates, the layered models were used. The layered configuration is convenient for flux computations, probably is a better lithologic analogue than the anisotropic configuration, and the average RMSE for the layered models (0.11) is lower than that for the anisotropic models (0.15). The average ground-water inflow for the layered models [2.0 $(ft^3/s)/mi$] is only 18 percent greater than the average for all six models [1.7 $(ft^3/s)/mi$]. Given the layered configuration, three distinct parts of the flow system contribute to the total ground-water inflow to the river: the shallow parts east and west of the river and the deep part beneath the layer. The percentage of ground-water inflow coming from each part of the flow system was estimated by analyzing the flux output from the calibrated layered model for each site (table 6). Combined with ground-water chemistry data, these percentages can be used to estimate the quality of ground water entering the San Joaquin River.

Table 6. Estimated percentage of ground-water inflow coming from the deep and shallow parts of the unconfined flow system at the cluster sites, using the layered models

Cluster site name	Estimated percentage of ground-water inflow from parts of the unconfined flow system		
	Deep	Shallow west	Shallow east
Newman	74	13	13
Crows Landing	27	63	10
Patterson	67	17	16

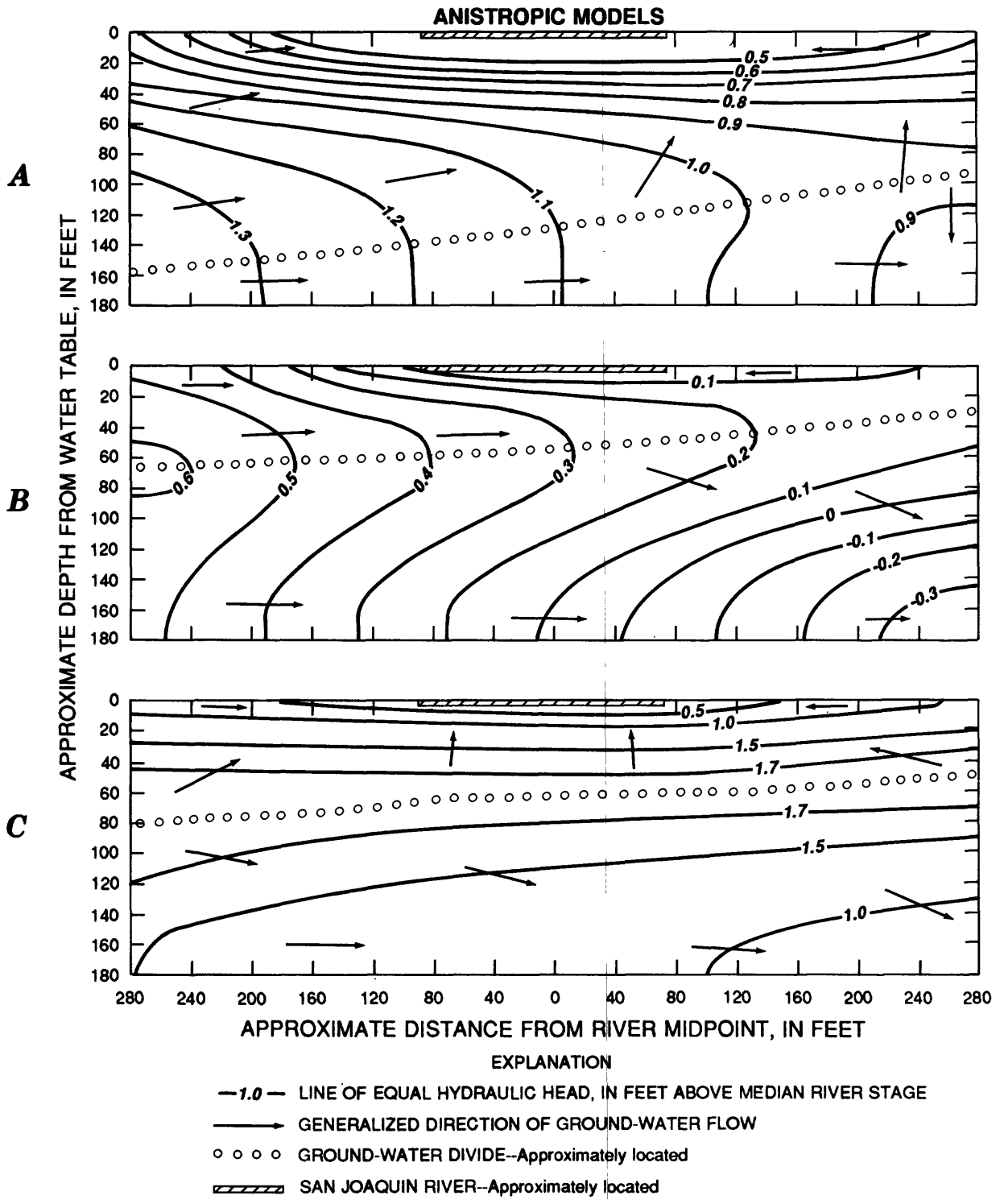

Figure 15. General directions of ground-water flow for the six calibrated solutions. *A*, Newman site. *B*, Crows Landing site. *C*, Patterson site.

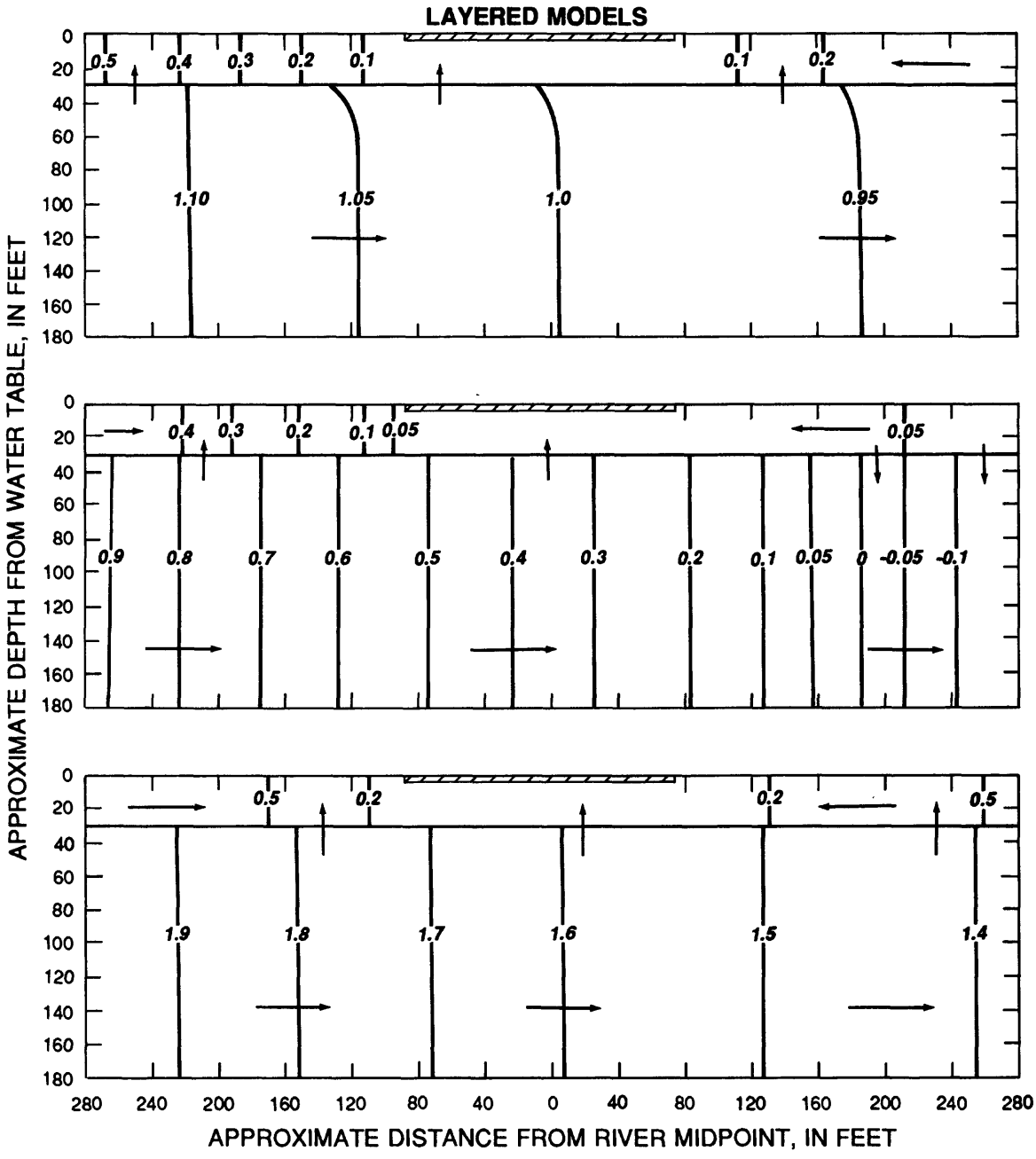

Figure 15. Continued.

ESTIMATION OF GROUND-WATER INFLOW USING WATER BALANCE

Ground-water inflow to the study reach was estimated using water-balance computations based on flow measurements made in all tributaries, canals, inflow pipes, and withdrawal pumps between the Newman and Patterson study sites. Streamflow and specific conductance were measured during two separate synoptic studies on October 28-29, 1986, (fig. 16*A*) and June 14, 1989 (fig. 16*B*).

For the 1986 synoptic study, the specific conductance of the San Joaquin River at Newman, where water from the Merced River has not completely mixed with the San Joaquin River, was measured in a discharge-weighted sample from the full cross section. For the 1989 synoptic study, specific conductance at the Newman site was determined from a monitor located downstream of the Newman site, where mixing of the rivers is complete; specific conductance data were not available for three small inflows near Crows Landing. These inflows were assumed to have the same specific conductance of river water at the Crows Landing site--1,538 µS/cm (microsiemens per centimeter at 25 degrees Celsius). Assuming no measurement error, no unmeasured surface-water inflows or withdrawals, and steady-flow conditions within the reach, the residual water resulting from the subtraction of all measured inflows to the study reach from the streamflow measured at Patterson, plus withdrawals, is an estimate of ground-water inflow. Sampling was done in October 1986 when the monthly mean streamflow was in the 60th percentile and in June 1989 during a low-flow period with a monthly mean streamflow in the 27th percentile of monthly means for 1975-89 (fig. 17).

Estimates of ground-water inflow to the San Joaquin River between Newman and Patterson were computed by:

$$Q_{gw} = Q_P - Q_N - \Sigma\, Q_{in} + \Sigma\, Q_{out}, \qquad (2)$$

where

Q_{gw} = ground-water inflow between the Newman and Patterson sites;

Q_P = river streamflow at the Patterson site;

Q_N = river streamflow at the Newman site;

$\Sigma\, Q_{in}$ = the sum of all inflows to the river between the Newman and Patterson sites; and

$\Sigma\, Q_{out}$ = the sum of all withdrawals of water from the river between the Newman and Patterson sites.

All flow values are in cubic feet per second.

Using equation 2 and values for streamflows, inflows, and withdrawals shown in figure 16*A*, ground-water inflow to the river was estimated to be 130 ± 69 ft^3/s during October 1986. The value of 69 ft^3/s is the standard error of the estimate at a 95-percent confidence interval based on the assumption that streamflows at Newman and Patterson were measured with a 5-percent standard error and all other flows with a 10-percent standard error. This inflow to the study reach is equivalent to an average of 6.7 ± 3.6 ft^3/s per river mile. Similar calculations for June 1989, using values for streamflows, inflows, and withdrawals shown in figure 16*B*, indicate 62 ± 41 ft^3/s of ground-water inflow. This inflow is equivalent to an average of 3.2 ± 2.1 (ft^3/s)/mi.

On the basis of estimated rates of ground-water inflow from the water-balance computations, the average salinity of ground water flowing into the river was estimated by a mass balance of dissolved solids using specific conductance. In the mass-balance computations, specific conductance was used as an indirect measure of dissolved-solids concentration. Although specific conductance is not in units of mass, it is linearly related to the concentration of dissolved solids in water and is frequently used as a measure of salinity. Because of the relatively constant linear relation between specific conductance and dissolved-solids concentration, specific conductance values can be used in water-mixing calculations in the same manner as for a nonreactive dissolved substance. Thus, the estimated contribution of a tributary source to the specific conductance of river water is equal to the product of tributary flow and specific conductance, divided by total riverflow.

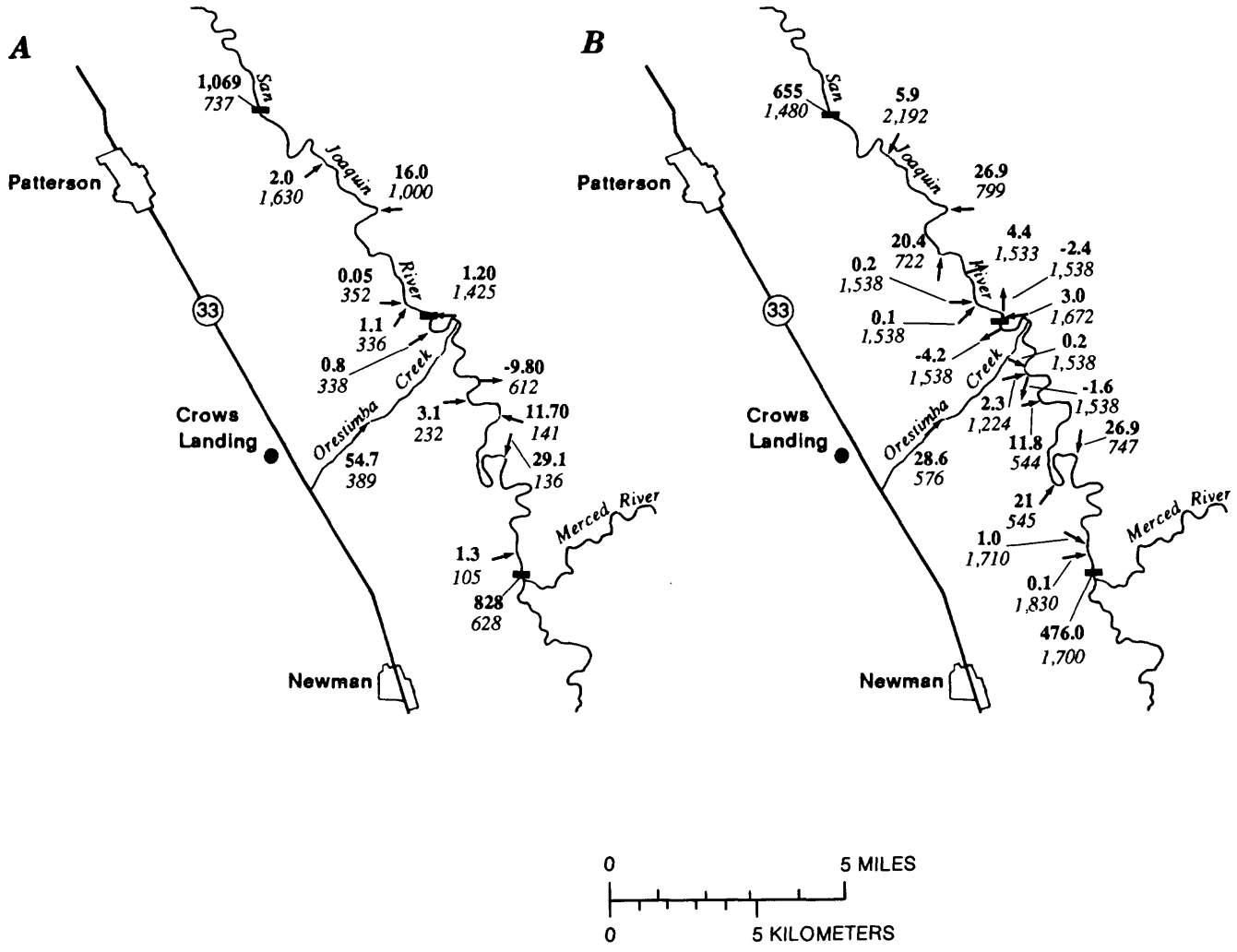

EXPLANATION

1.20
1,425 STREAMFLOW AND SPECIFIC CONDUCTANCE--**Top number** is streamflow, in cubic feet per second. Positive means flow into the reach; negative means flow out of the reach. *Bottom number* is specific conductance, in microsiemens per centimeter. Arrow indicates direction of flow

INSET FOR STUDY SITE--See figure 1

Figure 16. Streamflow and specific conductance in the San Joaquin River and its tributaries between Newman and Patterson for the water-balance synoptic studies. *A*, October 28-29, 1986. *B*, June 14, 1989.

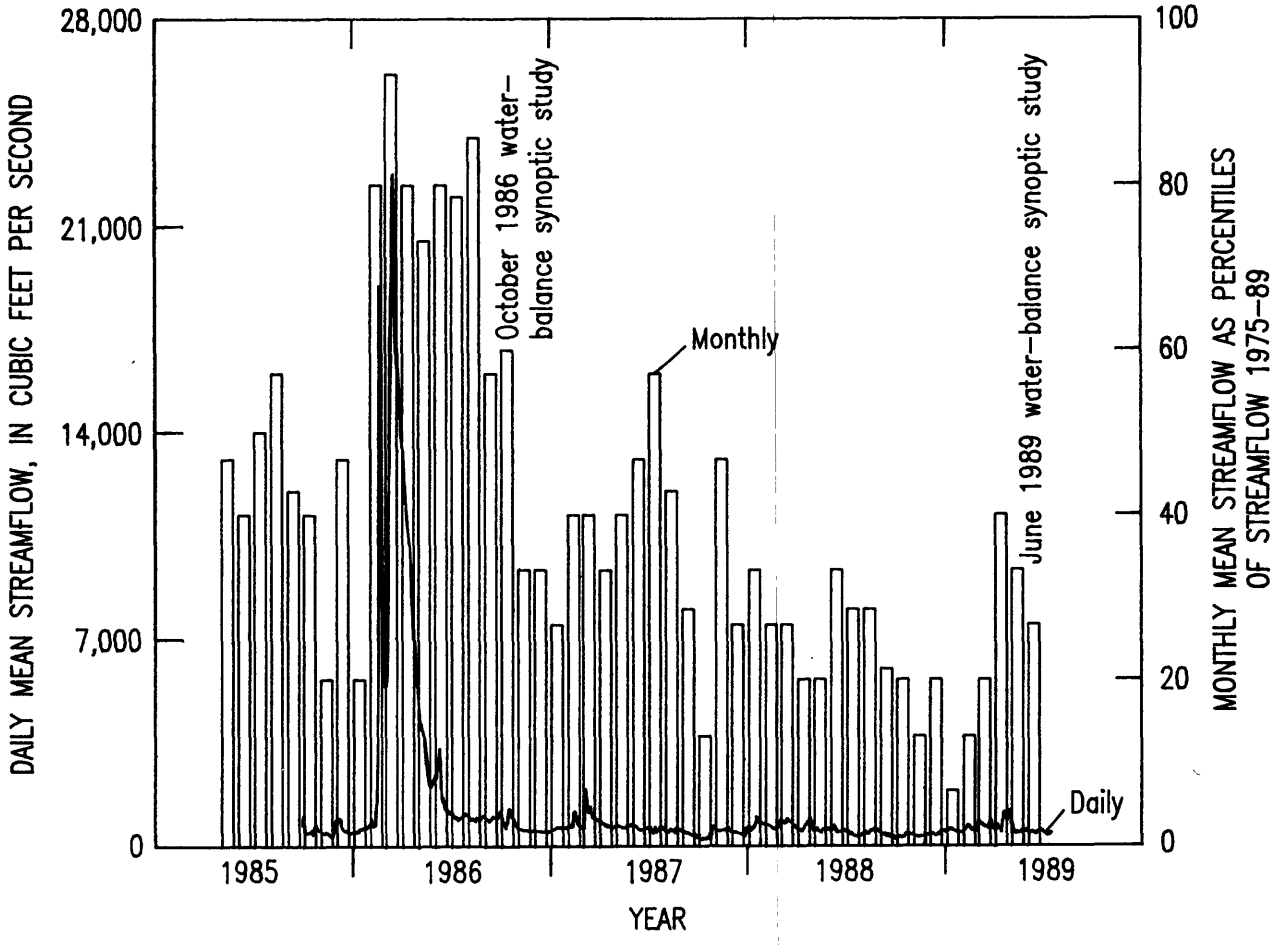

Figure 17. Daily mean streamflow at the Newman site compared with monthly mean streamflow as percentile of flows for the same month from 1975 to 1989.

The average specific conductance of ground water flowing into the river was computed by:

$$SC_{gw} = \frac{(SC_P \cdot Q_P) - (SC_N \cdot Q_N) - \Sigma(SC_{in} \cdot Q_{in}) + \Sigma(SC_{out} \cdot Q_{out})}{Q_{gw}} \quad (3)$$

where

SC_{gw} = specific conductance of ground water;

SC_P = specific conductance of river water at the Patterson site;

SC_N = specific conductance of river water at the Newman site;

$\Sigma(SC_{in} \cdot Q_{in})$ = sum of the products of specific conductance and flow for all inflows; and

$\Sigma(SC_{out} \cdot Q_{out})$ = sum of the products of specific conductance and flow for all withdrawals.

All other terms are as defined for equation 2; values of specific conductance are in microsiemens per centimeter at 25 degrees Celsius.

Using equation 3 and values for streamflows, inflows, and withdrawals shown in figure 16*A*, ground-water inflow to the river was estimated to have an average specific conductance of 1,730 ± 918 µS/cm during the October 1986 synoptic study. Similar calculations using values in figure 16*B* yield an estimate of 1,216 ± 804 µS/cm for June 1989. The standard errors were computed by assuming that all uncertainty was due to streamflow measurement. This approach may underestimate standard errors because of possible changes over time in tributary salinities during the study and uncertainty inherent in the measurement of specific conductance.

The ground-water inflows estimated from the October 1986 and June 1989 synoptic studies are reasonable in relation to the difference between San

Joaquin River flows measured at Newman and Patterson from 1986 to 1989 (fig. 18). At the time of both studies, ground-water inflow was a substantial component of the net gain in streamflow within this reach of river. The trend in within-reach gains in streamflow was downward during 1986-89, as drought conditions persisted. Seasonally, additions of water within the reach are greatest during the spring and summer irrigations.

The results of the water-balance calculations for the 1986 and 1989 synoptic studies indicate that ground-water inflow increases with increasing streamflow. As an increase in streamflow necessitates an increase in river stage, a greater increase in the ground-water system must occur for the ground-water inflow to increase. The peak of the 1986 flood was in February, about 6 months prior to the synoptic study (fig. 17). By October, the streamflow had

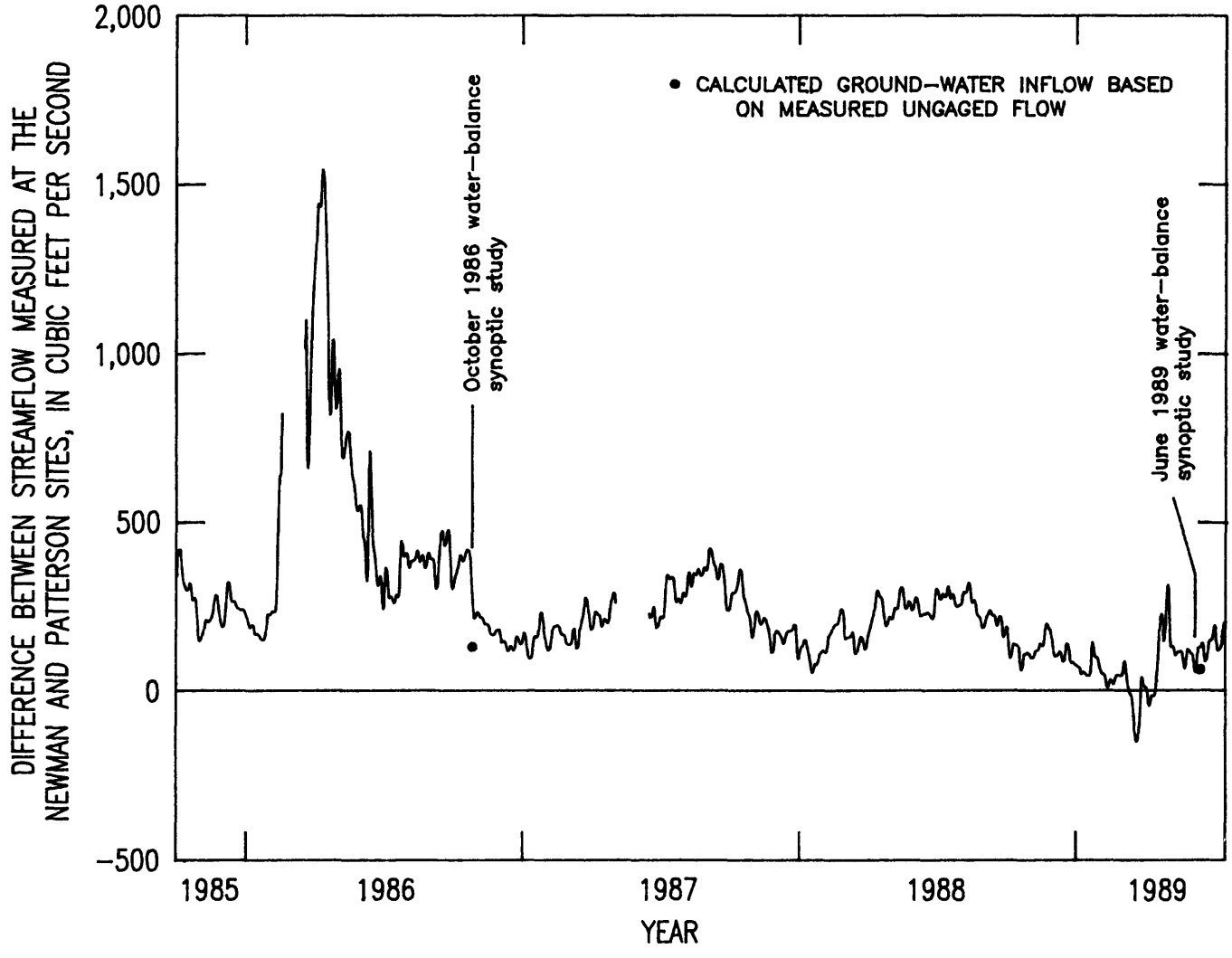

Figure 18. Difference between San Joaquin River flows measured at the Newman and Patterson sites from 1986 to 1989.

stabilized to about 880 ft^3/s, compared to about 500 ft^3/s during the 1989 synoptic study. The river stage at Newman was 49.78 ft during the 1986 study and 48.58 ft during the 1989 study for a difference of 1.2 ft.

Several factors could have caused relatively high water levels in the ground-water system in 1986:

(1) An abundance of irrigation water from surface-water sources in 1986, and shortages in 1989, may have resulted in differences in the total quantity of water applied during the two years;
(2) A low agricultural demand for ground water as a source of irrigation water in 1986 relative to 1989 may have resulted in lower pumping rates in 1986; and
(3) Infiltration of flood water over large areas in 1986 may have increased the hydraulic gradients toward the river.

If any combination of these factors resulted in a difference greater than 1.2 ft in water-table and (or) deep water levels, then ground-water inflow was greater in 1986 than in 1989, as the results of this study indicate.

CHEMICAL CHARACTER OF GROUND WATER

Ground-water inflow is a potential source of contaminants such as dissolved solids, selenium, boron, and molybdenum in the San Joaquin River (Kratzer and others, 1987). To evaluate the contribution of these contaminants to the river by ground water, an understanding is required of the chemical character of ground water in relation to the direction and magnitude of flow in different parts of the unconfined ground-water-flow system near the river. Ground water sampled at each study site was grouped into hydrochemical facies, each of which is believed to include ground water with a common origin and generally similar chemical characteristics. The distribution and characteristics of hydrochemical facies, combined with the analyses of the ground-water-flow system, provide the basis for estimating the chemical character of ground water flowing into the San Joaquin River.

HYDROCHEMICAL FACIES

The concept of hydrochemical facies, as described by Back (1966) and Hull (1984), is used to designate zones within a ground-water-flow system in which the water shares unique chemical characteristics. Ground water in each zone represents a hydrochemical facies that resulted from a particular combination of influences, such as lithology and mineralogy of aquifer sediments, flow patterns, and sources of recharge. The prefix hydro is used as a modifier of chemical to emphasize the interdependence of chemistry and hydrology. By considering ground water in relation to hydrochemical facies, the diverse chemical compositions of ground water near the San Joaquin River can better be understood in relation to factors governing composition, such as the sedimentary matrix holding the water and the sources of ground-water recharge.

Hydrochemical facies were determined by grouping ground water with similar chemical characteristics at each study site. Chemical characteristics of each sample analyzed for this study are in tables 9-12 (at back of report). Specific conductance was measured periodically in observation wells from November 1988 through August 1989; data for those wells with the most measurements are shown in figure 19. The steady nature of specific conductance over time implies that the temporal variability of ground-water chemistry is minimal.

Each hydrochemical facies at a particular site is believed to have ground water with a generally similar hydrologic history. The primary criteria used for grouping individual ground-water samples according to hydrochemical facies were stable-isotope composition and dissolved-solids concentration, selenium and boron concentrations, major-ion composition, and tritium distribution in relation to the simulated flow system.

STABLE ISOTOPES

Compositions of the stable isotopes of oxygen (oxygen-18) and hydrogen (deuterium) can be used as indicators to distinguish the source and evaporative history of water. Both oxygen and hydrogen isotopes are reported as ratios relative to the standard known

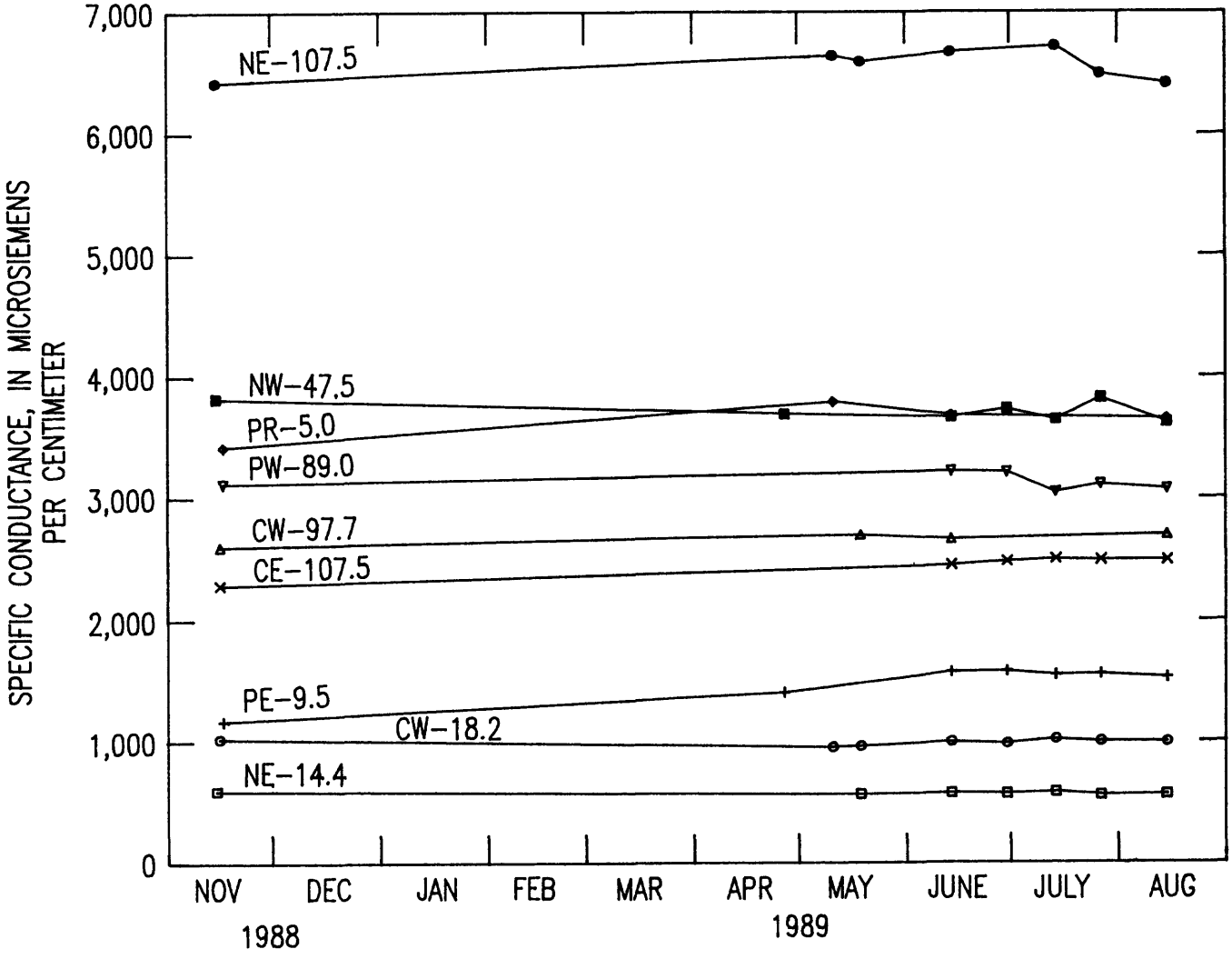

Figure 19. Measured specific conductance in selected observation wells. See table 1 for explanation of well identifier.

as Standard Mean Ocean Water (SMOW), in the per mil notation. The ratios of isotopes of oxygen and hydrogen in the vapor derived from seawater, the source of most precipitation, are relatively constant. However, as this vapor mass condenses and moisture precipitates, the heavier isotopes are removed in a greater proportion than the lighter isotopes. This process, known as isotopic fractionation, results in isotopic enrichment of precipitation and depletion of the vapor mass. The gradual depletion of heavy isotopes through repetitive rainfall as the vapor mass moves inland results in isotopic ratio values being more depleted inland than near coastal areas.

Oxygen-18 and deuterium are linearly correlated in precipitation with a slope similar to the Global Meteoric Water Line (Craig, 1961; Gat and Gonfiantini, 1981).

Biological processes, evaporation, freezing, and melting also contribute to isotopic fractionation (Freeze and Cherry, 1979). In particular, partial evaporation of water causes the ratio of deuterium to oxygen-18 to be lower than for precipitation because of greater enrichment in oxygen-18. When this occurs to varying degrees to water of similar origin, the slope of the relation between deuterium and

oxygen-18 is lower than the slope of the Global Meteoric Water Line. Figure 20 shows the relation between deuterium and oxygen-18 for all samples analyzed for this study. As a group, the range of values generally parallels the Global Meteoric Water Line, indicating relatively little evaporative concentration.

Under natural conditions in the San Joaquin Valley, recharge from Coast Ranges runoff was less depleted in oxygen-18 and deuterium than Sierra Nevada runoff, resulting in generally greater degrees of isotopic enrichment in native ground water of the western valley compared to the eastern valley. In places where evaporation occurred because of a shallow water table, oxygen-18 was further enriched. Davis and Coplen (1989) developed a general schematic showing deuterium levels in precipitation and runoff from the Coast Ranges to the Sierra Nevada (fig. 21). Table 7 shows oxygen-18 and deuterium compositions for imported irrigation water used in and around the study area (Delta-Mendota Canal and the California Aqueduct) and for the San Joaquin River at Patterson. Water at various positions in the ground-water-flow system near the river frequently is a variable mixture of water from these sources. For some samples collected during this study, the stable-isotope composition, combined with

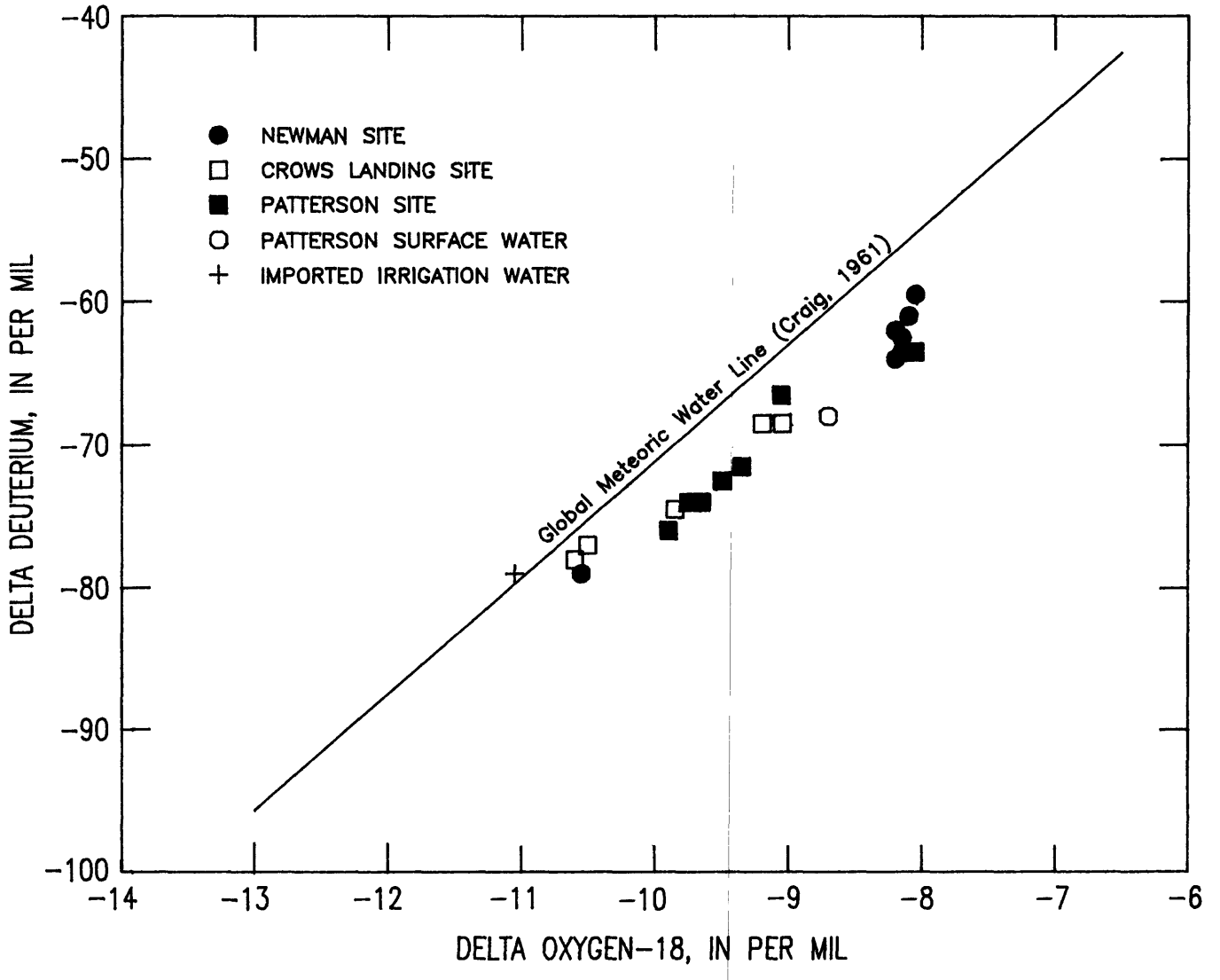

Figure 20. Relation between deuterium and oxygen-18 for all ground-water samples.

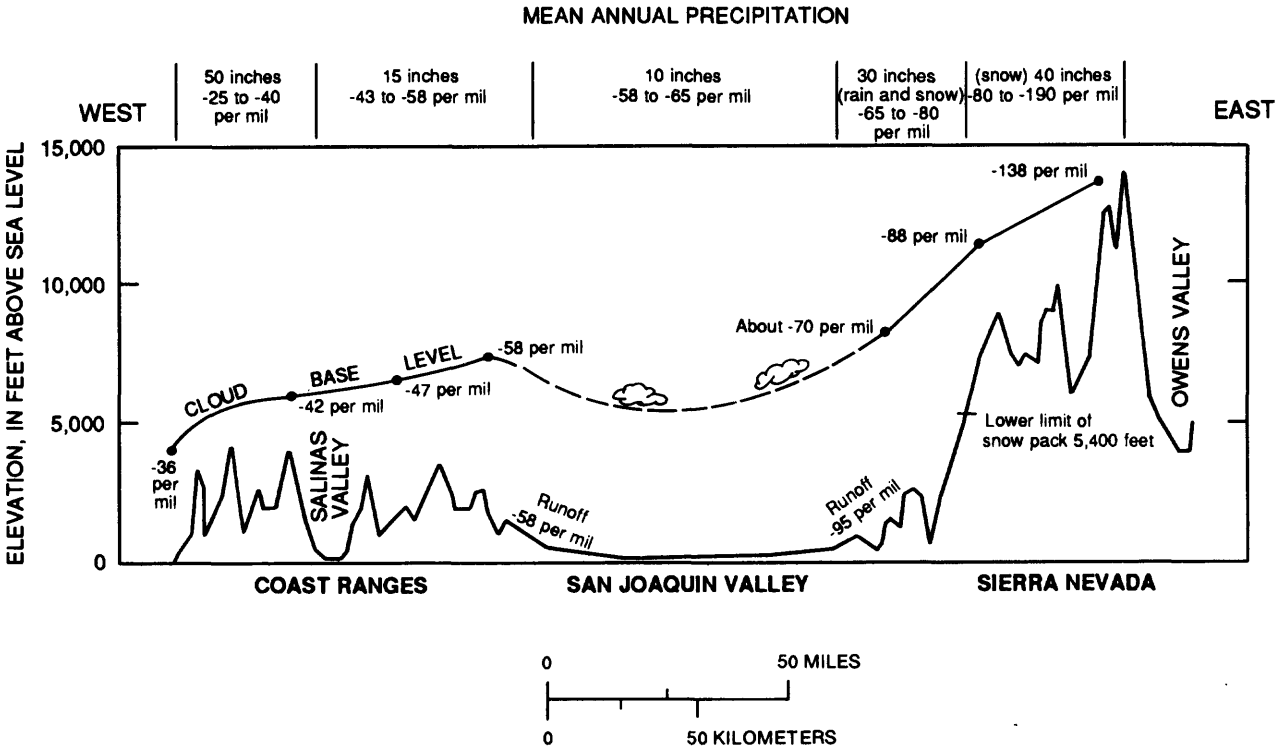

Figure 21. Modern meteorological model. Delta deuterium values are shown in per mil. Individual delta deuterium values shown above Coast Ranges are -36 per mil for Santa Maria precipitation, -42 per mil for Santa Clara Valley ground waters, -47 per mil for Hollister Valley ground waters, and -58 per mil for runoff from Coast Ranges to the San Joaquin Valley. Individual values shown above Sierra Nevada are about -70 per mil for Auburn precipitation, -88 per mil for Big Meadow snow core (7,595 feet), and -1.38 per mil for Bishop Pass snow core (11,205 feet). Modified from Davis and Coplen (1989).

Table 7. Stable-isotope composition of imported irrigation water

Source of water	Delta deuterium (per mil)	Delta oxygen-18 (per mil)
Delta-Mendota Canal[1]	-73.4	-9.80
California Aqueduct[1]	-71.8	-9.55
San Joaquin River at Patterson[2]	-68.0	-8.70

[1]Median of at least 12 measurements from 1987 to 1988.
[2]One measurement in 1989.

other characteristics, clearly indicates the source of recharge. For many samples, however, the range of possible mixtures results in no clear conclusion.

SELENIUM AND BORON

Selenium and boron were used to aid in identifying hydrochemical facies because of their significance to river-water quality and because of their varying geologic sources and mobility under different conditions. Selenium is clearly associated with Coast Ranges geologic sources and concentrations are low in Sierra Nevada-derived sediments (Tidball and others, 1987; Gilliom and others, 1989). Boron is present in about equal amounts in sedimentary (Coast Ranges) and igneous (Sierra Nevada) rocks (Deverel and Millard, 1988).

Selenium and boron occur as mobile oxyanions in alkaline and oxic conditions typical of shallow ground water in Coast Ranges alluvium (Deverel and Millard, 1988). Boron was equally correlated with dissolved

solids in ground water in Coast Ranges alluvium and in basin-trough deposits in which Sierra Nevada sediments dominate. Selenium was not correlated with dissolved solids in the basin-trough area, indicating the likely effect of the lower concentrations of selenium in Sierra Nevada-derived sediments. In addition, selenium mobility is much more sensitive than boron mobility to redox conditions. Generally, little or no dissolved selenium is detected in ground water with even mildly reducing conditions. In this study, the presence of detectable nitrate is used as an indicator of the presence of oxic conditions. The analyses reported in table 10 are for nitrogen in the form of nitrite and nitrite plus nitrate; however, nitrite was always an insignificant contribution to the total nitrogen in the samples analyzed. The nitrite plus nitrate values will be referred to as nitrate concentrations. Boron is expected to be generally correlated with dissolved solids in a much broader range of geologic settings and hydrochemical facies that occur in the San Joaquin Valley compared to selenium, which may be correlated with salinity only in oxic water associated with sediments derived from the Coast Ranges.

MAJOR-ION COMPOSITION

The major-ion composition of ground water reflects the geochemical characteristics of sources of recharge and the subsequent effects of geochemical processes such as sorption and mineral dissolution that occur when ground water is in contact with soils and aquifer material. Generally, sulfate-dominated water with high dissolved solids is associated with western valley ground water that originated from Coast Ranges runoff or recharge of irrigation water through saline soils derived from the Coast Ranges. Sodium and calcium bicarbonate water with low dissolved solids is characteristic of eastern valley ground water that originated from Sierra Nevada runoff and recharge through soils derived from the Sierra Nevada (Davis and others, 1959).

The ionic composition of water is depicted by using trilinear diagrams (Piper, 1944). Trilinear diagrams show the relative contribution of each major cation and anion to the overall ionic content of the water and are a convenient method for identifying water types. If one cation and one anion, such as sodium and bicarbonate, account for more than 50 percent of the total ion charge of a sample, the water is referred to and characterized by those particular ions, in this instance, a sodium bicarbonate water. If there is no dominant cation or anion and the water contains a comparable amount of two or three different ions, the water is referred to as a transitional or nondominant water type.

TRITIUM

Tritium is a radioactive isotope of hydrogen that is often used to determine the relative age of ground water. Large quantities of tritium were introduced into the environment through atmospheric nuclear weapons testing from 1952 through the early 1960's (Michel, 1990). Within the study area, tritium enters the ground-water system primarily by infiltration of irrigation water derived from surface-water sources and locally by seepage from surface-water bodies. The tritium concentration of water is expressed in tritium units (Tu), where 1 Tu is the equivalent of 1 ^{3}H atom in 10^{18} hydrogen atoms. The analytical method used in this study has a detection limit of 0.8 ± 0.8 Tu.

Prior to 1952, the tritium concentration in precipitation between 1 and 10 Tu occurred naturally (International Atomic Energy Agency, 1983). Recharge from surface-water sources that entered the ground-water system before 1952 presently would have a tritium concentration of less than 2 Tu because tritium decays over time, with a half life of 12.4 years. Recharge from surface-water sources since 1952 has had variable tritium, generally increasing to a peak in the 1960's and then decreasing after atmospheric nuclear weapons testing was ended (Michel, 1990). Figure 22 shows tritium concentrations currently (1989) expected in ground water that originated purely as recharge from surface water derived from precipitation during the indicated time period. These estimates are derived from Michel (1990) and have been corrected for radioactive decay through 1989. Imported irrigation water used near the study area presently has tritium concentrations ranging from 8.1 to 12.6 Tu (S.J. Deverel, U.S. Geological Survey, written commun., 1989).

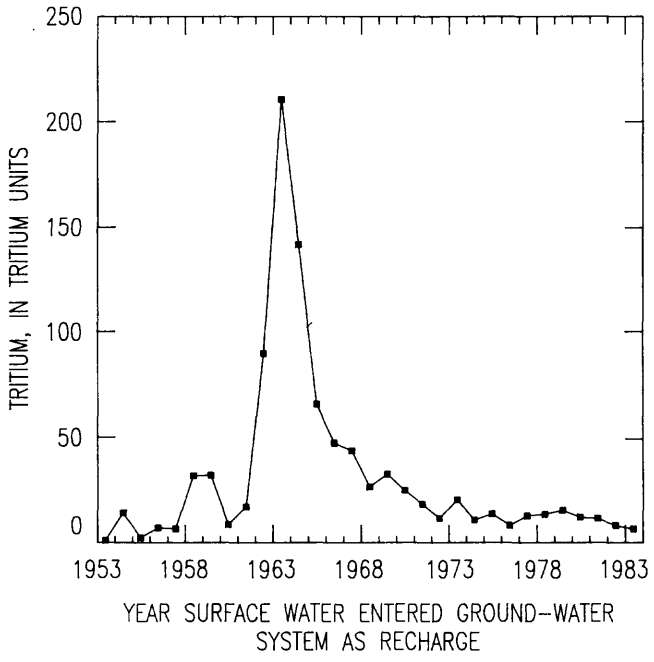

Figure 22. 1989 tritium levels expected in ground water that originated as precipitation during 1953-83. Modified from Michel (1990).

HYDROCHEMICAL FACIES IDENTIFIED

Three general hydrochemical facies were identified among the three study sites, with varying degrees of consistency at each site and among sites. Consistent with the ground-water-flow analysis, which indicates substantial west-to-east flow at all sites, the Coast Ranges hydrochemical facies is the most prevalent facies among all three sites. The Coast Ranges facies generally includes ground water that originated as recharge west of the river through sediments derived from the Coast Ranges. There are, however, important differences in the Coast Ranges facies among sites. A second hydrochemical facies, observed in shallow ground water at Newman and Crows Landing, is the flood-water facies, which is ground water believed to have originated as recharge of river water during high-flow conditions. The third hydrochemical facies, which is based more on general hydrologic origin than chemical character, is the local irrigation facies. The local irrigation facies is represented by one or more wells at all sites, is most commonly the shallowest ground water on either side of the river, and is believed to be water derived from local irrigation near the observation wells. In general, although there are important differences among sites, water of the Coast Ranges facies is the most saline, least depleted in oxygen-18 and deuterium, and has the highest selenium concentrations. The flood-water facies is lowest in dissolved solids, the most depleted in oxygen-18 and deuterium, and lowest in selenium. The local irrigation facies generally is intermediate between the Coast Ranges and flood-water facies.

NEWMAN SITE

Two hydrochemical facies were identified at the Newman study site. The most prevalent is the Coast Ranges facies, represented by samples from seven of the eight observation wells at the Newman site. This includes ground water sampled from all wells except for the shallowest well on the east side of the river, which was classified in the flood-water hydrochemical facies.

COAST RANGES FACIES

Samples of ground water representing the Coast Ranges facies at Newman (fig. 23) have relatively undepleted oxygen-18 (-8.20 to -8.05 per mil) and deuterium (-64.0 to -59.5 per mil) and relatively high dissolved-solids concentrations [1,820 to 4,620 mg/L (milligram per liter)]. The ratios of delta deuterium to delta oxygen-18 are similar for all seven samples and indicate isotopic composition typical of ground water that occurs above the Corcoran Clay Member of the Tulare Formation in Coast Ranges deposits of the central and northern San Joaquin Valley (Davis and Coplen, 1989; Dubrovsky and others, 1991). The narrow range of delta deuterium (-64.0 to -59.5 per mil) indicates that all samples probably originated as recharge dominated by Coast Ranges runoff (fig. 21). However, the greater depletion in deuterium compared to Coast Ranges runoff (typically -58 per mil), combined with the presence of detectable tritium (fig. 23), indicates that these samples are mixtures of water from different sources and probably include San Joaquin River water or imported canal water used for irrigation in the area. The substantially greater dissolved-solids concentration and undetectable tritium in the sample from NE-107.5, despite other chemical characteristics

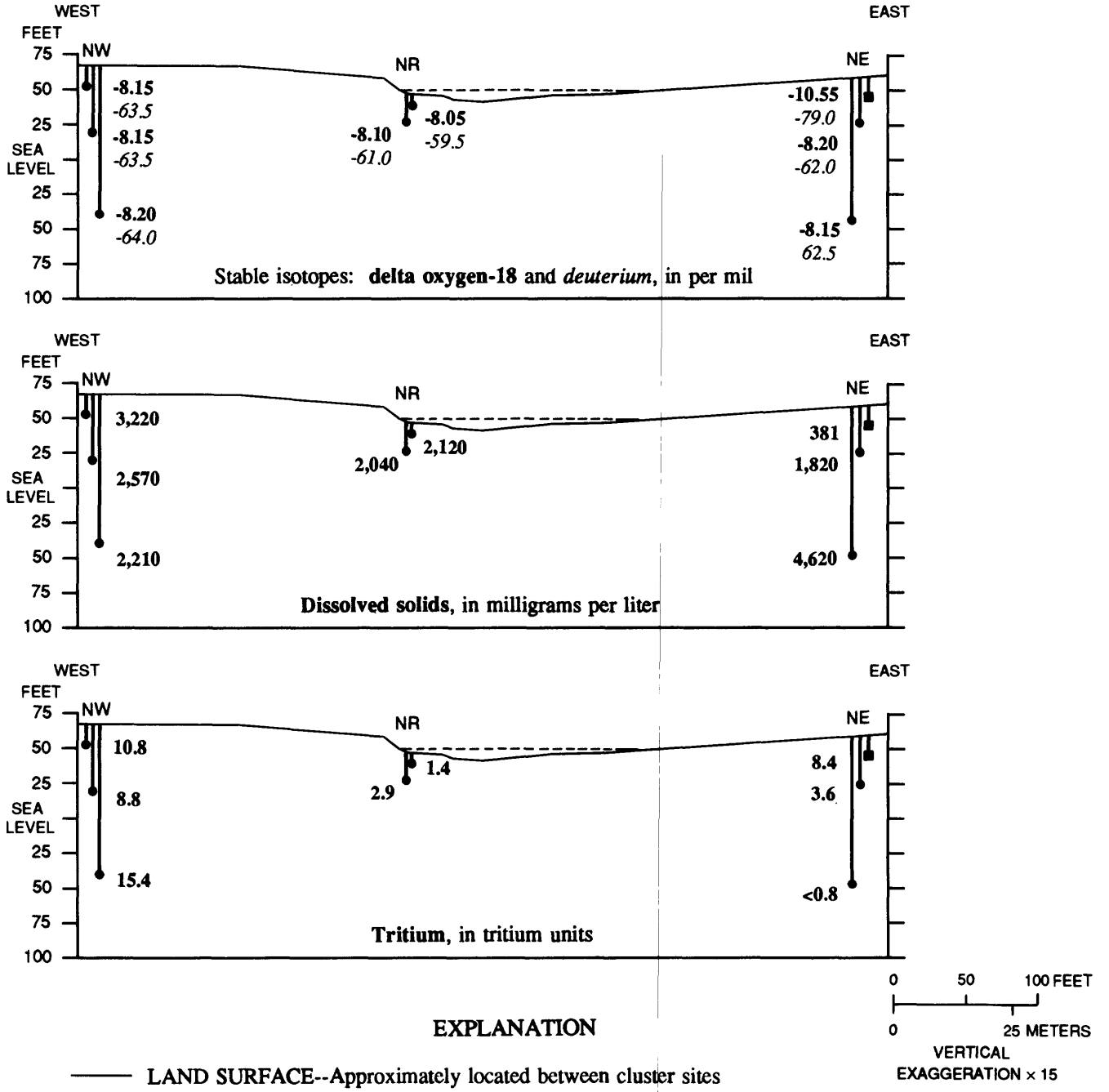

Figure 23. Distribution of constituents in water from observation wells at the Newman site.

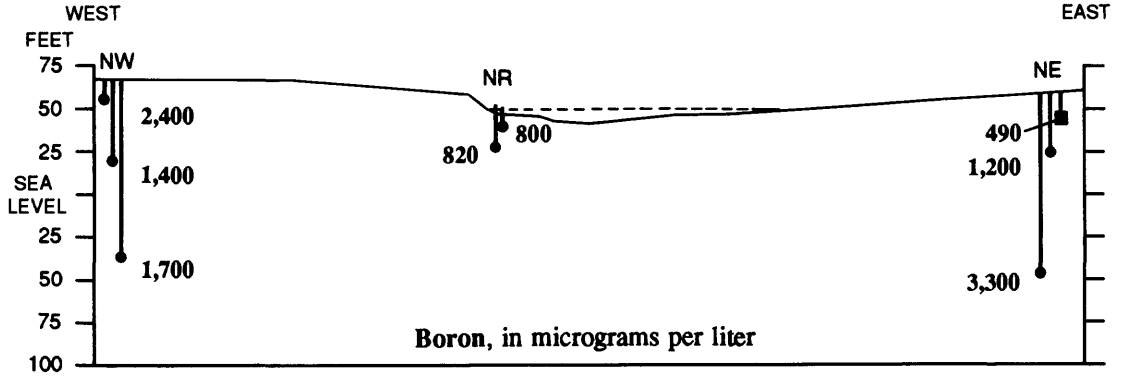

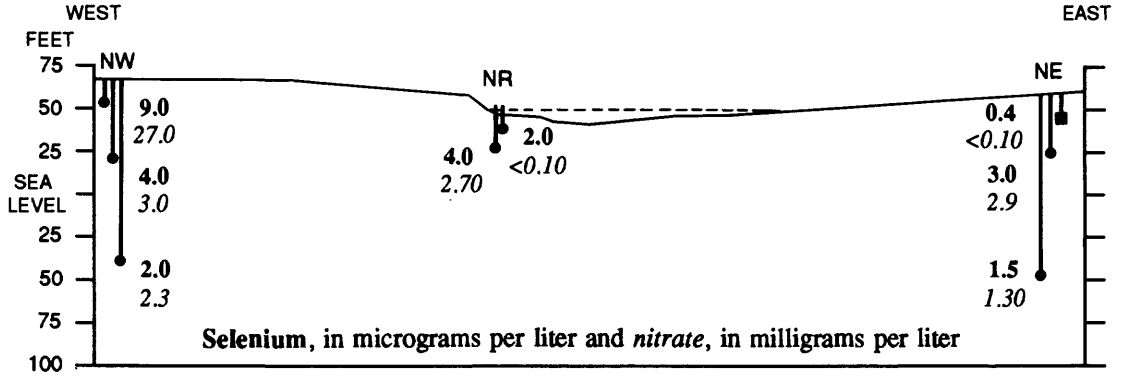

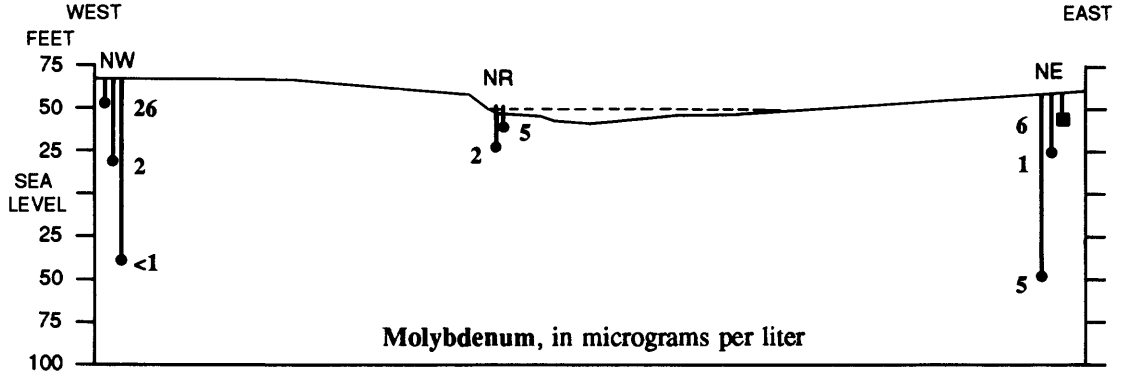

Figure 23. Continued.

and stable-isotope composition similar to other samples, indicate the possibility that this water originated as irrigation recharge prior to 1950 through saline west-side soils. At that time, soils of the area probably contained more abundant soluble salts than present-day (1990) soils because they had not been irrigated and leached for as long a period of time (Gilliom and others, 1989).

Boron concentrations in the Coast Ranges facies [800 to 3,300 µg/L (micrograms per liter)] are correlated with dissolved solids (rank r^2=0.67) but are independent of nitrate concentrations, suggesting that the relation between boron and salinity is relatively independent of redox conditions (fig. 23). In contrast, selenium (1.5 to 9 µg/L) is not correlated with dissolved solids within the range of concentrations measured but is highly correlated with nitrate (rank r^2=0.76), indicating the association between selenium and oxidizing conditions within the Coast Ranges hydrochemical facies at the Newman site (fig. 23).

Anionic composition (fig. 24) varies little for samples representing the Coast Ranges hydrochemical facies, with all samples dominated by sulfate and chloride. Cation composition is not clearly dominated by any single cation or pair of cations except for the sample from well NE-107.5 in which sodium is dominant.

Tritium concentrations measured in samples from the Coast Ranges facies indicate a general trend of high to low concentrations from west to east (fig. 23). This trend suggests a decreasing proportion of recent (since 1950) recharge from surface-water sources and thus increasing average time since recharge from west to east. In particular, tritium was undetectable in the deepest sample from the east side of the river (well NE-107.5) indicating no substantial presence of post-1950 recharge from surface-water sources at that position in the ground-water system.

The relatively consistent chemical composition of samples from the Coast Ranges facies at Newman and the distribution of tritium concentrations agree well with the flow-system analysis discussed earlier. Model results for the ground-water-flow system at Newman indicate that most ground water enters the study cross section from the west and then either discharges to the San Joaquin River or passes beneath the river to the east. This flow system is consistent with the occurrence of ground water of most recent origin on the west side of the river, the oldest ground water east of the river and at the greater depth, and ground water of intermediate age discharging to the river.

The dominant influence of Coast Ranges runoff and contact with Coast Ranges sediments on the chemical character of water in the Coast Ranges hydrochemical facies is evidenced by the combination of (1) relatively undepleted deuterium, (2) high dissolved solids even though ratios of delta deuterium to delta oxygen-18 indicate little evaporation, (3) the presence of selenium, and (4) sulfate-chloride anion composition. These characteristics are consistent at all cluster sites even though four of the seven samples are from observation wells completed in the Sierran sand. Thus, the origin of the ground water as Coast Ranges runoff and (or) recharge through sediments derived from the Coast Ranges seems to be controlling its character much more than the sediment matrix it now resides in.

FLOOD-WATER FACIES

The sample of ground water representing the flood-water hydrochemical facies at Newman is characterized by relatively depleted oxygen-18 and deuterium and a low dissolved-solids concentration (fig. 23). The stable-isotope composition is different from the samples from the Coast Ranges hydrochemical facies. The depleted deuterium (delta deuterium of -79.0 per mil) is within the range of a mixture of eastern valley and Sierra Nevada precipitation and runoff (fig. 21). The stable-isotope composition and low dissolved solids indicate little or no evaporative concentration and relatively little leaching of dissolved solids during recharge.

Both boron and selenium concentrations are low (490 and 0.4 µg/L), as shown in figure 23. Compared to the sample from well NR-7.0, which had similarly low nitrate (less than 0.1 mg/L), selenium is substantially lower (0.4 compared to 2 µg/L). In addition to reducing conditions, this may result from the relative absence of selenium in the aquifer matrix and the low concentrations of selenium in dilute flood waters.

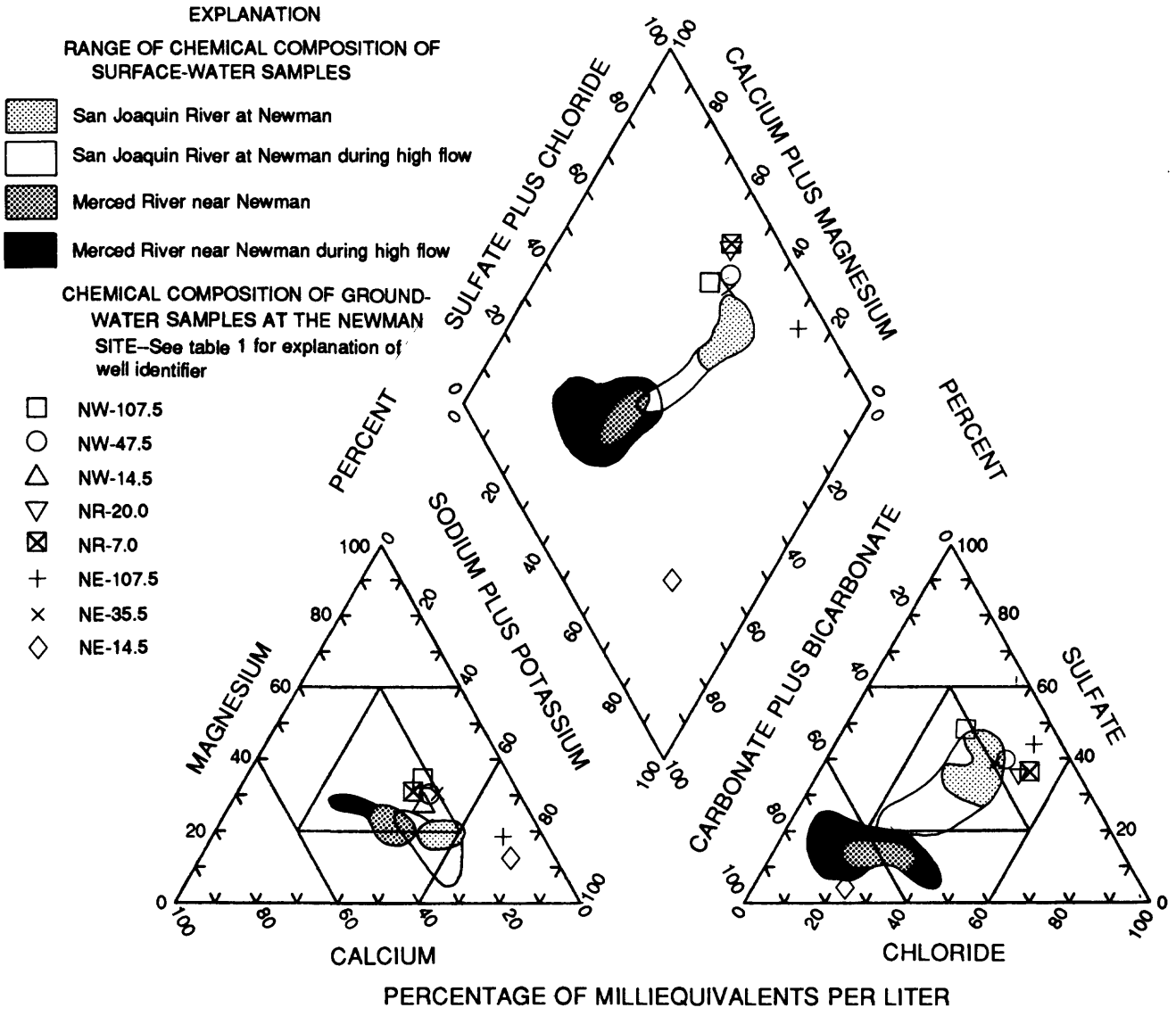

Figure 24. Distribution of major ions at the Newman site.

Anionic composition is strongly dominated by carbonate plus bicarbonate, and cation composition is dominated by sodium (fig. 24). The relative unimportance of sulfate indicates the absence of influence of runoff or sediments derived from the Coast Ranges on this sample. The anionic composition is similar to Merced River water, which is predominantly Sierra Nevada runoff.

The tritium concentration of 8.4 Tu indicates a substantial component of recharge of surface water after 1950, most likely since 1970 (fig. 22). The recharge probably was from Merced and (or) San Joaquin River flood waters. The sample from NE-14.5 may be a mixture of flood-water recharge and underlying ground water. The area surrounding the observation well is not irrigated but was inundated with flood water from the Merced and San Joaquin Rivers during the high-flow conditions in 1986 (table 2).

PATTERSON SITE

Two hydrochemical facies were identified at the Patterson site. As at the Newman site, the most prevalent is the Coast Ranges facies. The second, less distinct type of water occurs at the shallowest depths sampled on both sides of the river. This shallow ground water is the local irrigation facies.

COAST RANGES FACIES

Samples of ground water representing the Coast Ranges facies at Patterson have moderately depleted oxygen-18 (-9.90 to -9.35 per mil) and deuterium (-71.5 to -76.0 per mil) and relatively high dissolved solids (2,200 to 2,520 mg/L) (fig. 25). The constant ratio of delta deuterium to delta oxygen-18 among the five samples indicates that evaporative concentration since recharge has been minimal or similar for all samples (fig. 21). The values of delta oxygen-18 and delta deuterium are similar to imported irrigation water used in the area, and delta deuterium is between typical values for Coast Ranges and Sierra Nevada runoff (fig. 21).

Boron concentrations are consistently high in the Coast Ranges facies at Patterson, ranging from 2,200 to 2,500 µg/L (fig. 25). Selenium concentrations are low in all samples with low nitrate (less than 0.1 to 0.14 mg/L as N), but the highest selenium concentration measured in this study among all three sites (17 µg/L) was measured at well PW-22.5, where nitrate was 1.3 mg/L (fig. 25). As was found at Newman, the presence of oxic conditions in the Coast Ranges facies favors high selenium concentrations. The relatively high selenium concentration of 17 µg/L at Patterson is consistent with data for ground-water samples from two nearby production wells, which had 11 and 13 µg/L of selenium and were the highest selenium concentrations in a sampling of 44 production wells in the northern part of the western San Joaquin Valley (Dubrovsky and others, 1991). Dubrovsky and others (1991) discussed the possible origin of the elevated selenium in the area near Patterson.

The major-ion compositions of samples from the Coast Ranges facies vary little and indicate sodium and sulfate dominance (fig. 26). This composition indicates the influence of salts derived from the Coast Ranges.

The combination of tritium distribution (fig. 25) and the model analysis of the ground-water-flow system indicates that water of the Coast Ranges hydrochemical facies generally is moving from west to east, with discharge to the river and movement across the valley trough. The particularly high tritium concentrations in wells PW-22.5, PW-89.0, PR-5.0, and PR-30.7 (19.0 to 29.7 Tu) probably result from a substantial component of irrigation recharge that occurred during the 1960's when tritium in precipitation and runoff was highest (fig. 22). The sample from well PE-98.3 has lower tritium than the preceding samples but is farther along the simulated ground-water-flow path. This water probably originated as recharge during the late 1950's and early 1960's.

Water of the Coast Ranges hydrochemical facies at Patterson, though originating as irrigation water that primarily is derived from Sierra Nevada runoff and presently residing in a Sierra Nevada sand aquifer matrix, has been most strongly affected by solutes derived from Coast Ranges sediments. Apparently, the high dissolved solids and sulfate dominance result from the leaching of soluble salts from sediments derived from the Coast Ranges during irrigation recharge. The low selenium in all but one sample probably is the result of the chemically reducing conditions.

LOCAL IRRIGATION FACIES

The second, less distinct, hydrochemical facies observed at the Patterson site occurs in the shallowest ground water sampled on both sides of the river. This water probably is dominated by recent recharge from local irrigation. As indicated in table 2, the west side of the river historically has been irrigated with river water and the east side by secondary wastewater and local irrigation water derived from Sierra Nevada runoff. Both sites were flooded in 1986.

The stable-isotope composition indicates that shallow ground water on both sides of the river is more enriched in oxygen-18 and deuterium than imported irrigation water or flood water and that the values bracket the composition of typical river water (fig. 25). The low dissolved solids of the sample from well PW-11.5, however, suggest that this is not recharge of typical San Joaquin River water, which generally has greater than 500 mg/L of

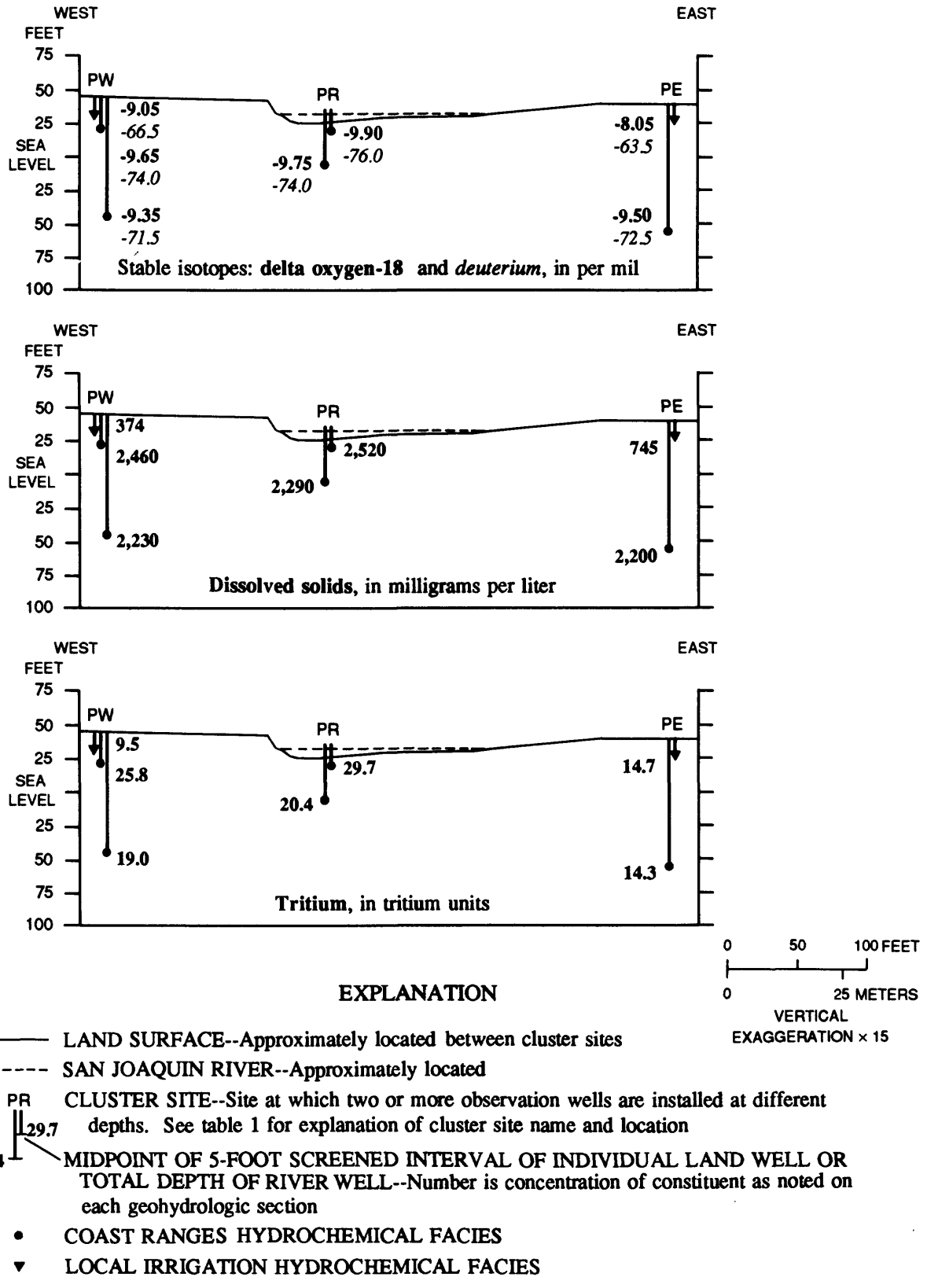

Figure 25. Distribution of constituents in water from observation wells at the Patterson site.

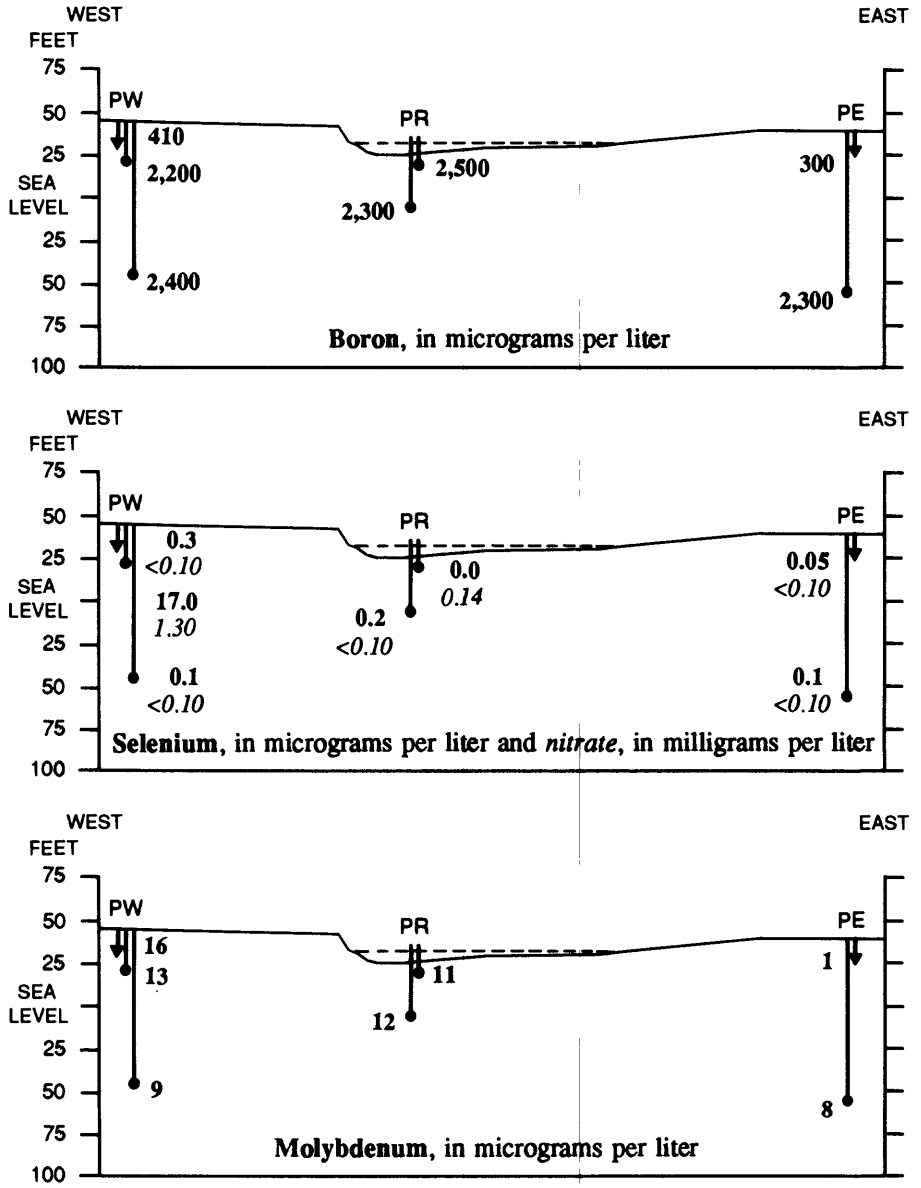

Figure 25. Continued.

dissolved solids at the Patterson site. This water could be a mixture of San Joaquin River water used for summer irrigation and flood waters recharged during 1986. The sample from well PE-9.5 was more evaporated, which is consistent with the particularly shallow water table at this site but also may have resulted from wastewater treatment.

Both boron and selenium concentrations are low (fig. 25), which is consistent with the low dissolved-solids concentrations. Nitrate was not detected in either sample.

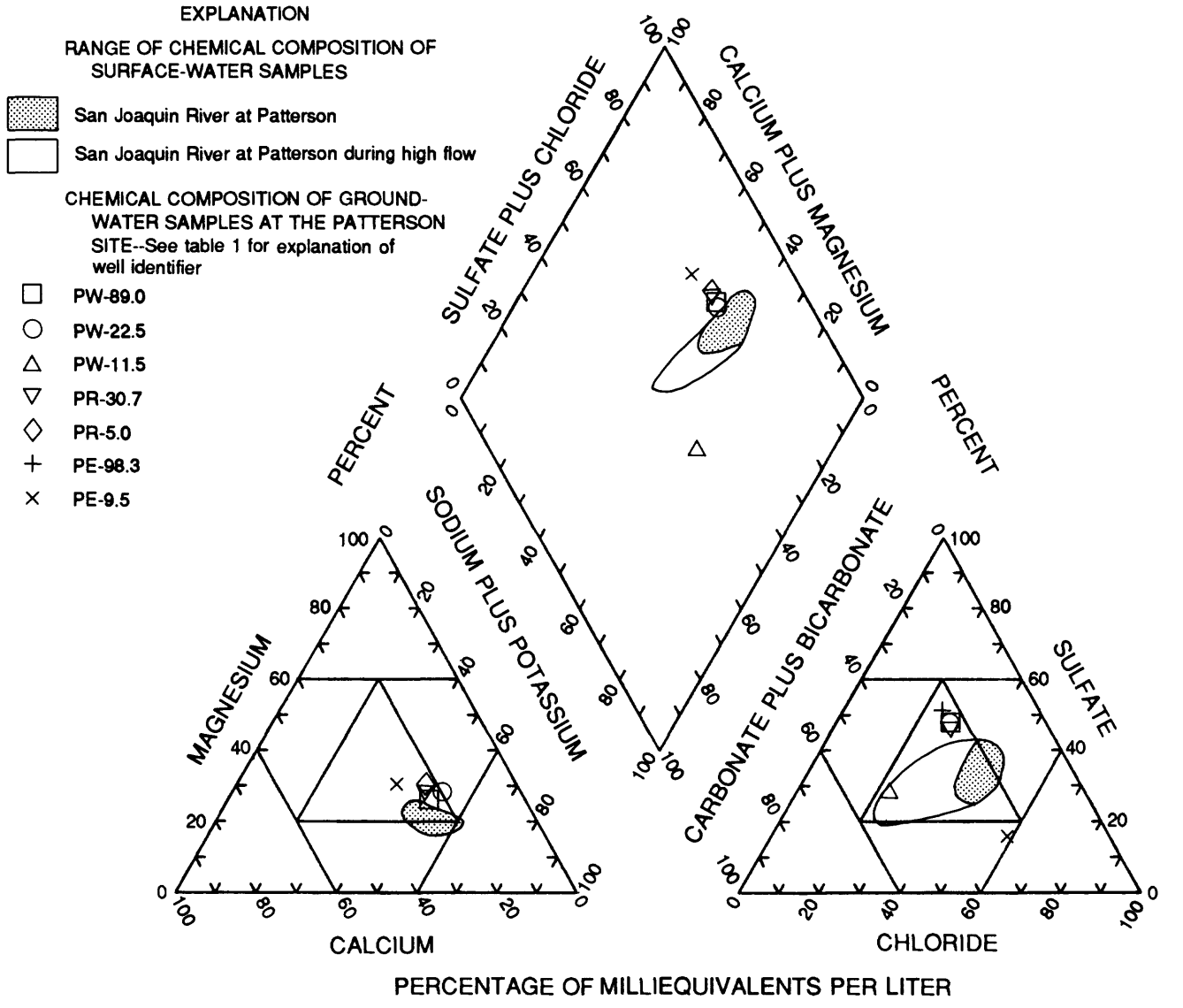

Figure 26. Distribution of major ions at the Patterson site.

Shallow ground water on both sides of the river has an anionic composition dominated more by chloride and carbonate plus bicarbonate than by sulfate, which dominated in the Coast Ranges facies. This composition is consistent with either San Joaquin River water (fig. 26) or irrigation water from Sierra Nevada sources (Deverel and Fujii, 1988).

CROWS LANDING SITE

The distinctions among hydrochemical facies for ground water sampled at the Crows Landing site are not as clear-cut as for the Newman or Patterson sites. The three hydrochemical facies identified are the Coast Ranges, flood-water, and local irrigation facies.

COAST RANGES FACIES

The single ground-water sample believed to represent the Coast Ranges hydrochemical facies is from well CW-97.7. This is the deepest ground water sample from the west side of the river at Crows Landing. This water has moderately depleted oxygen-18 and deuterium and the highest dissolved-solids concentration measured at Crows Landing (fig. 27). The delta deuterium of -68.5 per mil indicates that this water probably is a mixture of water originating from Coast Ranges and Sierra Nevada runoff (fig. 21).

The boron concentration at well CW-97.7 is high and, at 1,700 µg/L, falls within the range of the Coast Ranges facies at Newman (fig. 23) and Patterson (fig. 25). Selenium was detected at 1.0 µg/L, even though nitrate was undetectable.

The major-ion composition at CW-97.7 (fig. 28) also is similar to the water of the Coast Ranges facies at Newman (fig. 24) and Patterson (fig. 26). Anion composition is dominated by chloride and sulfate, and cation composition is dominated by sodium plus potassium.

The absence of detectable tritium (less than 0.8 Tu, fig. 27), combined with the ground-water-flow analysis that shows a strong component of west to east flow, indicates that the Coast Ranges facies at Crows Landing probably originated as pre-1950 recharge through Coast Ranges sediments west of the study area. The chemical characteristics are within the range characteristic of semiconfined ground water west of the San Joaquin River (Dubrovsky and others, 1991). The water sampled could be native ground water, recharge of irrigation water from local ground water or the river, or a mixture.

FLOOD-WATER FACIES

The flood-water facies is represented by shallow ground water sampled on the west side of the river (well CW-18.2) and by shallow ground water sampled from beneath the riverbed (well CR-5.0 and CR-20.0). Except for well NE-14.5, which also was identified as flood-water facies, samples from these wells have the most depleted oxygen-18 and deuterium among all sites. The isotopic composition is characteristic of water dominated by Sierra Nevada runoff, although it is probably a mixture. The three samples have among the lowest dissolved-solids concentrations (534 to 668 mg/L) but are higher than peak flood waters, which generally had dissolved-solids concentrations between 100 and 300 mg/L at Patterson (Shelton and Miller, 1988).

Boron concentrations are low (320 to 620 µg/L) and follow the relative distribution of dissolved solids (fig. 27). Selenium concentrations also are low (less than 0.1 to 0.4 µg/L), and the highest concentration occurred in the only sample with detectable nitrate.

The ground-water-flow system analysis indicates a much weaker gradient between ground water and the river than at the other study sites. Observations of water levels during the study showed that the gradient fluctuated in direction. These hydrologic conditions support the hypothesis that river water infiltrated the ground-water system beneath the river at high river stage. The tritium values in water of the flood-water facies range from 5.7 to 14.9, which is additional evidence that this water probably is recent recharge of surface water. In all respects, this water is similar to the water sampled from NE-14.5, which also was classified as a flood-water facies.

LOCAL IRRIGATION FACIES

The local irrigation facies at Crows Landing is represented by samples from both observation wells on the east side of the river, CE-19.5 and CE-107.5. This area is irrigated regularly during the summer with San Joaquin River water and receives occasional drainage from a dairy, which also uses river water (table 2). The samples have moderately depleted oxygen-18 and deuterium (fig. 27), which is similar to San Joaquin River water. The dissolved-solids concentrations of 969 and 1,430 mg/L are within the upper range of concentrations in river water at Newman and Patterson during low-flow periods (Shelton and Miller, 1988).

Boron and selenium concentrations (fig. 27) also are typical of San Joaquin River concentrations. The highest selenium concentration of 3 µg/L occurred in water with 7.1 mg/L of nitrate, and the lowest selenium concentration of 1.5 µg/L occurred in water with less than 0.1 mg/L of nitrate.

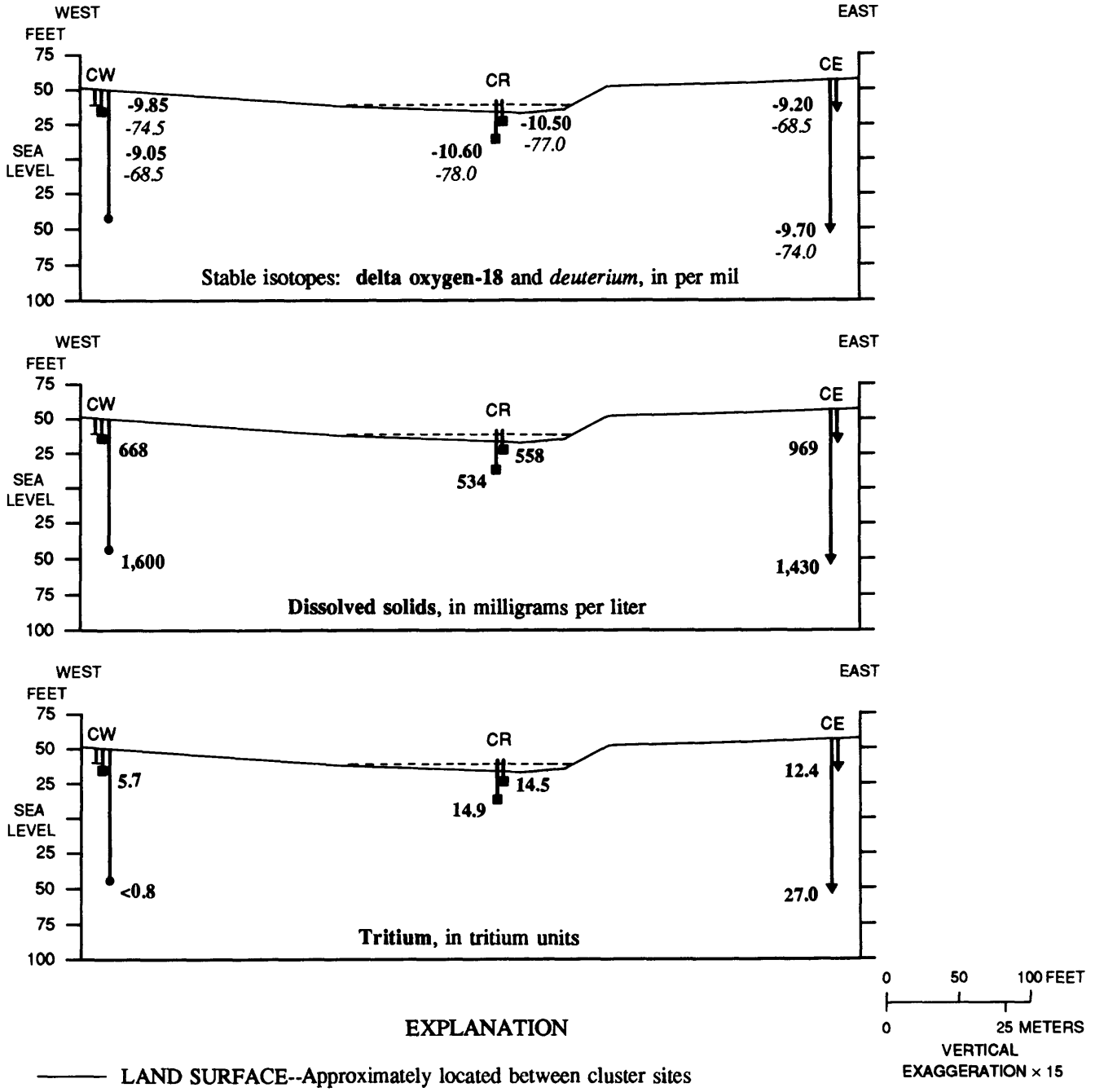

Figure 27. Distribution of constituents in water from observation wells at the Crows Landing site.

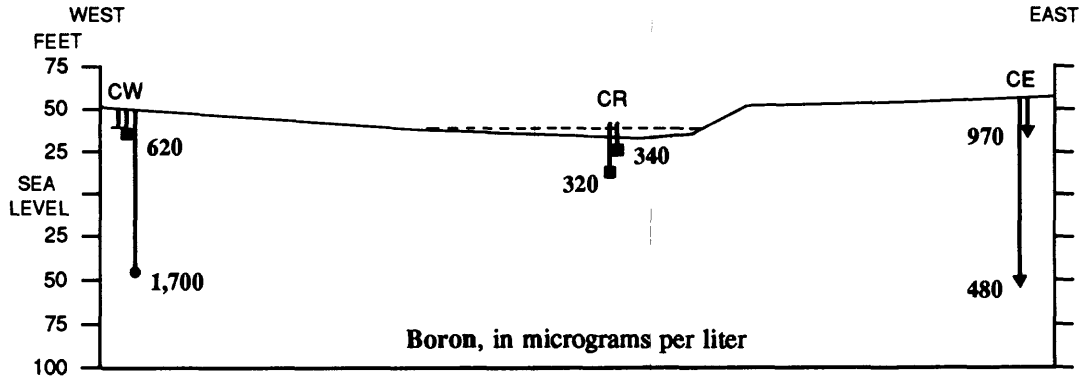

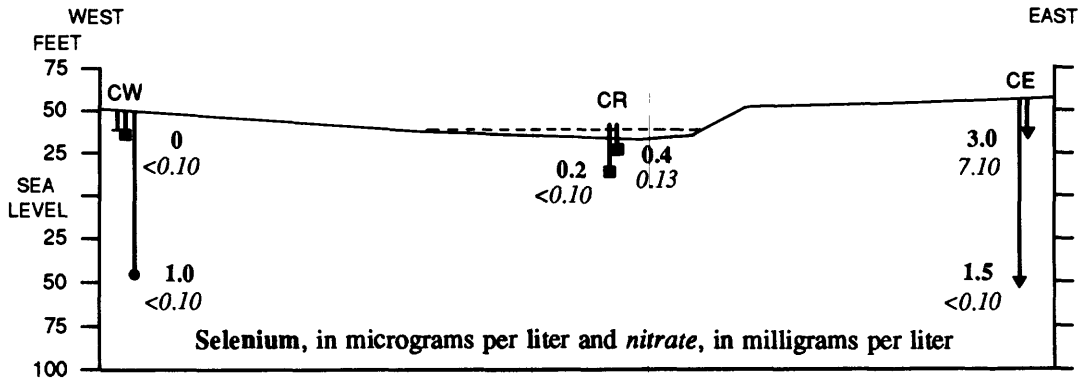

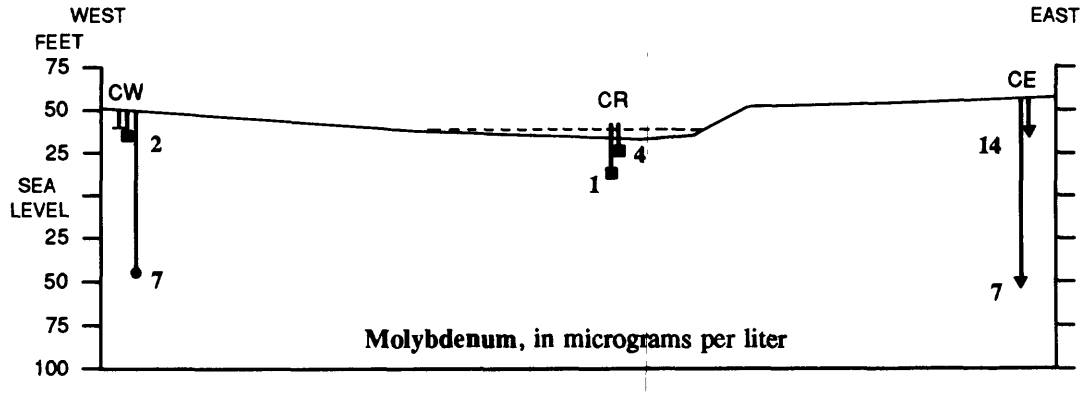

Figure 27. Continued.

Major-ion composition does not clearly support the explanation that this ground water originated as San Joaquin River water. The relative contribution of sulfate to anion composition is substantially lower in samples from CE-19.5 and CE-107.5 than in the San Joaquin River (fig. 28). This difference may be due to an alteration of ionic composition over time during residence in Sierran sand.

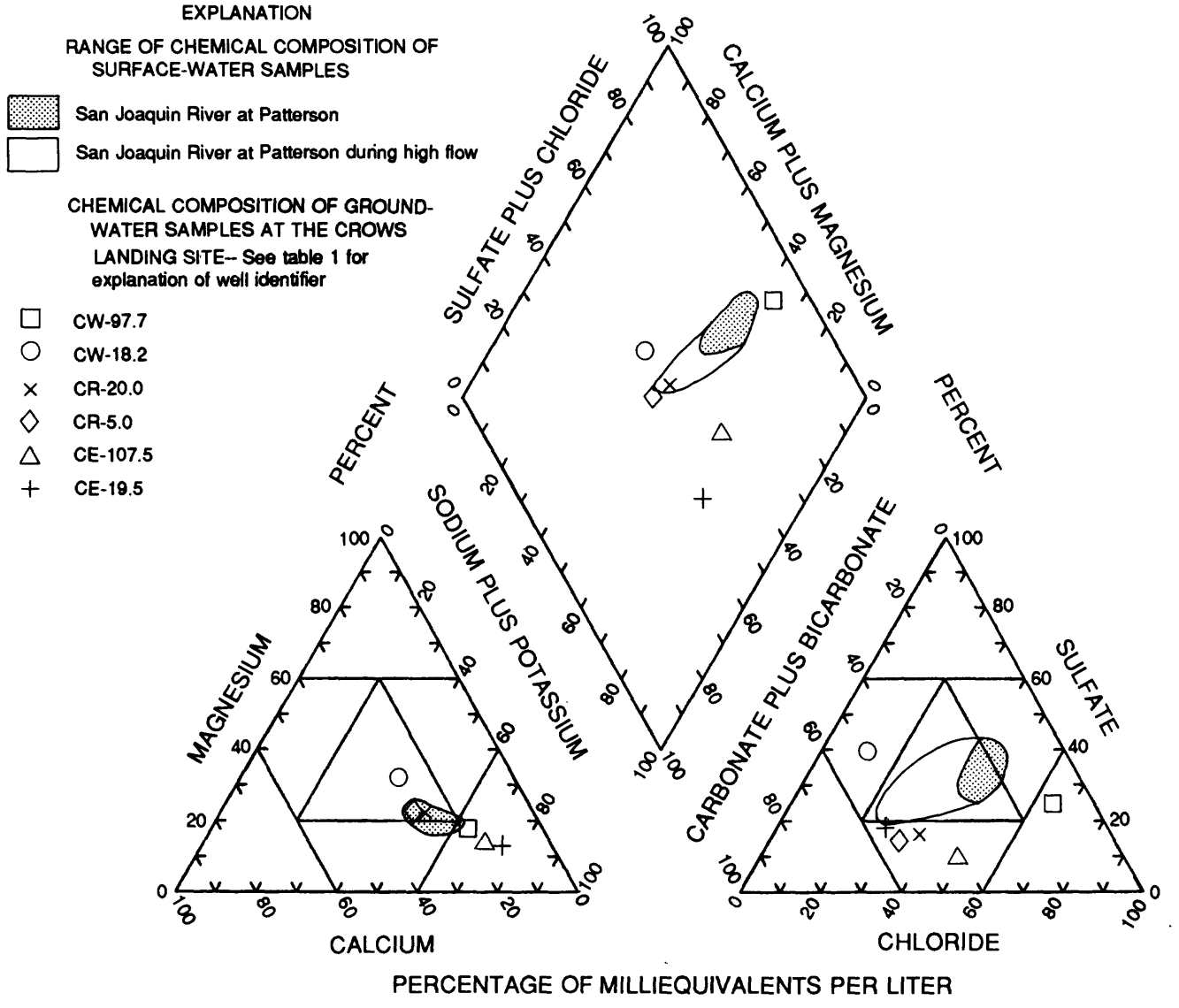

Figure 28. Distribution of major ions at the Crows Landing site.

The tritium distribution within the local irrigation facies at Crows Landing, combined with results from the ground-water-flow analysis, indicates a downward gradient on the east side of the river and shows that local irrigation recharge probably moves downward and eastward. The tritium concentration of 12.4 Tu in well CE-19.5 is consistent with recharge since 1970, whereas the concentration of 27.0 Tu in well CE-107.5 is indicative of recharge during the 1960's.

QUALITY OF GROUND WATER FLOWING INTO THE SAN JOAQUIN RIVER

The quality of ground water now flowing into the San Joaquin River was estimated in two ways: by the water-balance analysis for the entire study reach and by combining ground-water-flow model results and the assessment of ground-water chemistry for each of the three study sites. The water-balance analysis has the advantage of applying to the entire reach and the disadvantage of being limited to salinity. The two water-balance synoptic studies yielded estimates of 1,730 µS/cm (October 1986) and 1,216 µS/cm (June 1989) as the average specific conductance of ground water flowing into the river between Newman and Patterson. Based on direct measurements of ground water, the site-by-site analyses provided independent estimates of the chemical character of ground water flowing into the river.

The average chemical character of ground water flowing into the river at each site was computed by using estimates from the layered flow model of the amounts of inflow from three parts of the unconfined ground-water-flow system: the upper part west of the river, the upper part east of the river, and the lower part beneath the layer (table 6). The distributions of hydrochemical facies at each site in relation to the directions of ground-water flow were used to determine the chemical characteristics of each of the three components of total ground-water inflow. Concentrations for selected constituents were then computed as the flow-weighted average for each site.

NEWMAN SITE

For the Newman site, the layered configuration of the ground-water-flow model of the cross section yields a total flow into the San Joaquin River of 1.8 $(ft^3/s)/mi$, with 74 percent from the deep part of the unconfined zone beneath the low-permeability layer, 13 percent from the shallow part west of the river, and 13 percent from the shallow part east of the river. Shallow ground water sampled west of the river was classified in the Coast Ranges hydrochemical facies along with samples from all other locations along the cross section except for the shallowest sample on the east side of the river. Thus, ground-water inflow to the river is estimated to consist of 87 percent Coast Ranges facies (74 percent + 13 percent) and 13 percent flood-water facies.

For the seven samples included in the Coast Ranges facies, the median concentrations are 2,210 mg/L for dissolved solids, 1,400 µg/L for boron, 3 µg/L for selenium, and 2 µg/L for molybdenum. The median specific conductance is 3,380 µS/cm. For the single sample of the flood-water facies, the concentrations are 381 mg/L for dissolved solids, 490 µg/L for boron, 0.4 µg/L for selenium, and 6 µg/L for molybdenum. The specific conductance is 604 µS/cm. Based on the median concentrations in the Coast Ranges facies, the flow-weighted average concentrations of contributions of water from the two facies are 1,970 mg/L for dissolved solids, 1,280 µg/L for boron, 2.7 µg/L for selenium, and 2.5 µg/L for molybdenum. The average specific conductance is 3,019 µS/cm.

CROWS LANDING SITE

For the Crows Landing site, the layered configuration of the ground-water-flow model yields a total flow into the river of 1.1 $(ft^3/s)/mi$, with 27 percent from the deep part of the unconfined zone beneath the layer, 63 percent from the shallow part west of the river, and 10 percent from the shallow part east of the river. Shallow ground water sampled west of the river was classified in the flood-water facies, along with the samples from beneath the riverbed. At present, the flood-water facies probably best represent the character of ground water flowing into the river from the shallow flow system west of the river and from beneath the river, as a result of displacement towards the river by upward-flowing deeper ground water. Shallow ground water entering the river from the east was identified as the local irrigation facies. Ground-water inflow to the river, therefore, consists of 90 percent flood-water facies and 10 percent local irrigation facies, as characterized by the shallowest well sampled east of the river.

The three samples of the flood-water facies from west of the river and beneath the river have median concentrations of 558 mg/L for dissolved solids, 340 µg/L for boron, 0.2 µg/L for selenium, and 2 µg/L for molybdenum. The median specific conductance is 973 µS/cm. The single sample of shallow ground water of the local irrigation facies east of the river has 969 mg/L for dissolved solids, 970 µg/L for boron, 3 µg/L for selenium, and 14 µg/L for molybdenum. The specific conductance is 1,570 µS/cm. The flow-weighted average

concentrations in simulated ground-water inflow to the river at Crows Landing are 599 mg/L for dissolved solids, 403 µg/L for boron, 0.5 µg/L for selenium, and 3.2 µg/L for molybdenum. The average specific conductance is 1,033 µS/cm.

PATTERSON SITE

For the Patterson site, the layered configuration of the ground-water-flow model simulates a total inflow to the river of 3.2 $(ft^3/s)/mi$, with 67 percent from the deep part of the unconfined zone beneath the layer, 17 percent from the shallow part west of the river, and 16 percent from the shallow part east of the river. Shallow ground water on both sides of the river was classified as local irrigation facies with substantially different salinities. Ground water in the deep layer and beneath the river was classified as Coast Ranges facies.

Samples of the Coast Ranges facies have medians of 2,290 mg/L for dissolved solids, 2,300 µg/L for boron, 0.1 µg/L for selenium, 11 µg/L for molybdenum, and a median specific conductance of 3,360 µS/cm. The west and east side shallow ground waters have 374 and 745 mg/L for dissolved solids, 410 and 300 µg/L for boron, less than 0.1 and 0.1 µg/L for selenium, and 16 and 1 µg/L for molybdenum, respectively. The specific conductances are 591 and 1,250 µS/cm. The flow-weighted average concentrations of inflow to the river are 1,717 mg/L for dissolved solids, 1,659 µg/L for boron, 0.1 µg/L for selenium, and 10 µg/L for molybdenum. The average specific conductance is 2,552 µS/cm.

AVERAGE QUALITY OF GROUND WATER FLOWING INTO THE RIVER

Constituent levels estimated for the three study sites were averaged on a flow-weighted basis using the estimated rates of ground-water inflow at each site. The average rate of ground-water inflow determined using the layered models of the three study sites is 2.0 $(ft^3/s)/mi$ with a specific conductance of 2,230 µS/cm. The site estimates that were averaged range from 1.1 to 3.2 $(ft^3/s)/mi$ and 1,033 to 3,019 µS/cm. These values compare to estimates from the synoptic water-balance studies of 6.7 $(ft^3/s)/mi$ at 1,730 µS/cm in October 1986 and 3.2 $(ft^3/s)/mi$ at 1,216 µS/cm in June 1989. Thus, for 1989, the estimates for the study reach are 2.0 to 3.2 $(ft^3/s)/mi$ with specific conductance of 2,230 and 1,216 µS/cm. The dissolved-solids loads implied by these estimates are within 20 percent of each other (product of flow and specific conductance).

Average concentrations for dissolved solids, boron, selenium, and molybdenum can be estimated only from data for the three study sites because these constituents were not included in the synoptic water-balance studies. The flow-weighted average concentrations are 1,590 mg/L for dissolved solids, 1,321 µg/L for boron, 0.9 µg/L for selenium, and 6.6 µg/L for molybdenum. The estimated specific conductance from the synoptic water-balance study indicates that salinity may be lower than represented by the three study sites, and thus these estimated concentrations particularly for dissolved solids and boron may be high.

The greater inflow and specific conductance estimated from 1986 data indicate that ground-water inflow and salt load may vary substantially as hydrologic conditions change. Ground-water pumping may be a key control on the quantity and solute load of ground-water inflow to the San Joaquin River. The model results suggest that an average of about 76 percent of the total discharge from October 1988 through August 1989 was to pumping wells and the remaining 24 percent to the San Joaquin River. This ground-water pumping, which is primarily east of the river, induces flow from west to east across the valley trough, as evidenced by the distribution of measured water levels and ground-water chemistry at the study sites. Because the period simulated was the third year of a drought, the ground-water pumping probably was relatively high resulting in relatively low ground-water inflow to the river. This is consistent with the results from the 1986 and 1989 surface-water synoptic studies, which indicate that ground-water inflow in 1986, which was a wet year, was about twice that in 1989.

Relatively high pumping rates in 1989 also could have had an effect on the quality of ground water flowing into the San Joaquin River. As a result of the high pumping rates, the percentage of ground-water inflow from the deeper part of the unconfined aquifer probably was lower than average. Because water in the deeper part of the aquifer was highest in dissolved solids, the concentration of dissolved solids in water flowing into the river should have been relatively low in 1989. This is consistent with the surface-water synoptic studies, which resulted in estimates of 1,730 µS/cm for 1986 and 1,216 µS/cm for 1989.

SUMMARY AND CONCLUSIONS

Two approaches were used to estimate the quantity of ground-water inflow to a 19-mile reach of the San Joaquin River. The first approach was to develop ground-water-flow models of the unconfined zone at three sites on the 19-mile reach. The flow models, which are vertical cross sections oriented perpendicular to the river, were based on three conceptual models for the distribution of aquifer materials that control vertical flow. The models were calibrated on the basis of water levels measured in clusters of observation wells at each site.

Two of the three conceptual models produced reasonable results; one of which proved superior in several respects. The best results were obtained using the layered model, which is based on assuming an isotropic homogeneous system except for one low-conductivity layer within 30 ft of the land surface. The layered models were used for determining the quantity of ground-water inflow coming from various parts of the unconfined zone at each site. The average ground-water inflow predicted by the layered models for all three sites was 2.0 $(ft^3/s)/mi$, with a range of 1.1 to 3.2 $(ft^3/s)/mi$. The model results indicate that during the study period ground-water pumpage was the dominant mechanism of ground-water discharge from the modeled cross sections, capturing an average of 76 percent of the total recharge to the cross sections of the three sites. This pumpage induced significant flow from west to east across the valley trough.

The second approach used to estimate the quantity of ground-water inflow along the 19-mile reach was based on a volumetric balance of measured surface-water flows. During synoptic studies in October 1986 and June 1989, streamflow and specific conductance were measured at all known tributaries and diversions along the 19-mile reach and for the San Joaquin River at the Newman and Patterson sites, the endpoints of the reach. The estimated ground-water inflow was computed as the residual of the measured streamflow. Measured specific conductance provided an indirect assessment of the quality of ground-water inflow. Residual inflow and salt load were attributed to ground water.

Results for the 1986 synoptic study were 6.7 $(ft^3/s)/mi$ for ground-water inflow, with an associated specific conductance of 1,730 µS/cm. The corresponding results for the 1989 synoptic study, done after 2.5 years of drought conditions, were 3.2 $(ft^3/s)/mi$ and 1,216 µS/cm.

The quality of ground water at the study sites was directly assessed through analysis of ground-water samples from observation wells installed at each site. Chemical analyses include tritium, stable isotopes, major ions, trace elements, and dissolved solids. Results from the analyses were used to classify ground water at each site into hydrochemical facies with common origin and chemical characteristics. Three hydrochemical facies were identified by the chemical characteristics and interpreted hydrologic history of the ground water sampled: the Coast Ranges, flood-water, and local irrigation facies. For each of the three sites, the median concentrations of selected constituents were determined for each of the two or three hydrochemical facies present. The quality of ground-water inflow at each site was estimated by combining the results from the layered flow models with the concentrations of key constituents present in the appropriate hydrochemical facies.

Ground water flowing into the 19-mile reach of the San Joaquin River was estimated to have the following average chemical characteristics: 1,590 mg/L for dissolved solids, 1,321 µg/L for boron, 0.9 µg/L for selenium, and 6.6 µg/L for molybdenum. Specific conductance averaged 2,230 µS/cm for estimated ground-water inflow at the three sites. The conclusion from the model analysis, indicating that eastward flow across the valley trough is significant, was reinforced by the chemistry and interpreted hydrologic history of the ground-water samples.

The 1989 dissolved-solids loads implied by the results of the surface-water balance approach and the ground-water flow model approach are within 20 percent of each other. The results of the 1986 and 1989 water-balance synoptic studies indicate that the quantity and quality of ground-water inflow may vary substantially with changing hydrologic conditions. The degree to which the constituent load may vary with changing hydrologic conditions is an important consideration because 1989 did not represent typical conditions.

References Cited

Back, William, 1966, Hydrochemical facies and ground-water flow patterns in northern part of Atlantic Coastal Plain: U.S. Geological Survey Professional Paper 498-A, 42 p.

Belitz, Kenneth, and Heimes, F.J., 1990, Character and evolution of the ground-water flow system in the central part of the western San Joaquin Valley, California: U.S. Geological Survey Water-Supply Paper 2348, 28 p.

Bull, W.B., and Miller, R.E., 1975, Land subsidence due to ground-water withdrawal in the Los Banos-Kettleman City area, California. Part 1. Changes in the hydrologic environment conducive to subsidence: U.S. Geological Survey Professional Paper 437-E, 71 p.

Clifton, D.G., and Gilliom, R.J., 1989, Sources and concentrations of dissolved solids and selenium in the San Joaquin River and its tributaries, California, October 1985 to March 1987: U.S. Geological Survey Water-Resources Investigations Report 88-4217, 33 p.

Compton, R.R., 1985, Geology in the field: New York, John Wiley and Sons, 398 p.

Cooper, H.H., Bredehoeft, J.D., and Papadopulos, I.S., 1967, Response of a finite diameter well to an instantaneous charge of water: Water Resources Research, v. 3, no. 1, p. 263-269.

Craig, H., 1961, Isotopic variations in meteoric waters: Science, v. 133, p. 1702-1703.

Davis, G.H., and Coplen, T.B., 1989, Late Cenozoic paleohydrology of the western San Joaquin Valley, California, as related to structural movements in the central Coast Ranges: Geological Society of America Special Paper 234, 40 p.

Davis, G.H., Green, J.H., Olmsted, F.H., and Brown, D.W., 1959, Ground-water conditions and storage capacity of the San Joaquin Valley, California: U.S. Geological Survey Water-Supply Paper 1469, 287 p.

Deverel, S.J., and Fujii, Roger, 1988, Processes affecting the distribution of selenium in shallow groundwater of agricultural areas, western San Joaquin Valley, California: Water Resources Research, v. 24, no. 4, p. 516-524.

Deverel, S.J., and Millard, S.P., 1988, Distribution and mobility of selenium and other trace elements in shallow groundwater of the western San Joaquin Valley, California: Environmental Science and Technology, v. 22, no. 6, p. 697-707.

Dietrich, R.V., Dutro, J.T., and Foose, R.M., 1982, AGI data sheets for geology in the field, laboratory, and office: American Geological Institute, data sheets 15.1-18.2, and 25.1.

Dubrovsky, N.M., Neil, J.M., Welker, M.C., and Evenson, K.D., 1991, Geochemical relations and distribution of selected trace elements in ground water of the northern part of the western San Joaquin Valley, California: U.S. Geological Survey Open-File Report 90-108, 55 p.

Epstein, S., and Mayeda, T., 1953, Variation of the O-18 content of waters from natural sources: Geochimica et Cosmochimica Acta, 4, p. 213-224.

Fishman, M.J., and Bradford, W.L., 1982, A supplement to methods for the determination of inorganic substances in water and fluvial sediments: U.S. Geological Survey Open-File Report 82-272, 136 p.

Fishman, M.J., and Friedman, L.C., eds., 1989, Methods for determination of inorganic substances in water and fluvial sediments: U.S. Geological Survey Techniques of Water-Resources Investigations, book 5, chap. A1, 709 p.

Freeze, R.A., and Cherry, J.A., 1979, Groundwater: Englewood Cliffs, New Jersey, Prentice-Hall, 604 p.

Gat, J.R., and Gonfiantini, R., eds., 1981, Stable isotope hydrology--Deuterium and oxygen-18 in the water cycle: International Atomic Energy Agency Technical Reports Series No. 210, 335 p.

Gilliom, R.J., and others, 1989, Preliminary assessment of sources, distribution, and mobility of selenium in the San Joaquin Valley, California: U.S. Geological Survey Water-Resources Investigations Report 88-4186, 129 p.

Hull, L.C., 1984, Geochemistry of ground water in the Sacramento Valley, California: U.S. Geological Survey Professional Paper 1401-B, 36 p.

International Atomic Energy Agency, 1983, Guidebook on nuclear techniques in hydrology: International Atomic Energy Agency Technical Report Series No. 91, 439 p.

Johnson, A.I., Moston, R.P., and Morris, D.A., 1968, Physical and hydrologic properties of water-bearing deposits in subsiding areas in central California: U.S. Geological Survey Professional Paper 497-A, 71 p.

Kendall, Carol, and Coplen, T.B., 1985, Multisample conversion of water to hydrogen by zinc for stable isotope determination: Analytical Chemistry, v. 57, p. 1437-1440.

Kipp, K.L., Jr., 1985, Type curve analysis of inertial effects in the response of a well to a slug test: Water Resources Research, v. 21, no. 9, p. 1397-1408.

Kratzer, C.R., Pickett, P.J., Rashmawi, E.A., Cross, C.L., and Bergeron, K.D., 1987, An input-output model of the San Joaquin River from the Lander Avenue bridge to the Airport Way bridge: Appendix C of the State Water Resources Control Board Technical Committee Report on Regulation of Agricultural Drainage to the San Joaquin River, 173 p.

Loeltz, O.J., and Leake, S.A., 1983, A method for estimating ground-water return flow to the lower Colorado River in the Yuma area, Arizona and California: U.S. Geological Survey Water-Resources Investigations Report 83-4220, 86 p.

McDonald, M.G., and Harbaugh, A.W., 1988, A modular three-dimensional finite-difference ground-water flow model: U.S. Geological Survey Techniques of Water Resources Investigations, book 6, chap. A1, 586 p.

Michel, R.L., 1990, Tritium deposition in the continental United States, 1953-1983: U.S. Geological Survey Water-Resources Investigations Report 89-4072, 46 p.

Munsell Color, 1975, Munsell soil color charts: Baltimore, Maryland, Munsell Color, MacBeth Division of Kollmorgen Corporation.

National Research Council, 1947, Report of the Subcommittee on Sediment Terminology: Eos, Transactions of the American Geophysical Union, v. 28, no. 6, p. 936-938.

Page, R.W., 1986, Geology of the fresh ground-water basin of the Central Valley, California, with texture maps and sections: U.S. Geological Survey Professional Paper 1401-C, 54 p.

Papadopulos, I.S., Bredehoeft, J.D., and Cooper, H.H., Jr., 1973, On the analysis of "slug test" data: Water Resources Research, v. 9, no. 4, p. 1087-1089.

Phillips, S.P., and Belitz, Kenneth, 1990, Calibration of a texture-based model of a ground-water flow system, western San Joaquin Valley, California: U.S. Geological Survey Open-File Report 90-573, 30 p.

Piper, A.M., 1944, A graphical procedure in the geochemical interpretation of water analyses: Eos, Transactions of the American Geophysical Union, v. 25, p. 914-923.

Rashmawi, E.A., Grober, L.F., Grismer, M.E., and Kratzer, C.R., 1989, Data refinements and modeling results for the lower San Joaquin River basin: University of California Davis report to the State Water Resources Control Board, 101 p.

Shelton L.R., and Miller, L.K., 1988, Water-quality data, San Joaquin Valley, California, March 1985 to March 1987: U.S. Geological Survey Open-File Report 88-479, 210 p.

Tidball, R.R., Severson, R.C., Gent, C.A., and Riddle, G.O., 1987, Element associations in soils of the San Joaquin Valley, California: U.S. Geological Survey Open-File Report 86-583, 15 p.

Table 8. Lithologic logs for wells at cluster sites

[See table 1 for explanation of well identifier]

Depth (feet) From	Depth (feet) To	Description
		NW-107.5
Altitude of land surface, approximately 66.0 feet. Drilled with an auger rig by the U.S. Bureau of Reclamation, July 25 and 26, 1988. Total depth of borehole, 113.0 feet. Screen interval 105.0-110.0 feet.		
Core		
0	1.7	Clay, very silty, brownish gray (5YR 4/1), abundant rootlets; dry.
1.7	3.0	Sand (very fine), very silty, dark yellowish brown (10YR 4/2); dry.
3.0	3.5	Sand (very fine), very silty, abundant gravel, dark yellowish brown (10YR 4/2); dry.
3.5	4.9	Clay, very silty, brownish gray (5YR 4/1); dry.
4.9	8.3	Sand (very fine), moderately silty, dark yellowish brown (10YR 4/2), mica content increases with depth; dry.
8.3	12.0	Sand (medium to coarse), composed of predominantly quartz and some mica and interbeds of fine silty sand, moderate yellowish brown (10YR 5/4), sand coarsens with depth; damp.
12.0	28.3	Sand (coarse), pale yellowish brown (10YR 6/2), predominantly quartz and mica; saturated at 13.6 feet.
28.3	40.6	Clay, grayish green (5G 5/2) with some white (N9) and moderate yellowish brown (10YR 5/4) mottling, occasional thin layers of very micacous clay, sharp contact with overlying sand; damp.
40.6	43.3	Clay, greenish black (5G 2/1) grading to dark greenish gray (5G 4/1), some layers of mica rich silt, 1-inch thick layer of coarse sand at 42.4 feet; saturated.
43.3	49.3	Sand (fine to coarse), dusky yellow green (5GY 5/2), predominantly quartz and mica, sand coarsens with depth; saturated.
Cuttings		
49.3	113.0	Sand (fine to coarse), predominantly quartz and mica; saturated.
		NR-20.0
Cuttings		
River well jetted August 19, and September 9, 1988. Total depth, 20.0 feet, open ended.		
0	6.5	Clay, medium bluish gray (5B 5/1).
6.5	9.0	Sand (medium to coarse).
9.0	17.0	Clay, yellowish gray (5Y 8/1).
10.0	20.0	Sand, very silty, abundant mica.

Table 8. Lithologic logs for wells at cluster sites–*Continued*

Depth (feet) From	Depth (feet) To	Description
		NE-107.5
Altitude of land surface, approximately 58.0 feet. Drilled with an auger rig by the U.S. Bureau of Reclamation, June 13, 1988. Total depth of borehole, 113.0 feet. Screened interval 105.0-110.0 feet.		
Core		
0	3.4	Sand (medium), grayish orange (10YR 7/4), composed of mostly quartz and moderate amounts of mica, loose; damp.
3.4	9.4	Sand (medium), grayish orange (10RY 7/4), composition similar to above, with evenly spaced 6-inch layers of micaceous sandy silt, layers are moderate yellowish brown (10YR 5/4), slightly cohesive; damp.
9.4	13.4	Sand and silty sand, alternating layers of olive gray (5Y 3/2) micaceous sand (medium to coarse) and silty sand (as much as 3.0 inches wide), cohesive; damp.
13.4	15.9	Sand (medium), slightly silty, olive gray (5Y 3/2), predominantly quartz and some mica, loose; saturated.
15.9	18.4	Clay, slightly sandy, olive gray (5Y 3/2), very cohesive; saturated.
18.4	23.4	Sand (medium), silty, olive gray (5Y 3/2), silty sand grading downward to sand with occasional wood chips, mica content increases with depth, slightly cohesive; saturated.
23.4	25.4	Clay, grayish green (5G 5/2) with moderate yellowish brown (10YR 5/4) mottling.
25.4	26.2	Clay, pale olive (10Y 6/2).
26.2	29.5	Clay, yellowish gray (5Y 7/2) with dark yellowish orange (10YR 6/6) mottling and specks of light brown (5YR 5/6) and very pale orange (10YR 8/2).
29.5	31.4	Sand (medium) and clay, alternating layers of sandy clay, micaceous quartz sand, and clay; sandy clay is yellowish gray (5Y 7/2) with small patches of dark yellowish orange (10YR 6/6) color, sand and clay layers are yellowish gray (5Y 7/2); saturated.
31.4	33.4	Sand (medium), top section of sample is yellowish gray (5Y 7/2) and grade into light olive gray (5Y 5/2), composed of mostly quartz with abundant mica with occasional lamina of micaceous sand; saturated.
Cuttings		
33.4	113.0	Sand (very fine to coarse), cuttings show sand grading in and out of coarse-grained sands; saturated.

Table 8. Lithologic logs for wells at cluster sites--*Continued*

Depth (feet) From	Depth (feet) To	Description
		CW-97.7
Altitude of land surface, approximately 50.0 feet. Drilled with an auger rig by the U.S. Bureau of Reclamation, June 28 and 29, 1988. Total depth of borehole, 103.2 feet. Screened interval 95.2-100.2.		
Core		
0	1.5	Sand (coarse), pale yellowish brown (10YR 4/2), predominantly quartz with some mica, loose; dry.
1.5	2.3	Clay, some fine-grained sand; dry.
2.3	3.6	Sand (fine), some silt, moderate yellowish brown (10YR 5/4), loose; dry.
3.6	8.0	Sand (fine to medium grained), pale yellowish brown (10YR 6/2), predominantly quartz with moderate amounts of mica, loose; dry.
8.0	8.9	Sand (very fine), very silty, moderate brown (5YR 4/4), oxidized burrows and lamina, crumbly; dry.
8.9	9.4	Sand (very fine), abundant silty clay, light brown (5YR 5/6), crumbly; dry.
9.4	12.2	Sand (medium), pale yellowish brown (10YR 6/2), loose; dry to 10.2 feet, damp thereafter.
11.4	13.9	Sand (fine), silt and wood chips, alternating layers sand, silt and wood chips up to 3 inches thick, sand is medium gray (N4), silt is dark gray (N2), occasional thin lamina of very oxidized fine-grained sand, slightly cohesive; saturated.
Cuttings		
13.9	103.2	Sand (medium to coarse), between light bluish gray (5B 7/1) and medium bluish gray (5B 5/1), predominantly composed of quartz and feldspar with moderate amounts of mica, loose; saturated.
		CR-20.0
River well jetted September 2, 1988. Total depth, 20.0 feet; open ended.		
Cuttings		
0	6.5	Sand (medium to coarse).
6.5	16.5	Clay.
16.5	20.0	Sand.
		CE-107.5
Altitude of land surface, approximately 57.0 feet. Drilled with an auger rig by the U.S. Bureau of Reclamation, July 12 and 13, 1988. Total depth of borehole, 113.0 feet. Screened interval 105.0-110.0 feet.		
Core		
0	1.7	Clay, between dark yellowish brown (10YR 4/2) and dusky yellowish brown (10YR 2/2), abundant rootlets very cohesive; dry.
1.7	2.5	Clay, moderately silty, yellowish gray (5Y 8/1), abundant rootlets dry and crumbly.
2.5	3.0	Clay, very silty, yellowish gray (5Y 8/1); dry.

Table 8. Lithologic logs for wells at cluster sites--*Continued*

Depth (feet) From	To	Description
		CE-107.5--*Continued*
Core--*Continued*		
3.0	4.2	Sand (very fine), moderately silty, light brown (5Y 8/1), extremely oxidized; dry.
4.2	7.8	Sand (very fine), some silt, pale yellowish brown (10YR 6/2), some oxidized patched; dry.
7.8	8.6	Sand (fine to medium), grayish orange (10YR 7/4), predominantly quartz and feldspar with some mica; dry.
8.6	13.8	Sand (medium to coarse), grayish orange (10YR 7/4), composition similar to preceding sample; slightly moist at 10.5 feet.
13.8	20.0	Sand (coarse to very coarse), predominantly quartz and feldspar with some mica, no apparent oxidation, loose; saturated at 17.6 feet.
20.0	20.3	Sand as above, very oxidized.
20.3	21.5	Sand (very fine to fine), no apparent oxidation, occasional thin black lamina, loose; saturated.
Cuttings		
21.5	113.0	Sand (medium to very coarse), no apparent oxidation, no clay observed, loose; saturated.
		PW-89.0
Altitude of land surface, approximately 45.0 feet. Drilled with an auger rig by the U.S. Bureau of Reclamation, June 7-9, 1988. Total depth of borehole, 98.0 feet. Screened interval, 86.5-91.5 feet.		
Core		
0	2.0	Sand (fine to medium), pale yellowish brown (10YR 6/2), composed of predominantly quartz with some mica and yellow and orange grains, moderately well sorted; loose; sample dry.
2.0	5.8	Clay, moderately silty, dusky yellowish brown (10YR 2/2) with dusty brown (5YR 2/2) mottling and some oxidized patches; an organically rich sandy clay lens (0.2 foot thick) at 5.6 feet deep; abundant animal burrows throughout top half of sample; very cohesive; slightly damp.
5.8	9.0	Sand (fine to medium), some silt, predominantly quartz with moderate amounts of mica, slightly cohesive; slightly damp.
9.0	16.6	Sand (fine to medium), pale yellowish brown (10YR 6/2) to dark yellowish brown (10YR 4/2), composed of predominantly quartz with moderate amounts of mica, loose; saturated.
16.6	17.0	Wood chips (as much as 0.4 inch), some medium-grained sand; saturated.
17.0	18.2	Sand (medium to coarse), predominantly quartz with moderate amounts of mica, some small clay clasts (as much as 0.25 inch), loose; saturated.
18.2	32.0	Sand (medium to coarse), light bluish gray (5B 7/1), predominantly quartz and feldspar with moderate amounts of mica, loose; saturated.
32.0	38.0	Sand (medium to coarse), light bluish gray (5B 7/1), predominantly quartz and feldspar with moderate amounts of mica, occasional clay stringers (as much as 1.0 inch) also (5B 7/1); saturated.

Table 8. Lithologic logs for wells at cluster sites--*Continued*

Depth (feet) From	Depth (feet) To	Description
		PW-89.0--*Continued*
Cuttings		
38.0	98.0	Sand (medium to coarse), light bluish gray (5B 7/1), predominantly quartz and feldspar with moderate amounts of mica, very little clay observed, loose; saturated.
		PR-30.7
River well jetted August 25, and September 2, 1988. Total depth, 30.7 feet; open ended.		
Cuttings		
0	19.5	Sand (medium to coarse).
19.5	24.5	Clay, dusky blue green (5BG 3/2), very dense, crumbly.
24.5	30.7	Sand, (medium to coarse).
		PE-98.3
Altitude of land surface, approximately 40.0 feet. Drilled with an auger rig by the U.S. Bureau of Reclamation, June 14 and 15, 1988. Total depth of borehole, 103.8 feet. Screened interval 95.8-100.8 feet.		
Core		
0	3.5	Sand (medium), some silt, pale yellowish brown (10YR 6/2), composed predominantly of quartz, moderate amounts of yellow, orange, and mica grains, slightly cohesive; slightly damp.
3.5	3.8	Sand (medium), moderately silty, pale yellowish brown (10YR 6/2), cohesive; damp.
3.8	8.5	Sand (medium), moderately silty, silt in top section of sample is pale yellowish brown (10YR 6/2), olive gray (5Y 3/2) in middle section and alternating back to (10YR 6/2) in bottom part of sample; cohesive; very damp; sharp contact between sandy silt on the underlying sand at 8.5 feet.
8.5	9.5	Sand (medium to coarse), light bluish gray (5B 7/1) with occasional streaks of moderate yellowish brown (10YR 5/4) sand, loose; saturated.
9.5	10.4	Sand (medium to coarse), moderate yellowish brown (10YR 5/4) with occasional streaks of light bluish gray (5B 7/1) sand including small silty clay nodules, loose; saturated.
10.4	23.5	Sand (medium to coarse), light bluish gray (5B 7/1), predominantly quartz and feldspar with moderate amounts on mica, some occasional clay layers, sand is loose; saturated.
Cuttings		
23.5	103.8	Sand (medium to coarse), similar to previous sample; cuttings on deepest auger flight showed light bluish gray (5B 7/1) clay.

Table 9. Stable-isotope ratios and tritium concentrations

[TU, tritium unit; <, actual value is less than value shown]

Well identifier (see table 1)	Date	Delta deuterium (per mil)	Delta oxygen-18 (per mil)	Tritium (TU)
NW-14.5	11-15-88	-63.5	-8.15	10.8
NW-47.5	11-15-88	-63.5	-8.15	8.8
NW-107.5	11-15-88	-64.0	-8.20	15.4
NR-7.0	11-15-88	-59.5	-8.05	1.4
NR-20.0	11-15-88	-61.0	-8.10	2.9
NE-14.5	11-15-88	-79.0	-10.55	8.4
NE-35.5	11-15-88	-62.0	-8.20	3.5
NE-107.5	11-15-88	-62.5	-8.15	<.8
CW-18.2	11-16-88	-74.5	-9.85	5.7
CW-97.9	11-16-88	-68.5	-9.05	<.8
CR-5.0	11-16-88	-77.0	-10.50	14.5
CR-20.0	11-16-88	-78.0	-10.60	14.9
CE-19.5	11-16-88	-68.5	-9.20	12.4
CE-107.5	11-16-88	-74.0	-9.70	27.0
PW-11.5	11-17-88	-66.5	-9.05	9.5
PW-22.5	11-17-88	-74.0	-9.65	25.8
PW-89.0	11-17-88	-71.5	-9.35	19.0
PR-5.0	11-17-88	-76.0	-9.90	29.7
PR-30.7	11-17-88	-74.0	-9.75	20.4
PE-9.5	11-17-88	-63.5	-8.05	14.7
PE-98.3	11-17-88	-72.5	-9.50	14.3

Table 10. Analyses of ground-water properties and constituents

[Dissolved major ions are given in milligrams per liter; <, actual value is less than value shown]

Well identifier (see table 1)	Date	pH, field (standard units)	Calcium	Magnesium	Sodium	Potassium	Alkalinity, carbonate, field (as $CaCO_3$)	Sulfate	Chloride
NW-14.5	11-15-88	7.1	250	170	540	3.9	443	1,100	730
NW-47.5	11-15-88	7.6	180	150	440	4.0	364	850	680
NW-107.5	11-15-88	7.4	160	140	350	3.3	413	870	400
NR-7.0	11-15-88	7.5	170	130	330	3.8	226	640	680
NR-20.0	11-15-88	7.5	160	120	320	3.7	246	600	640
NE-14.5	11-15-88	7.9	14	9.7	110	1.9	226	15	48
NE-35.5	11-15-88	7.5	120	110	330	3.4	289	580	460
NE-107.5	11-15-88	7.8	150	160	1,200	5.7	272	1,600	1,300
CW-18.2	11-16-88	6.9	63	42	95	2.3	282	220	48
CW-97.7	11-16-88	7.5	99	56	380	3.2	130	320	620
CR-5.0	11-16-88	7.2	57	26	100	3.6	253	65	110
CR-20.0	11-16-88	7.0	50	24	100	3.3	220	72	120
CE-19.5	11-16-88	7.3	42	25	280	2.7	449	140	140
CE-107.5	11-16-88	8.0	82	43	400	3.4	507	120	430
PW-11.5	11-17-88	7.2	21	12	89	.9	148	82	48
PW-22.5	11-17-88	7.5	160	130	450	3.9	497	950	430
PW-89.0	11-17-88	7.4	170	110	400	3.6	443	870	380
PR-5.0	11-17-88	7.7	180	140	430	4.2	514	980	450
PR-30.7	11-17-88	7.6	170	120	410	3.7	462	870	410
PE-9.5	11-17-88	6.6	75	45	110	3.0	174	100	280
PE-98.3	11-17-88	7.5	170	110	390	3.7	438	880	350

Well identifier (see table 1)	Date	Fluoride	Bromide	Iodide	Silica	Solids, sum of constituents, dissolved	Nitrogen, nitrite (as N)	Nitrogen, nitrite plus nitrate (as N)	Phosphorus ortho, (as P)
NW-14.5	11-15-88	0.2	2.4	0.06	27	3,220	0.08	27	1.3
NW-47.5	11-15-88	.2	2.1	.08	26	2,570	.03	3.0	.14
NW-107.5	11-15-88	.2	1.3	.07	26	2,210	<.01	2.3	.05
NR-7.0	11-15-88	.2	2.1	.32	25	2,120	<.01	<.10	.09
NR-20.0	11-15-88	.2	2.0	.07	28	2,040	<.01	2.7	.06
NE-14.5	11-15-88	.3	0.1	.06	37	381	.04	<.10	2.4
NE-35.5	11-15-88	.2	1.4	.04	27	1,820	<.01	2.9	.09
NE-107.5	11-15-88	.1	3.3	.13	25	4,620	.19	1.3	.86
CW-18.2	11-16-88	.3	.2	.01	24	668	<.01	<.10	.05
CW-97.7	11-16-88	.2	2.2	.45	36	1,600	.05	<.10	.13
CR-5.0	11-16-88	.2	.2	.09	38	558	.01	.13	.94
CR-20.0	11-16-88	.2	.3	.07	30	534	<.01	<.10	.02
CE-19.5	11-16-88	.9	.5	.08	32	969	.03	7.1	.82
CE-107.5	11-16-88	.1	.6	.12	33	1,430	<.01	<.1	2.2
PW-11.5	11-17-88	.4	.2	.03	31	374	<.01	<.10	.06
PW-22.5	11-17-88	.3	1.1	.12	24	2,460	.04	1.3	.04
PW-89.0	11-17-88	.3	.9	.12	26	2,230	<.01	<.10	.02
PR-5.0	11-17-88	.4	1.0	.13	23	2,520	<.01	.14	.02
PR-30.7	11-17-88	.4	1.0	.14	26	2,290	<.01	<.10	.04
PE-9.5	11-17-88	.1	.3	.10	26	745	.01	<.10	.04
PE-98.3	11-17-88	.3	.8	.14	25	2,200	<.01	<.10	.06

Table 11. Specific conductance measured in observation wells

[Specific conductance in microsiemens per centimeter at 25 degrees Celsius; --, no data]

Well identifier (see table 1)	1988	1989							
	Nov. 15-17 field	Apr. 27	May 11	May 19	June 14	June 30	July 14	July 27	Aug. 15
NW-14.5	4,640	--	--	--	5,170	--	--	--	5,130
NW-47.5	3,820	3,690	--	--	3,660	3,730	3,640	3,820	3,620
NW-107.5	3,150	--	--	3,090	3,410	--	--	--	3,310
NR-7.0	3,380	--	--	--	3,380	--	--	--	3,540
NR-20.0	3,200	--	--	--	3,310	--	--	--	3,280
NE-14.5	595	--	--	562	573	567	581	554	560
NE-35.5	2,690	--	--	2,860	2,850	--	--	--	2,920
NE-107.5	6,420	--	6,640	6,590	6,670	--	6,720	6,490	6,410
CW-12.8	--	--	--	--	--	--	--	--	--
CW-18.2	1,024	--	950	960	996	979	1,018	998	994
CW-97.7	2,600	--	--	2,700	2,660	--	--	--	2,700
CR-5.0	910	--	--	--	1,406	1,322	1,383	1,384	1,381
CR-20.0	850	--	--	--	1,237	--	--	--	1,266
CE-19.5	1,480	--	--	--	1,549	--	--	--	1,772
CE-107.5	2,290	--	--	--	2,450	2,480	2,500	2,490	2,490
PW-11.5	574	--	--	--	854	916	--	--	995
PW-22.5	3,440	--	--	--	3,650	--	--	--	3,600
PW-89.0	3,120	--	--	--	3,220	3,210	3,040	3,110	3,070
PR-5.0	3,420	--	3,790	--	3,680	--	--	--	3,650
PR-30.7	2,980	--	--	--	--	--	--	--	3,300
PE-9.5	1,170	1,404	--	--	1,572	1,580	1,547	1,553	1,527
PE-98.3	2,890	--	--	--	3,150	--	--	--	3,140

Table 12. Chemical analyses of dissolved trace elements

[Trace elements in micrograms per liter; <, actual value is less than value shown; --, no data]

Well identifier (see table 1)	Date	Aluminum	Arsenic	Boron	Cadmium	Chromium	Cobalt	Copper
NW-14.5	11-15-88	20	3	2,400	<1	4	2	2
NW-47.5	11-15-88	<10	3	1,400	<1	20	2	1
NW-107.5	11-15-88	10	1	1,700	2	10	1	1
NR-7.0	11-15-88	<10	3	800	<1	2	2	1
NR-20.0	11-15-88	<10	2	820	<1	20	1	1
NE-14.5	11-15-88	--	3	490	1	3	1	2
NE-35.5	11-15-88	<10	2	1,200	<1	20	2	1
NE-107.5	11-15-88	<10	7	3,300	<1	10	1	1
CW-18.2	11-16-88	<10	1	620	<1	1	<1	<1
CW-97.7	11-16-88	<10	2	1,700	<1	2	1	<1
CR-5.0	11-16-88	<10	40	340	1	<1	4	1
CR-20.0	11-16-88	30	3	320	<1	<1	3	1
CE-19.5	11-16-88	120	4	970	1	2	2	3
CE-107.5	11-16-88	170	9	480	<1	1	<1	1
PW-11.5	11-17-88	<10	4	410	<1	2	1	1
PW-22.5	11-17-88	<10	2	2,200	<1	2	1	<1
PW-89.0	11-17-88	<10	5	2,400	<1	1	1	1
PR-5.0	11-17-88	<10	1	2,500	<1	1	2	<1
PR-30.7	11-17-88	<10	3	2,300	<1	1	2	<1
PE-9.5	11-17-88	10	16	300	2	<1	5	<1
PE-98.3	11-17-88	20	3	2,300	<1	2	<1	<1

Well identifier (see table 1)	Date	Iron	Lead	Lithium	Manganese	Mercury	Molybdenum	Nickel
NW-14.5	11-15-88	40	<5	10	70	<0.1	26	7
NW-47.5	11-15-88	20	<5	40	10	<.1	2	3
NW-107.5	11-15-88	20	<5	40	70	<.1	<1	4
NR-7.0	11-15-88	180	<5	40	300	<.1	5	4
NR-20.0	11-15-88	20	<5	30	<10	<.1	2	2
NE-14.5	11-15-88	640	<5	<4	120	<.1	6	3
NE-35.5	11-15-88	<10	<5	40	<10	<.1	1	2
NE-107.5	11-15-88	10	<5	60	30	<.1	5	2
CW-18.2	11-16-88	2,300	<5	17	180	<.1	2	2
CW-97.7	11-16-88	20	<5	30	30	<.1	7	2
CR-5.0	11-16-88	1,400	<5	13	--	<.1	4	7
CR-20.0	11-16-88	690	<5	8	820	<.1	1	3
CE-19.5	11-16-88	130	<5	9	340	.4	14	--
CE-107.5	11-16-88	210	<5	20	100	.1	7	3
PW-11.5	11-17-88	49	<5	8	67	<.1	16	3
PW-22.5	11-17-88	160	<5	100	30	<.1	13	6
PW-89.0	11-17-88	340	<5	120	60	<.1	9	1
PR-5.0	11-17-88	80	<5	100	100	<.1	11	3
PR-30.7	11-17-88	520	<5	110	60	<.1	12	1
PE-9.5	11-17-88	--	<5	18	--	<.1	1	7
PE-98.3	11-17-88	1,600	<5	100	250	<.1	8	1

Table 12. Chemical analyses of dissolved trace elements--*Continued*

Well identifier (see table 1)	Date	Selenium	Silver	Strontium	Vanadium	Zinc
NW-14.5	11-15-88	9	<1.0	2,900	25	<10
NW-47.5	11-15-88	4	<1.0	3,300	20	10
NW-107.5	11-15-88	2	1.0	2,700	10	10
NR-7.0	11-15-88	2	<1.0	2,800	15	10
NR-20.0	11-15-88	4	<1.0	2,600	15	<10
NE-14.5	11-15-88	.4	<1.0	190	26	8
NE-35.5	11-15-88	3	<1.0	2,000	13	<10
NE-107.5	11-15-88	1.5	<1.0	2,900	48	20
CW-18.2	11-16-88	0	<1.0	860	<1	11
CW-97.7	11-16-88	1	<1.0	1,400	15	<10
CR-5.0	11-16-88	.4	<1.0	670	3	20
CR-20.0	11-16-88	.2	<1.0	480	3	13
CE-19.5	11-16-88	3	<1.0	480	13	17
CE-107.5	11-16-88	1.5	<1.0	1,200	8	<10
PW-11.5	11-17-88	.3	<1.0	180	2	6
PW-22.5	11-17-88	17	<1.0	2,700	35	<10
PW-89.0	11-17-88	.1	<1.0	2,900	6	<10
PR-5.0	11-17-88	0	1.0	3,100	8	20
PR-30.7	11-17-88	.2	<1.0	3,000	7	<10
PE-9.5	11-17-88	<.1	<1.0	750	2	16
PE-98.3	11-17-88	.1	<1.0	2,900	5	<10

☆U.S. GOVERNMENT PRINTING OFFICE: 1991-587-665/59255